



UNIVERSIDAD  
DE LOS ANDES  
Mérida - Venezuela

ISSN: 1856-5301

# Avances en Química

Septiembre - Diciembre 2021

Volumen 16  
Número 3



# Avances en Química

## Contenido

---

Volumen 16, número 3, cuatrimestre septiembre – diciembre 2021

Página

---

### Artículos científicos

Síntesis y caracterización estructural del compuesto hidantoína de D,L-valina .....	49
<b>Ronald Márquez, Lusbely M. Belandria, Marilia Guillén, Teresa González, Asiloé J. Mora, Gerzon E. Delgado</b>	Venezuela
Capacidad base o inicial de retención de fósforo en un suelo soporte de un establecimiento de engorde a corral.....	57
<b>Ileana C. Ciapparelli*, Alicia Rosa Fabrizio de Iorio, Ana Rosa García</b>	Argentina
Phytochemical study and in vitro biological activities of Chlorella vulgaris, Chlorella pyrenoidosa and Chlorella minutissima extracts .....	71
<b>Antonio Menezes-Filho*, Matheus Ventura, Hellen Batista-Ventura, Carlos Castro, Celiana Triches, Cinthia Porfiro, Jacqueline Guimarães, Marconi Teixeira, Frederico Soares, Aparecida Taques</b>	Brasil

### Revisiones bibliográficas

Residuos lignocelulósicos como materia prima de segunda generación en procesos de biorrefinación.....	81
<b>Andrea Briones Muñoz*, María A. Riera</b>	Ecuador
Cell encapsulation using chitosan: chemical aspects and applications .....	89
<b>Maura Rojas Pirela, Verónica Rojas, Elizabeth Pérez Pérez, Cristóbal Lárez Velásquez*</b>	Venezuela/Chile

---

# Avances en Química

## Consejo Editorial

### Comité Editorial

Dra. Marcela Pascu de Burguera, [pascu@ula.ve](mailto:pascu@ula.ve)  
Dr. Issa Katime, [issakatime@ehu.es](mailto:issakatime@ehu.es)  
Dr. Wilmer Olivares, [wilmer@ula.ve](mailto:wilmer@ula.ve)  
Dr. Jairo Márquez, [jamar@ula.ve](mailto:jamar@ula.ve)  
Dr. Enrique Millán Barrios, [ejmb@ula.ve](mailto:ejmb@ula.ve)

### Editor Jefe

Dr. Cristóbal Lárez Velásquez, [clarez@ula.ve](mailto:clarez@ula.ve)

### Consejo de Editores por Área

Área	Principales Suplentes	Direcciones electrónicas	Área	Principales Suplentes	Direcciones electrónicas
Analítica	Froylan Contreras Alexis Zambrano	<a href="mailto:fcontrer@ula.ve">fcontrer@ula.ve</a> <a href="mailto:alexisz@ula.ve">alexisz@ula.ve</a>	Productos Naturales	Juan M. Amaro Carmelo Rosquete	<a href="mailto:jamaro@ula.ve">jamaro@ula.ve</a> <a href="mailto:carmelor@ula.ve">carmelor@ula.ve</a>
Electroquímica	Enrique Millán B. Yris Martínez	<a href="mailto:ejmb@ula.ve">ejmb@ula.ve</a> <a href="mailto:ymartin@ula.ve">ymartin@ula.ve</a>	Cinética y Catálisis	Freddy Imbert Pedro Rodríguez	<a href="mailto:imbert@ula.ve">imbert@ula.ve</a> <a href="mailto:pedrojrs@ula.ve">pedrojrs@ula.ve</a>
Orgánica	Alí Bahsas Andrés Abad	<a href="mailto:bahsas@ula.ve">bahsas@ula.ve</a> <a href="mailto:abadjos@ula.ve">abadjos@ula.ve</a>	Química Ecológica	María P. Calcagno Alberto Oliveros	<a href="mailto:mariapia@ula.ve">mariapia@ula.ve</a> <a href="mailto:aloliver@ula.ve">aloliver@ula.ve</a>
Polímeros	Hugo Martínez P. Cristóbal Lárez V.	<a href="mailto:hmartin@ula.ve">hmartin@ula.ve</a> <a href="mailto:clarez@ula.ve">clarez@ula.ve</a>	Espectroscopía Analítica	Xiomara de Navarro María A. Sánchez	<a href="mailto:roxio@ula.ve">roxio@ula.ve</a> <a href="mailto:angelisa@ula.ve">angelisa@ula.ve</a>
Inorgánica y Organometálicos	Bernardo Fontal Ricardo Contreras	<a href="mailto:fontal@ula.ve">fontal@ula.ve</a> <a href="mailto:ricardo@ula.ve">ricardo@ula.ve</a>	Espectroscopía Molecular	Pablo Carrero Carlos Rondón	<a href="mailto:pcarrero@ula.ve">pcarrero@ula.ve</a> <a href="mailto:crondon@ula.ve">crondon@ula.ve</a>
Química Teórica	Wilmer Olivares Luis Rincón	<a href="mailto:wilmer@ula.ve">wilmer@ula.ve</a> <a href="mailto:lrincon@ula.ve">lrincon@ula.ve</a>	Cristalográfia	Graciela Díaz Gerzon Delgado	<a href="mailto:diaz@ula.ve">diaz@ula.ve</a> <a href="mailto:gerzon@ula.ve">gerzon@ula.ve</a>
Farmacia	Alfredo Usbillaga Sabino Menolasina	<a href="mailto:usbillaga@ula.ve">usbillaga@ula.ve</a> <a href="mailto:sabino@ula.ve">sabino@ula.ve</a>			

# Consejo editorial

## Comité Editorial

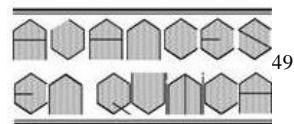
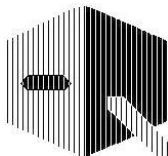
Dra. Marcela Pascu de Burguera, [pascu@ula.ve](mailto:pascu@ula.ve)  
Dr. Issa Katime, [issakatime@chu.es](mailto:issakatime@chu.es)  
Dr. Wilmer Olivares, [wilmer@ula.ve](mailto:wilmer@ula.ve)  
Dr. Jairo Márquez, [jamar@ula.ve](mailto:jamar@ula.ve)  
Dr. Enrique Millán Barrios, [ejmb@ula.ve](mailto:ejmb@ula.ve)

## Editor Jefe

Dr. Cristóbal Lárez Velásquez, [clarez@ula.ve](mailto:clarez@ula.ve)

## Consejo de Editores por Área

Área	Principales Suplentes	Direcciones electrónicas	Área	Principales Suplentes	Direcciones electrónicas
Analítica	Froylan Contreras Alexis Zambrano	<a href="mailto:fcontrer@ula.ve">fcontrer@ula.ve</a> <a href="mailto:alexisz@ula.ve">alexisz@ula.ve</a>	Productos Naturales	Juan M. Amaro Carmelo Rosquete	<a href="mailto:jamaro@ula.ve">jamaro@ula.ve</a> <a href="mailto:carmelor@ula.ve">carmelor@ula.ve</a>
Electroquímica	Enrique Millán B. Yris Martinez	<a href="mailto:ejmb@ula.ve">ejmb@ula.ve</a> <a href="mailto:vmartin@ula.ve">vmartin@ula.ve</a>	Cinética y Catálisis	Freddy Imbert Pedro Rodriguez	<a href="mailto:imbert@ula.ve">imbert@ula.ve</a> <a href="mailto:pedroirs@ula.ve">pedroirs@ula.ve</a>
Orgánica	Ali Bahsas Andrés Abad	<a href="mailto:bahsas@ula.ve">bahsas@ula.ve</a> <a href="mailto:abadjos@ula.ve">abadjos@ula.ve</a>	Química Ecológica	Maria P. Calcagno Alberto Oliveros	<a href="mailto:mariapia@ula.ve">mariapia@ula.ve</a> <a href="mailto:aloliver@ula.ve">aloliver@ula.ve</a>
Polímeros	Hugo Martínez P. Cristóbal Lárez V.	<a href="mailto:hmartin@ula.ve">hmartin@ula.ve</a> <a href="mailto:clarez@ula.ve">clarez@ula.ve</a>	Espectroscopía Analítica	Xiomara de Navarro María A. Sánchez	<a href="mailto:roxio@ula.ve">roxio@ula.ve</a> <a href="mailto:angelisa@ula.ve">angelisa@ula.ve</a>
Inorgánica y Organometálicos	Bernardo Fontal Ricardo Contreras	<a href="mailto:fontal@ula.ve">fontal@ula.ve</a> <a href="mailto:ricardo@ula.ve">ricardo@ula.ve</a>	Espectroscopía Molecular	Pablo Carrero Carlos Rondón	<a href="mailto:pcarrero@ula.ve">pcarrero@ula.ve</a> <a href="mailto:crondon@ula.ve">crondon@ula.ve</a>
Química Teórica	Wilmer Olivares Luis Rincón	<a href="mailto:wilmer@ula.ve">wilmer@ula.ve</a> <a href="mailto:lrincon@ula.ve">lrincon@ula.ve</a>	Cristalografía	Graciela Diaz Gerzon Delgado	<a href="mailto:diaz@ula.ve">diaz@ula.ve</a> <a href="mailto:gerzon@ula.ve">gerzon@ula.ve</a>
Farmacia	Alfredo Usobilaga Sabino Menolasina	<a href="mailto:usubilla@ula.ve">usubilla@ula.ve</a> <a href="mailto:sabino@ula.ve">sabino@ula.ve</a>			



## Síntesis y caracterización estructural del compuesto hidantoína de *D,L*-valina

Ronald Márquez<sup>1</sup>, Lusbely M. Belandria<sup>1</sup>, Marilia Guillén<sup>1</sup>,  
Teresa González<sup>2</sup>, Asiloé J. Mora<sup>1</sup>, Gerzon E. Delgado<sup>1\*</sup>

<sup>1</sup>) Laboratorio de Cristalografía, Departamento de Química, Facultad de Ciencias,  
Universidad de Los Andes, Mérida 5101, Venezuela

<sup>2</sup>) Centro de Química, Instituto Venezolano de Investigaciones Científicas (IVIC),  
Caracas, Venezuela

(\*) [gerzon@ula.ve](mailto:gerzon@ula.ve)

Recibido: 30/11/2021

Revisado: 23/12/2021

Aceptado: 25/12/2021

### Resumen

La hidantoína de *D,L*-vailna, un nuevo derivado hidantóico de  $\alpha$ -aminoácido, con fórmula  $C_6H_{10}N_2O_2$ , ha sido sintetizado y caracterizado estructuralmente mediante las técnicas IR, RMN, y difracción de rayos-X. Los resultados espectroscópicos son consistentes con el esqueleto molecular. El patrón de difracción de rayos-X en polvo confirma la pureza de la muestra cristalina. El análisis por difractometría de cristal único indica que el compuesto cristaliza en el sistema monoclinico, grupo espacial  $P2_1/c$  (Nº14), con parámetros de celda unidad:  $a= 5,493(3) \text{ \AA}$ ,  $b= 23,53(2) \text{ \AA}$ ,  $c= 6,254(3) \text{ \AA}$  y  $\beta= 115,09(4)^\circ$ ,  $V= 732,1(9) \text{ \AA}^3$ ,  $Z= 4$ . El empaquetamiento cristalino está estabilizado por enlaces de hidrógeno fuertes del tipo N-H···O entre los anillos hidantoinicos vecinos; formando los grafos:  $C(5)$ ,  $R^2_2(8)$  y  $R^4_4(16)$ . Además, la estructura cristalina presenta enlaces de hidrógeno no convencionales del tipo  $C5\text{-}H5\cdots O2$  e interacciones  $\pi\cdots\pi$  entre los bordes del anillo hidantoína. La interacción de todos estos tipos de enlaces de hidrógeno, junto a fuerzas dispersivas presentes en las regiones donde se encuentran los grupos isopropilos, estabilizan el eficiente empaquetamiento de la estructura con un índice de espacio ocupado de 66,3%.

**Palabras claves:**  $\alpha$ -aminoácidos; hidantoínas; difracción de rayos-X; estructura cristalina

### Abstract

**Synthesis and structural characterization of the *D,L*-valine hydantoin compound:** The title compound, *D,L*-valine hydantoin, a new  $\alpha$ -amino acid hydantoin derivative with formula  $C_6H_{10}N_2O_2$  has been synthesized and structurally characterized by FT-IR, NMR, and X-ray diffraction techniques. Spectroscopy results are consistent with the skeleton structure. The powder X-ray diffraction data confirm the phase purity of the crystalline sample. Single-crystal X-ray diffraction analysis indicated that crystallizes in the monoclinic space group  $P2_1/c$  (Nº14),  $Z= 4$ , and unit cell parameters  $a= 5.493(3) \text{ \AA}$ ,  $b= 23.53(2) \text{ \AA}$ ,  $c= 6.254(3) \text{ \AA}$ ,  $\beta= 115.09(4)^\circ$ ,  $V= 732.1(9) \text{ \AA}^3$ . The crystalline packing is stabilized by strong hydrogen bonds of the N-H···O type between the neighboring hydantoin rings; forming the graphs:  $C(5)$ ,  $R^2_2(8)$  y  $R^4_4(16)$ . In addition, the crystalline structure presents unconventional hydrogen bonds of the  $C5\text{-}H5\cdots O2$  type and  $\pi\cdots\pi$  interactions between the edges of the hydantoin ring. The interaction of all these types of hydrogen bonds, together with dispersive forces present in the regions where the isopropyl groups are found, stabilize the efficient packing of the structure with a space-occupied index of 66.3%.

**Keywords:**  $\alpha$ -amino acids; Hydantoins; X-ray diffraction; crystal structure

### Introducción

Las hidantoínas o imidazolidina-2,4-dionas son compuestos con un anillo de imidazol que poseen grupos ceto en las posiciones 2 y 4 (figura 1). Dependiendo de la naturaleza y el tipo de sustitución en el anillo heterocíclico, estos compuestos pueden mostrar actividad farmacéutica y biológica con una variedad de aplicaciones<sup>1,3</sup>.

En particular, las hidantoínas sustituidas en la posición 5, como Norantoína (3-metil-5-fenilhidantoína), Mefenitoína (5-

ethyl-3-metil-5-fenilhidantoína), Nirvanol (5-etil-5-fenilhidantoína), Metetoína (5-etil-1-metil-5-fenilhidantoína) o Fenitoína (5,5-difenilhidantoína), son precursores valiosos de una gran variedad de sistemas heterocíclicos que están asociados con una amplia gama de actividades biológicas, incluida la antiarritmia<sup>4</sup>, anticonvulsivantes<sup>5</sup> y agentes antitumorales<sup>6</sup>. La hidantoína 5,5-difenilhidantoína más conocida, la fenitoína, es un compuesto anticonvulsivo que tiene eficacia en el tratamiento de la epilepsia convulsiva y psicomotora generalizada<sup>7</sup>.

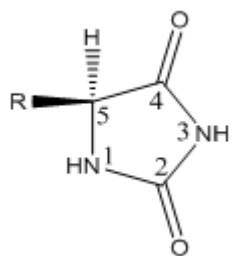


**Fig. 1:** Estructura química general de una hidantoína.

Estos heterociclos se usan comúnmente como modelos en química combinatoria debido a que poseen un núcleo altamente reactivo con cuatro posibles puntos de sustitución. Estas moléculas poseen el mismo número de grupos donantes de enlaces de hidrógeno (NH de dos anillos) y átomos aceptores (dos carbonilo CO), adecuados para formar arquitecturas supramoleculares a través de enlaces de hidrógeno, que a su vez desempeñan un papel clave en el reconocimiento molecular y la ingeniería de cristales<sup>8,9</sup>. Continuando con nuestros estudios estructurales de pequeñas moléculas biológicamente activas, incluyendo hidantoínas y tiohidantoínas<sup>10-15</sup>, en este trabajo reportamos la síntesis y caracterización estructural del nuevo compuesto hidantoína de *D,L*-valina.

## Parte experimental

En la figura 2 se representa esquemáticamente la ruta de síntesis de la hidantoína de *D,L*-valina. El derivado se sintetizó realizando algunas modificaciones de la ruta sintética Bucherer-Bergs propuestas en la literatura<sup>10,11</sup>. Se disolvieron 4mmol de la *D,L*-valina en 20 mL de agua destilada y se acidificó con unas gotas de HCl concentrado (37%) hasta alcanzar un pH por debajo de su punto isoeléctrico. A continuación, se añadieron 12 mmol de KOCN en una relación 1:3 respecto a la valina. Esta solución se sometió a calentamiento y agitación constante durante 4 horas a 60 °C. Una vez transcurrido el tiempo de reacción se dejó enfriar la solución y se acidificó nuevamente con HCl hasta la formación del N-carbamoiilo. El precipitado se disolvió en HCl hasta alcanzar un pH ácido ( $\text{pH} \approx 1-2$ ) y esta mezcla se sometió a refluo durante 4 horas a 60 °C, con agitación constante, obteniéndose la hidantoína. El producto se recristalizó por evaporación lenta de solvente en una mezcla etanol:agua en proporción 1:1. Luego de algunas semanas se obtuvieron cristales incoloros en forma de paralelepípedos, óptimos para el estudio por difracción de rayos-X de cristal único. Punto de fusión: 140-142°C.

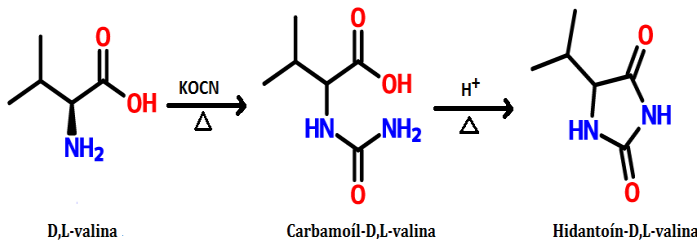


**Fig. 2:** Ruta de síntesis de la hidantoína de *D,L*-valina.

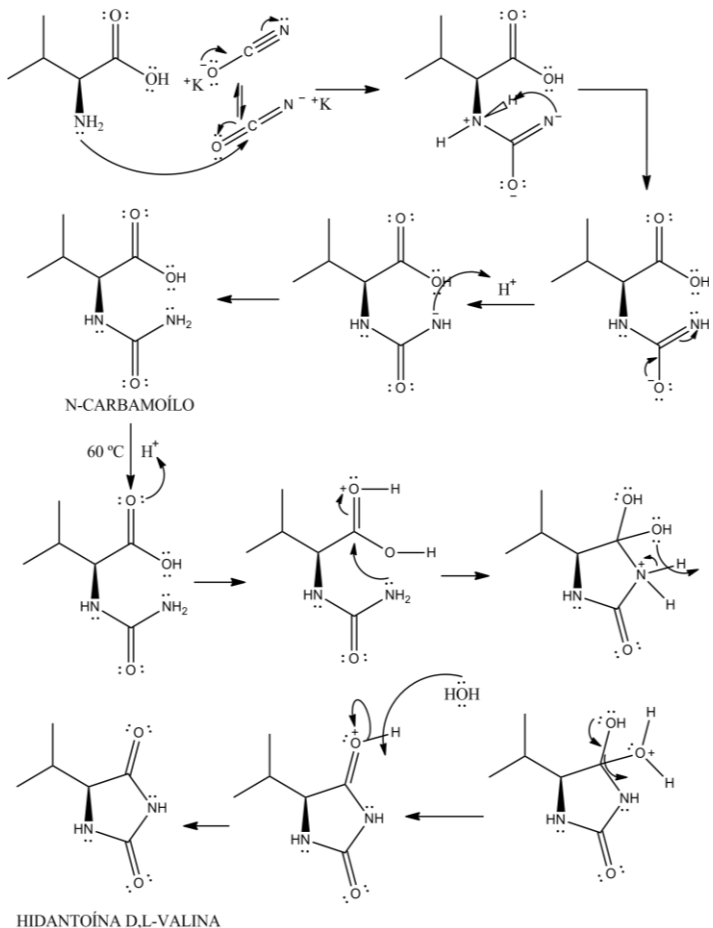


**Fig. 3:** Mecanismo de reacción propuesto para la formación de la hidantoína *D,L*-valina.

En la figura 3 se muestra el mecanismo de reacción propuesto para la síntesis del derivado hidantoína de *D,L*-valina. La reacción consiste en la adición nucleofílica del carbono electrofílico de cianato de potasio sobre el nitrógeno del grupo amina. El producto de reacción sufre un reordenamiento intramolecular para formar el N-carbamoiilo de la valina. Una vez obtenido el N-carbamoiilo, este se somete a refluo bajo condiciones ácidas para lograr la deshidratación y ciclación del α-aminoácido, obteniendo así el anillo hidantoína sustituido en la posición 5 por un grupo isopropilo.

El punto de fusión se midió en un aparato Electrothermal modelo 9100.

El espectro infrarrojo (FT-IR) se midió en un equipo Perkin-Elmer 1600 en pastillas de KBr. Los espectros de resonancia magnética nuclear RMN-<sup>1</sup>H y RMN-<sup>13</sup>C, se obtuvieron en un espectrómetro Bruker Avance DRX 400, utilizando DMSO.

Los datos de difracción de rayos-X en muestra policristalina se registraron en un difractómetro Siemens D5005 utilizando radiación de CuKα ( $\lambda = 1,5418 \text{ \AA}$ ). Los datos se colectaron en un rango de 5-65° en  $2\theta$  con pasos de 0,02° y un tiempo de 10 segundos por paso. Se utilizó silicio como estándar externo.

La toma de datos de intensidad de difracción de rayos-X de cristal único se realizó, a temperatura ambiente, en un difractómetro Rigaku AFC-7S, empleando radiación de Mo K $\alpha$  ( $\lambda = 0,71073 \text{ \AA}$ ) y detector Mercury-CCD, en un rango de  $1,7\text{--}28,1^\circ$  en  $2\theta$ .

## Discusión de resultados

### Difracción de rayos-X en monocrystal

La estructura cristalina de la hidantoína D,L-valina se determinó con métodos directos empleando el programa SHELXS<sup>16</sup> y se refinó mediante cálculos de mínimos cuadrados de matriz completa utilizando el programa SHELXL<sup>17</sup>.

**Tabla 1.** Datos cristalográficos de la hidantoína de D,L-valina obtenidos por difracción de rayos-X de monocrystal.

Código CCDC	2130728	Temperatura (K)	293
Fórmula	C <sub>6</sub> H <sub>10</sub> N <sub>2</sub> O <sub>2</sub>	Radiación (Å)	MoKa (0,71070)
Peso molecular	142.16	Rango en $2\theta$	1,7 - 28,1
Sistema cristalino	Monoclínico	D <sub>cal</sub> (g/cm <sup>3</sup> )	1,290
Grupo espacial	P2 <sub>1</sub> /c (Nº14)	Mu(MoKa) (mm)	0,098
a (Å)	5,493(3)	F(000)	304
b (Å)	23,53(2)	Refl. únicas (R <sub>int</sub> )	1237 (0,065)
c (Å)	6,254(3)	R(F <sup>2</sup> ) [I > 2σ(I)]	0,0746
β (°)	115,09(4)°	wR(F <sup>2</sup> ) [I > 2σ(I)]	0,2119
Volumen (Å <sup>3</sup> )	732,1(9)	S	1,21
Z	4		

La hidantoína D,L-valina cristaliza en una celda monoclinica con grupo espacial centrosimétrico P2<sub>1</sub>/c (Nº14) y 4 unidades fórmula por celda unidad (Z=4). En la figura 4 se muestra la estructura molecular del compuesto. Las elipsoides se dibujaron con una probabilidad del 50% y los átomos de hidrógeno se muestran como esferas con radio arbitrario.

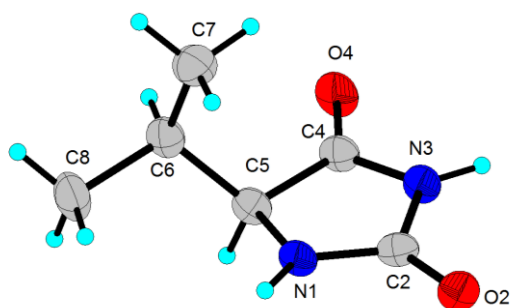


**Fig. 4:** Unidad asimétrica de la hidantoína D,L-valina.

La estructura molecular de la hidantoína D,L-valina está constituida por un anillo heterocíclico de cinco miembros; con dos grupos carbonilos en las posiciones 2 y 4, dos nitrógenos en las posiciones 1 y 3 y sustituido en la posición 5 por un grupo isopropilo. El átomo C5 es un centro quiral, sin embargo, en el arreglo cristalino coexisten la mezcla de enantiómeros D- y L- relacionados por centros de inversión propio del grupo espacial centrosimétrico P2<sub>1</sub>/c.

En el anillo hidantoína, los enlaces C2-N1, C2-N3 y C4-N3, poseen distancias de 1,337(5) Å, 1,389(6) Å y 1,354(6) Å,

Los átomos de hidrógeno se colocaron en posiciones calculadas y tratados usando un modelo rígido con distancias C-H 0,96-0,98 Å y Uiso(H) = 1,2 Ueq(C)], O-H 0,82 Uiso(H) = 1,2 Ueq(O)], N-H 0,86 Å y Uiso(H)= 1,2 Ueq(N)]. Los datos cristalográficos aquí reportados se depositaron en la base de datos Cambridge Crystallographic Data Centre<sup>18</sup> ([www.ccdc.cam.ac.uk](http://www.ccdc.cam.ac.uk)).

En la tabla 1 se muestran los parámetros de celda y figuras de mérito del refinamiento. Los parámetros de celda concuerdan muy bien con los encontrados con difractometría de polvo, lo cual es un indicativo de la homogeneidad de la muestra cristalizada.

siendo estos valores intermedios a las distancias reportadas para un enlace sencillo C-N (1,47 Å) y un enlace doble C=N (1,29 Å). Adicional a esto, el anillo hidantoínico es casi plano, con una ligera desviación del átomo C5, con hibridación sp<sup>3</sup> de 0,117(4) Å por encima del plano conformado por los átomos O2-O4-N1-N3-C2-C4. Estas características evidencian la deslocalización de carga del anillo heterocíclico.

El análisis de los ángulos torsionales de la hidantoína de la D,L-valina a través del enlace C5-C6, muestra que los grupos CH<sub>3</sub> unidos al carbono C6 se encuentran en una posición oblicua con respecto al grupo N-H unido al carbono C5 del anillo hidantoínico, formando un ángulo de torsión de 52,2(5)° para C7-C6-C5-N1 y -74,3(6)° para C8-C6-C5-N1. Esta conformación se comparó con la hidantoína de la L-valina monohidratada reportada<sup>17</sup> encontrando ligeras diferencias en la conformación espacial de estos grupos cuyos ángulos son 58,5(2)° y -67,6(2)°, respectivamente.

El empaquetamiento cristalino de la hidantoína D,L-valina, está estabilizado por interacciones de enlace de hidrógeno del tipo N--H···O y C--H···O, cuyos parámetros geométricos se resumen en la tabla 2. El bloque de construcción básico en empaquetamiento cristalino corresponde a dímeros imida-imida a través de enlaces de hidrógeno del tipo N3--H3···O2 descrito por el grafo R<sub>2</sub>(8), donde enantiómeros D- y L- se relacionan simétricamente por centro de inversión. Estos dímeros se apilan a lo largo del eje c unidos por enlaces de

hidrógeno del tipo N1--H1…O4, descrito con el grafo C(5). La combinación de ambos enlaces construye un macrociclo descrito con el grafo R<sup>4</sup>(16). Este arreglo da lugar a la formación de cintas que se extienden de manera infinita a lo largo del eje *c* y se alternan con regiones hidrofóbicas a lo largo del eje *b* del cristal, tal como se muestra en la figura 5(a).

Adicional a esto, la cintas de dímeros imida-imida se unen a lo largo del eje *a* mediante interacciones de enlace de hidrógeno no convencionales del tipo C5--H5…O2, construyendo

anillos descrito por el grafo R<sup>2</sup>(12), donde O2 actúa como aceptor bifurcado, tal como se observa en la figura 5(b). Este arreglo también es asistido por interacciones del tipo  $\pi\cdots\pi$  con distancia de 3,529(6) Å entre bordes con carga deslocalizada del anillo hidantoína. Este tipo de enlace también se ha encontrado en algunas hidantoínas 5,5-sustituidas como la 5-metil-5-fenilhidantoína<sup>12</sup>, y las tiohidantoínas de la valina<sup>15</sup> y la tirosina<sup>16</sup>, respectivamente. El índice de empaquetamiento (KPI) de la hidantoína D,L-valina es de 66,3% sin espacios intersticiales disponibles para moléculas de solvente.

**Tabla 2.** Parámetros geométricos de los enlaces de hidrógeno presentes en la hidantoína D,L-valina.

D-H…A	D-H (Å)	H…A (Å)	D…A(Å)	D-H…A(°)
N3-H3…O2 <sup>a</sup>	0,860	1,980	2,817(5)	164,0
N1-H1…O4 <sup>b</sup>	0,860	2,060	2,912(5)	171,0
C5-H5…O2 <sup>c</sup>	0,980	2,480	3,295(7)	140,0

Código de simetría: <sup>a</sup> 2-x, 1-y, 2-z; <sup>b</sup> x, y, -1+z; <sup>c</sup> -1+x, y, z.

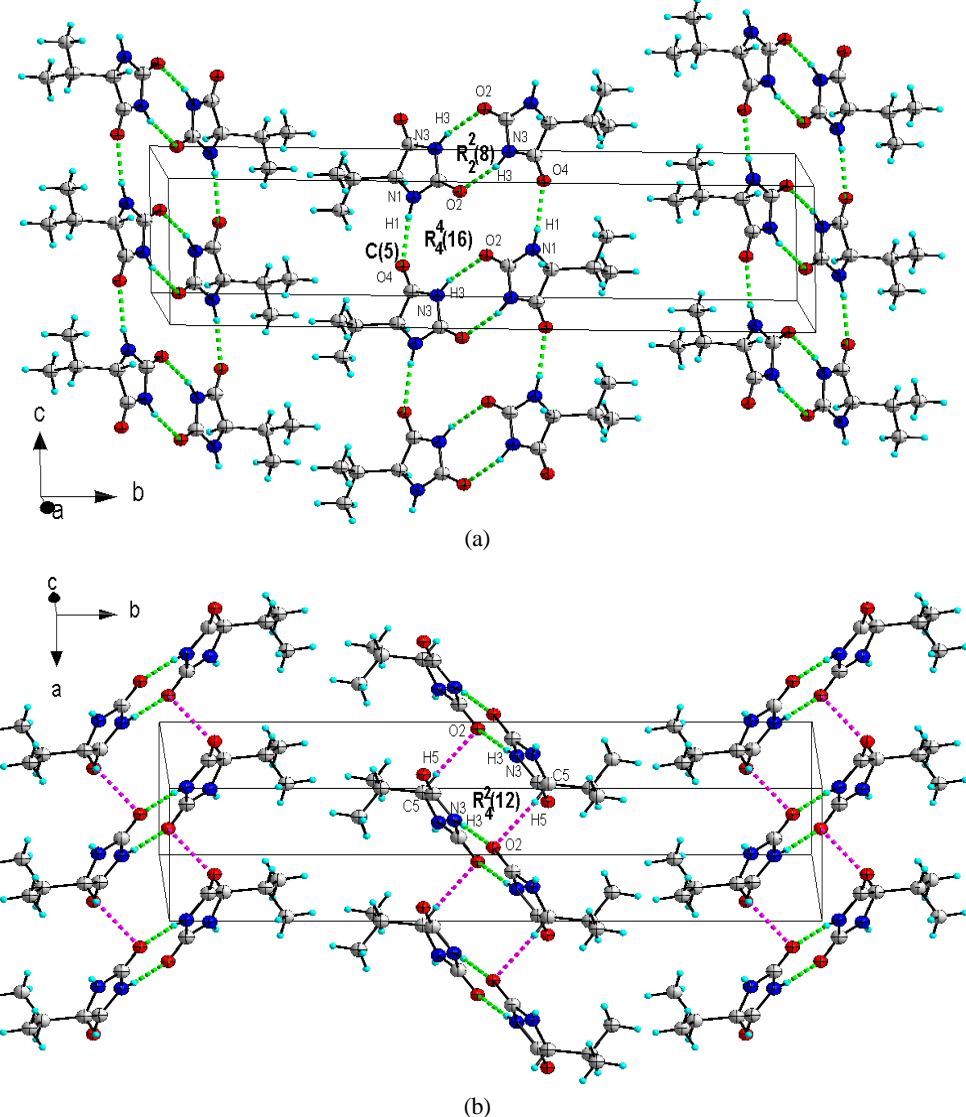
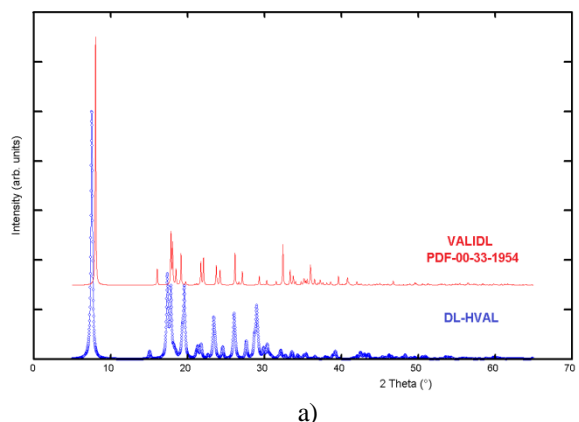


**Fig. 5:** Vista del empaquetamiento cristalino de la hidantoína D,L-valina en (a) el plano *cb* donde la región hidrofólica es estabilizada por enlaces de hidrógeno N3--H3…O2 y N1--H1…O4. (b) la diagonal [102] en la que dímeros imida-imida se apilan por interacciones de enlace de hidrógeno C5--H5…O2 e interacciones  $\pi\cdots\pi$  a lo largo del eje *a*.

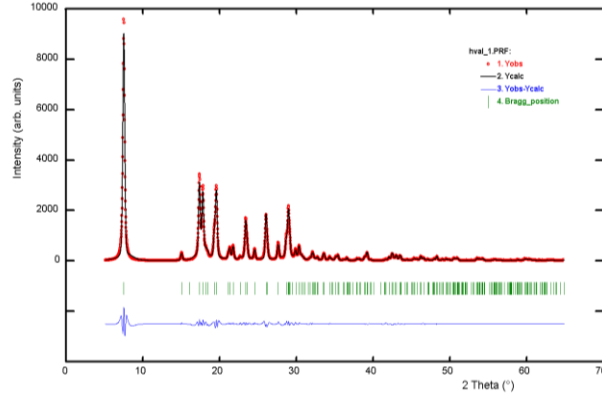
### Difracción de rayos-X en muestras policristalinas (XRPD)

El patrón de difracción indica la presencia de una sola fase (Figura 6a). En esta figura se compara el patrón experimental obtenido con el patrón calculado partiendo de la información de su estructura cristalina reportada en la base de datos de Cambridge (CSD, versión 5.42, septiembre de 2021)<sup>18</sup> para *D,L*-valina (código VALIDL), la cual se corresponde con el patrón de polvo reportado, para el mismo amonoácido, en la base de datos de polvo del ICDD<sup>19</sup> con código PDF-00-033-1954. La diferencia entre los patrones de polvo evidencia la formación de un nuevo compuesto. El indexado del patrón de di-

fracción se realizó utilizando el programa Dicvol06<sup>20</sup>. La hidantoína cristaliza en una celda monoclinica con los parámetros de celda indicados en la tabla 3. Los figuras de mérito  $M_{(20)}$ <sup>21</sup> y  $F_{(20)}$ <sup>22</sup> indican la calidad del indexado. Las celdas obtenidas se refinaron sin modelo estructural por el método de Le Bail<sup>23</sup> utilizando el programa Fullprof<sup>24</sup>. La figura 6b muestra el resultado del refinamiento observándose un buen ajuste entre los patrones observado y calculado para la hidantoína. Las figuras de mérito del refinamiento fueron  $R_{\text{exp}} = 6.69$ ,  $R_p = 7.69$ ,  $R_{\text{wp}} = 8.95$ ,  $S = 1.3$ <sup>24</sup>.



a)



b)

**Fig. 6:** a) Patrón de difracción de la hidantoína *D,L*-valina comparada con la *D,L*-valina y b) Gráfica del ajuste final Le Bail.

**Tabla 3.** Parámetros de celda unidad obtenidos para la hidantoína de *D,L*-valina luego del indexado.

a (Å)	b (Å)	c (Å)	$\beta$ (°)	V (Å <sup>3</sup> )	$M_{(20)}$	$F_{(20)}$
5,4917	23,5226	6,2546	115,09	731,73	35,0	47,1 (0,0048)

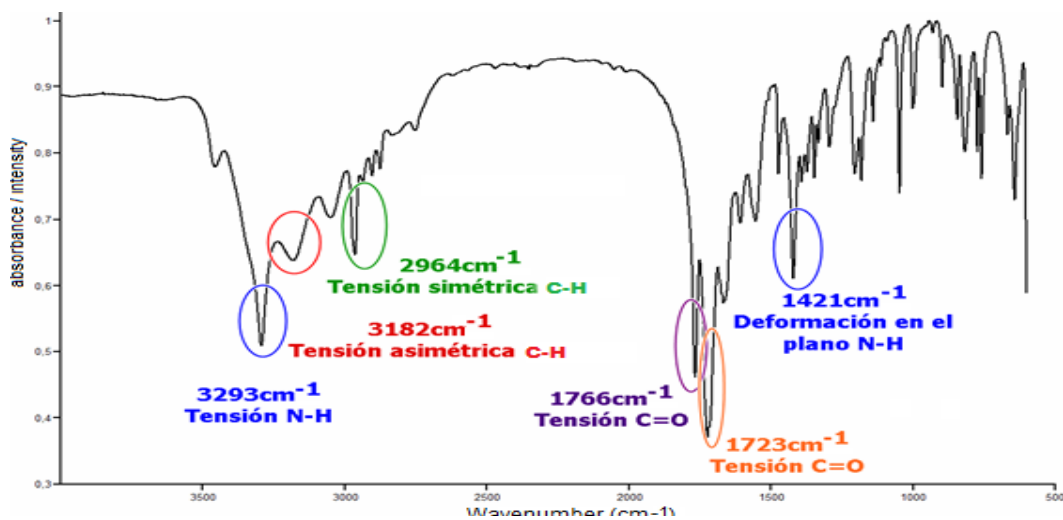


**Fig. 7:** FT-IR espectro del hidantoína *D,L*-valina.

### Espectroscopía infrarroja (FT-IR)

En la figura 7 se observa el espectro FT-IR obtenido para la hidantoína de *D,L*-valina. En el espectro, se identifican las señales de vibración características de los grupos funcionales presentes en el compuesto estudiado.

En la tabla 4 se resumen las bandas de absorción más signifi-

cativas de dicho espectro. Se aprecia la vibración de tensión a 3293 cm<sup>-1</sup> correspondiente al grupo imida N-H ubicado en la posición 3. También se aprecian bandas de absorción que corresponden a vibraciones de tensión asimétrica y simétrica en 3182 cm<sup>-1</sup> y 2964 cm<sup>-1</sup> respectivamente, de los enlaces C-H de los grupos metilo (CH<sub>3</sub>) presentes en la cadena isopropilo.

**Tabla 4.** Asignaciones de las bandas características de la hidantoína *D,L*-valina.

Banda	Frecuencia (cm <sup>-1</sup> )	Asignación
1	3293	Tensión N-H
2	3182	Tensión asimétrica C-H
3	2964	Tensión simétrica C-H
4	1766	Tensión C=O
5	1723	Tensión C=O
6	1421	Deformación N-H en el plano

También se observan las bandas correspondiente a la vibración de tensión de los dos grupos carbonilo C=O de la hidantoína en 1766 cm<sup>-1</sup> y 1723 cm<sup>-1</sup>; la primera se debe al carbonilo sustituido en la posición 4 del anillo, mientras que la de menor frecuencia se debe al carbonilo en la posición 2; el desplazamiento de esta banda a menor frecuencia se debe a la contribución de dos estructura de resonancia con los pares

libres del nitrógeno, haciendo que el doble enlace del carbonilo se debilite alargando la distancia C=O y ensanchando la banda. Además, se aprecia la señal de flexión débil del grupo N-H a una frecuencia de 1421 cm<sup>-1</sup>.

#### Resonancia magnética nuclear (RMN-<sup>1</sup>H y RMN-<sup>13</sup>C)

En la figura 8 se muestran los espectros RMN-<sup>1</sup>H (a) y RMN-<sup>13</sup>C (b) para la hidantoína *D,L*-valina. Se obtuvieron las siguientes señales de desplazamiento químico para RMN-<sup>1</sup>H δ (ppm): N3-H3 imida en 10,0 (s, 1H), N1-H1 urea en 6,0 (s, 1H), C5-H5 metino -CH en 4,52 (d, 1H), C6-H6 isopropilo CH(CH<sub>3</sub>)<sub>2</sub> en 2,65 (m, 1H), C7-H7 y C8-H metilo CH<sub>3</sub> en 0,91 (d, 6H). RMN-<sup>13</sup>C δ (ppm): 156,9 (C4), 173,5 (C2), 57,5 (C5), 30,8 (C6), 18,5 (C7-C8).

Los estudios espectroscópicos confirman el esqueleto molecular de la hidantoína *D,L*-valina.

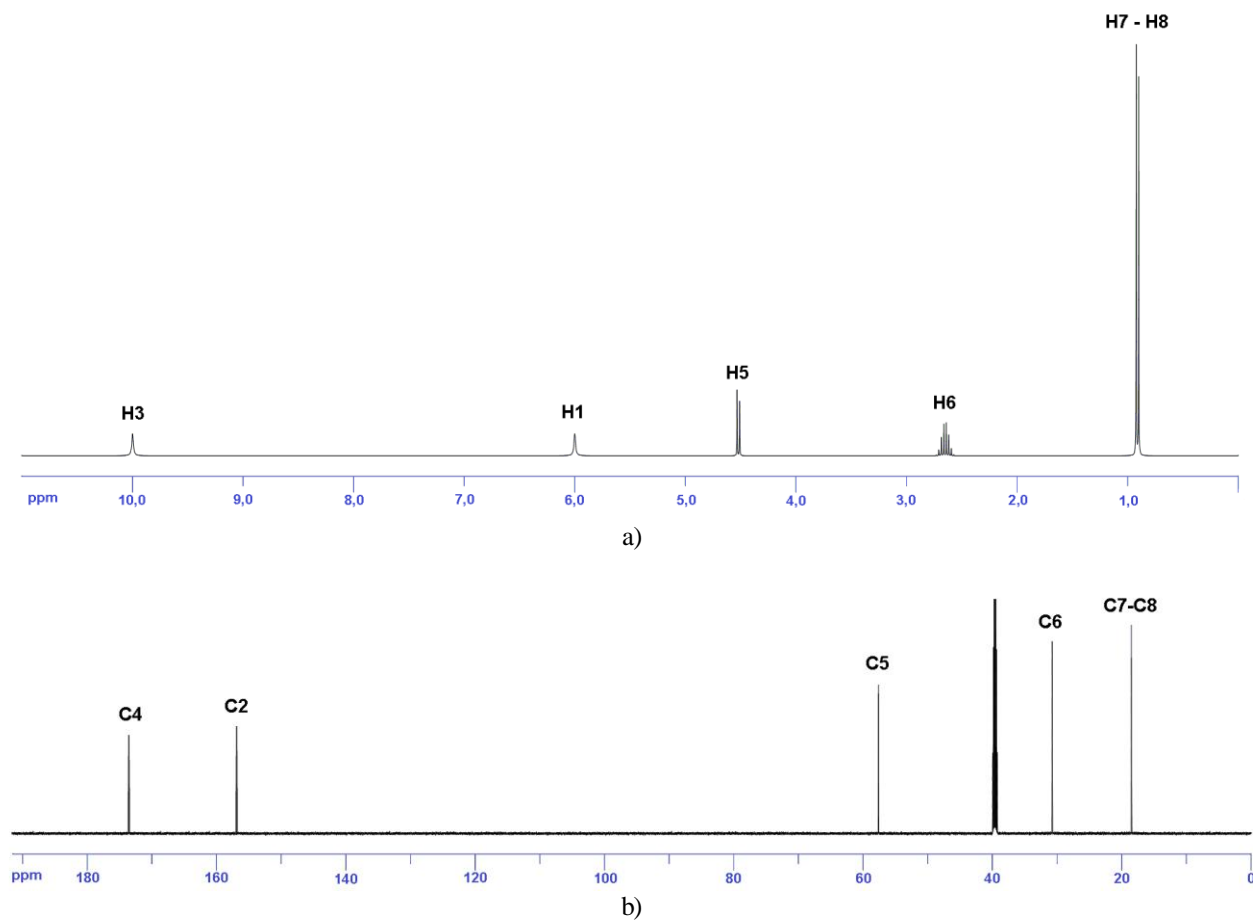


**Fig. 8:** Espectros RMN-<sup>1</sup>H (a) y RMN-<sup>13</sup>C (b) de la hidantoína de *D,L*-valina.

#### Conclusiones

El nuevo compuesto hidantoína de *D,L*-valina se sintetizó mediante la reacción de Bucherer-Bergs. Los datos espectroscópicos permitieron elucidar el esqueleto molecular del compuesto y fueron consistentes con los resultados estructurales. La estructura fue determinada utilizando difracción de rayos-X en monocristal y cristaliza en el sistema monoclínico.

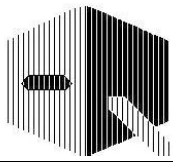
El cristal está conformado por enantiómero *D* y *L* relacionados simétricamente por el centro de inversión asociado al grupo espacial centrosimétrico P2<sub>1</sub>/c. El empaquetamiento cristalino de la hidantoína *D,L*-valina está estabilizado por interacciones de enlaces de hidrógeno del tipo N--H···O y enlaces de hidrógeno no convencionales del tipo C5--H5···O<sub>2</sub>, así como interacciones π···π.

## Agradecimientos

Este trabajo ha sido financiado gracias al CDCHT-ULA y al CONICIT (LAB-97000821).

## Referencias

1. C Avendaño López, G González Trigo. The chemistry of hydantoins, **Adv. Heter. Chem.**, **38**(1), 177-228 (1985).
2. M Meusel, M Güttschow. Recent developments in hydantoin chemistry. A review. **Org. Prep. Proced. Int.**, **36**(5), 391-443 (2004).
3. M Kalník, P Gabko, M Bella, M Koós. The Bucherer–Bergs multicomponent synthesis of hydantoins-excellence in simplicty. **Molecules**, **26**(13), 4024(33) (2021).
4. J Knabe, J Baldauf, A Ahlhem. Racemates and enantiomers of basic, substituted 5-phenylhydantoins, synthesis and antiarrhythmic action. **Pharmazie**, **52**(12), 912-919 (1997).
5. G Singh, PH Driever, JW Sander. Cancer risk in people with epilepsy: the role of antiepileptic drugs. **Brain**, **128**(1), 7-17 (2005).
6. C Carmi, A Cavazzoni, V Zuliani, A Lodola, F Bordi, PV Plazzi, RR Alfieri, PG Petronini, M Mor. 5-Benzylidene-hydantoins as new EGFR inhibitors with antiproliferative activity. **Bioorg. Med. Chem. Lett.**, **16**(15), 4021-4025 (2006).
7. TJ Putnam, HH Merrit. Experimental determination of the anti-convulsant properties of some phenyl derivatives. **Science**, **85**(1), 525-526 (1937).
8. GR Desiraju. Crystal engineering: A brief overview. **J. Chem. Sci.**, **122**(5), 667-675 (2010).
9. T Steiner. The hydrogen bond in the solid state. **Angew. Chem. Int. Ed.**, **41**(1), 48-76 (2002).
10. LE Seijas, GE Delgado, AJ Mora, A Bahsas, J Uzcátegui. Síntesis y caracterización de los derivados N-carbamolio e hidantoína de la L-proolina. **Av. Quím.**, **1**(2), 3-7 (2006).
11. GE Delgado, AJ Mora, JE Contreras, J Bruno-Colmenárez, R Atencio. Synthesis, crystal and molecular structure, and hydrogen-bonding patterns in hydantoin-L-aspartic acid. **Av. Quím.**, **8**(2), 59-63 (2013).
12. GE Delgado, JA Rodríguez, AJ Mora, J Bruno-Colmenárez, J Uzcátegui, C Chacón. Supramolecular structure of 5-methyl-5-phenyl hydantoin and hydrogen-bonding patterns in 5, 5'-substituted hydantoins. **Mol. Cryst. Liq. Cryst.**, **629**(1), 96-104 (2016).
13. GE Delgado, AJ Mora, LE Seijas, R Almeida, C Chacón, L Azotla-Cruz, J Cisterna, A Cárdenas, I Brito. N-acetyl-5-isopropyl-2-tioxoimidazolidin-4-one: Synthesis, spectroscopic characterization, crystal structure, DFT calculations, Hirshfeld surface analysis and energy framework study. **J. Mol. Struct.**, **1219**(1), 128630(13) (2020).
14. GE Delgado, AJ Mora, LE Seijas, L Rincón, G Marroquin, J Cisterna, A Cárdenas, I Brito. Combined DFT calculation, Hirshfeld surface analysis, and Energy framework study of non-covalent interactions in the crystal structure of (Z)-5-ethylidene-2-thiohydantoin determined by powder X-ray diffraction. **J. Mol. Struct.**, **1236**(1), 130361 (11) (2021).
15. GE Delgado, AJ Mora, P Narea, C Chacón, G Marroquin, B Hernández, J Cisterna, I Brito. Synthesis, crystal structure, hydrogen bond patterns and Hirshfeld surface analysis of (S)-5-(4-hydroxybenzyl)-imidazolidine-2,4-dione. **J. Mol. Struct.**, **1250**(1), 131757 (7) (2022).
16. GM Sheldrick. A short history of SHELX. **Acta Cryst.**, **A64**(1), 112-122 (2008).
17. GM Sheldrick. Crystal structure refinement with SHELXL, **Acta Cryst.**, **C71**(1), 3-8 (2015).
18. CR Groom, IJ Bruno, MP Lightfoot, SC Ward. The Cambridge structural database. **Acta Cryst.**, **B72**, 171-179 (2016).
19. International Centre for Diffraction Data. PDF-ICDD-Powder Diffraction File (Set 1-71). Newtown Square: International Centre for Diffraction Data (2019).
20. A Boultif, D Löuer. Powder pattern indexing with the dichotomy method. **J. Appl. Cryst.**, **37**, 724-731 (2004).
21. PM de Wolff. A simplified criterion for the reliability of a powder pattern indexing. **J. Appl. Cryst.**, **1**, 108-113 (1968).
22. GS Smith, RL Snyder.  $F_N$ : A criterion for rating powder diffraction patterns and evaluating the reliability of powder-pattern indexing. **J. Appl. Cryst.**, **12**, 60-65 (1979).
23. A Le Bail. Whole powder pattern decomposition methods and applications: A retrospection. **Powder Diffr.**, **20**, 316-326 (2005).
24. J Rodriguez-Carvajal. Fullprof, versión 7.40, LLB, CEA-CNRS, France (2021).



# Capacidad base o inicial de retención de fósforo en un suelo soporte de un establecimiento de engorde a corral

Ileana Cecilia Ciapparelli\*, Alicia Rosa Fabrizio de Iorio, Ana Rosa García

Facultad de Agronomía, Universidad de Buenos Aires (UBA), Av. San Martín 4453, CP 1417,  
Ciudad Autónoma de Buenos Aires, Buenos Aires, Argentina.

(\*) [ciappare@agro.uba.ar](mailto:ciappare@agro.uba.ar)

Recibido: 03/11/2021

Revisado: 07/12/2021

Aceptado: 23/12/2021

## Resumen

Con el propósito de determinar la capacidad base o inicial de retención de fósforo en un suelo Argialbol, soporte de un establecimiento de engorde intensivo de Argentina, se tomaron muestras del mismo en profundidad y se analizaron sus características. Se realizaron ensayos de isotermas de adsorción de fósforo y los modelos de Langmuir, Freundlich, Temkin y Dubinin-Radushkevich fueron ajustados a los datos experimentales. Los tres horizontes superiores presentaron partículas con sitios de mayor afinidad y energía de enlace que las de los horizontes profundos. Se demostró una adsorción favorable en todo el perfil, influenciada principalmente por variables como materia orgánica, arcilla y potasio.

**Palabras clave:** arcilla; fósforo; isotermas de adsorción; materia orgánica; suelo

## Abstract

**Background capacity of phosphorus retention in a supporting soil of a feedlot.** In order to determine the background capacity of phosphorus retention on an Argialboll soil, of a feedlot from Argentina, samples of it were taken in depth and its properties were analyzed. Phosphorus adsorption isotherms were performed and the Langmuir, Freundlich, Temkin and Dubinin-Radushkevich models were fitted to the experimental data. Particles with higher affinity and binding energy sites were exhibited for the three upper horizons than those of the lower horizons. A favorable adsorption was demonstrated throughout the profile. Clay, organic matter and potassium were some of the main parameters influencing the process.

**Keywords:** Adsorption isotherms; Clay; Organic matter; Phosphorus; Soil

## Introducción

Es ampliamente difundido que la producción intensiva de ganado bovino (*feedlot*) aporta un gran volumen de estiércol sólido y líquido, y que uno de sus principales componentes es el fósforo (P). Cuando estos residuos son depositados en el suelo, el exceso de P puede migrar hacia cursos de agua superficiales, y/o perderse verticalmente alcanzando la napa freática. En los cursos superficiales de agua, el enriquecimiento con P favorece el proceso de eutrofificación, generando efectos adversos que limitan su funcionamiento ecosistémico.

Para evitar los procesos de eutrofificación derivados de las actividades de engorde a corral y para cumplimentar con las normativas vigentes nacionales<sup>1</sup> e internacionales<sup>2,3</sup> relacionadas con la preservación del ambiente, se vienen realizando investigaciones para comprender las vías, los procesos y mecanismos que determinan el movimiento de fósforo hacia los cursos de agua.

La transferencia de P mediante escorrentía superficial y subsuperficial desde el estiércol hacia cuerpos de agua ha sido ampliamente investigada<sup>4-9</sup>, en tanto que las pérdidas de P a través de la matriz del suelo y por caminos preferenciales se han estudiado en menor grado. Considerando que en la región

Pampa Ondulada la napa freática se interconecta con los cursos superficiales dentro de una gran red hidrológica, el movimiento vertical de P en el suelo merece atención dado que gobierna el traslado de P hacia la napa<sup>10</sup> influyendo indirectamente en el proceso de eutrofificación.

La migración de P dentro del suelo se ve condicionada tanto por su propia movilidad como por las características del medio en el que se encuentra, pudiendo ser evaluada mediante procesos de transporte de solutos y procesos de intercambio y transformación<sup>11,12</sup>. Los procesos de intercambio y transformación son aquellos que involucran reacciones físicas, químicas y/o biológicas que determinan la liberación, retención, degradación y/o pérdida de un contaminante en el suelo. Ejemplos de ellos son los procesos de sorción-desorción, disolución-precipitación, inmovilización-mineralización, reacciones ácido-base, de óxido-reducción, complejación iónica y filtración física<sup>13</sup>.

Los mecanismos de sorción-desorción son los que participan más activamente en la retención-liberación de este nutriente a la solución del suelo. Dichos mecanismos dependen entre otros factores de: la concentración de fosfatos y de P orgánico en la solución del suelo, la presencia de óxidos de hierro y aluminio y de carbonato de calcio, el pH, las condiciones

redox y el contenido de arcilla<sup>14,15</sup>. La materia orgánica (MO) incorporada con el estiércol determina que la concentración de ácidos orgánicos también sea otro factor de importancia a tener en cuenta<sup>16-18</sup>.

El estudio de la capacidad de sorción de P de un suelo permite entender qué capacidad tiene ese suelo para retener al nutriente y frenar así su salida del sistema. Las isotermas de adsorción permiten cuantificar la adsorción de P sobre la matriz del suelo a temperatura y presión constante, a través de la relación entre la cantidad del soluto sorbido y la concentración en el equilibrio del mismo<sup>19</sup>. La fórmula general de las isotermas explica que cuanto mayor sea la superficie ocupada con P adsorbido, menor será la energía con que ese P es retenido por el sorbente<sup>20</sup>. A partir de las isotermas también se puede cuantificar la máxima capacidad de retención que permite estimar el grado de saturación de ese suelo con el nutriente<sup>18</sup>.

El riesgo potencial de contaminación de un curso de agua superficial y/o subterránea puede ser evaluado considerando la vulnerabilidad del medio y la carga del contaminante presente<sup>21</sup>. Mientras los residuos generados por los establecimientos de engorde a corral (EEC) se caracterizan por tener una alta carga de P, la vulnerabilidad de cada ambiente es sitio-específica y necesita ser considerada en forma particular. Por consiguiente, en un sitio sobre el cual se asienta o se asentará un EEC uno de los primeros aspectos a diagnosticar es la capacidad de retención química de nutrientes del suelo y, en este caso específico de P, para luego elaborar estrategias de manejo de los residuos. El objetivo entonces fue determinar la capacidad base o inicial de retención de fósforo (también llamada capacidad *background*) en un suelo Argialbol, soporte de un EEC de la Pampa ondulada (Argentina), y estimar las variables edáficas que la favorecen. Esta información servirá como precedente en trabajos subsiguientes, en los cuales se espera evaluar cómo se ve afectada dicha capacidad cuando el suelo recibe aplicaciones de estiércol bovino.

## Materiales y métodos

### Área de estudio

El estudio se realizó en un EEC de Argentina, ubicado en la provincia de Buenos Aires dentro de la región Pampa Ondulada. La principal actividad de este establecimiento es el engorde intensivo de bovinos a corral, principalmente de las razas Bradford y Brangus. Desde hace alrededor de 20 años mantiene una producción con una capacidad de hasta 12000 animales por ciclo productivo. En cuanto a sus instalaciones,

además de los corrales, cuenta con: lagunas, parcelas destinadas a la producción agrícola y forrajera, y con parcelas destinadas al apilamiento del estiércol sólido cuando es removido de los corrales, entre otras áreas.

Los datos meteorológicos provistos por la Estación Meteorológica Ezeiza AERO (Lat. -34°49' Long. -58°32') del Servicio Meteorológico Nacional<sup>22</sup> para el período 1981-2010 indicaron una temperatura media anual de 16,7°C y una precipitación anual media de 1020 mm.

La unidad taxonómica dominante del suelo en estudio es el Argialbol típico cuyo rasgo característico es la presencia de al menos un horizonte iluvial Bt. Según la carta de suelos<sup>23</sup> los principales horizontes que lo conforman son: A (0-30 cm), E (30-40 cm), 2Bt1 (40-90 cm, en adelante Bt1), 2Bt2 (90-140 cm, en adelante Bt2), 3BCt (140-180 cm, en adelante BCt).

### Muestreo

Dentro del EEC se seleccionó una superficie destinada a la producción de forraje, que no recibió influencia de estiércol ni de efluentes. Allí se definieron cinco puntos de muestreo equidistantes entre sí (a más de 50 m), constituyendo cada uno de ellos una réplica.

La recolección de muestras se realizó en forma sistemática, cada 10 cm desde la superficie hacia los horizontes más profundos; los estratos 80-90 cm, 150-160 cm y 160-170 cm no se muestrearon dado que sus características morfológicas se veían representadas por los demás estratos del horizonte al que pertenecían cada uno. Las muestras se acondicionaron en bolsas plásticas, se rotularon y llevaron al laboratorio. Luego se dejaron secar al aire, se molieron y tamizaron utilizando una malla de 2 mm de diámetro. Finalmente se las conservó en bolsas plásticas para posteriores análisis.

### Caracterización del suelo

Para determinar la capacidad de retención de fosfatos del suelo del EEC fue necesario establecer previamente las propiedades físicas y químicas del mismo. Las variables pH, P Bray, carbono orgánico (CO), nitrógeno Kjeldahl (NKj), carbonato de calcio equivalente ( $\text{CaCO}_3$  Eq), cationes intercambiables ( $\text{Na}^+$ ,  $\text{K}^+$ ,  $\text{Ca}^{2+}$ ,  $\text{Mg}^{2+}$ ), capacidad de intercambio catiónico (CIC) y conductividad eléctrica (CE) fueron medidas siguiendo métodos estandarizados<sup>24-25</sup>, en el laboratorio de la cátedra de Química Inorgánica y Analítica de la Facultad de Agronomía de la Universidad de Buenos Aires (FAUBA). En la tabla 1 se presentan algunas de las características analizadas.

**Tabla 1.** Características físicas y químicas de los horizontes del perfil del suelo (valores medios junto a sus desvíos estándar).

Variable	Horizonte Profundidad (cm)	A (0-30)	E (30-40)	Bt1 (40-90)	Bt2 (90-140)	BCt (140-180)
pH (en agua 1:2,5)		5,8±0,6	6,7±0,8	7,0±1,0	7,6±0,8	7,1±0,1
CE (mS.cm <sup>-1</sup> )		0,36±0,19	0,38±0,25	0,59±0,24	0,54±0,15	0,41±0,02
CO (%)		1,80±0,43	0,63±0,34	0,56±0,20	0,29±0,16	0,31±0,05
P Bray (mg.kg <sup>-1</sup> )		6,5±5,2	2,3±1,8	2,1±1,6	2,0±1,2	2,9±0,5
n*		15	5	19	12	2

\* El número de muestras depende de las réplicas y del espesor de cada horizonte muestreado. En algunos casos no se pudo contar con réplicas como en BCt.

**Tabla 2.** Clases texturales, composición de roca total, de la mineralogía de la fracción arcilla y contenido de hierro y aluminio del perfil del suelo.

Horizonte	Textura	Roca Total						Filosilicatos			Fe	Al
		Qz	Fel K	Pl	Fil	Afb	Amf	Sm	I/M	C	g.100g <sup>-1</sup>	
A	FL	xxx	x	xx	xx	x	xx	xxx	xxx	x	2,13	4,03
E	FL	xxx	x	xx	xx	x	xx	-	xxx	xx	2,34	4,10
Bt1	AL	xxx	x	xx	xx	x	xx	xxx	xx	x	4,66	9,73
Bt2	FAL	xxx	x	xx	xx	x	xx	xxx	xx	x	4,03	8,39
BCt	AL	xxx	x	xx	xx	x	xx	xxx	xx	x	4,34	7,50

FL: franco limosa; AL: arcillo limosa; FAL: franco arcillo limosa. Qz: cuarzo; Fel K: feldespatos potásicos; Pl: plagioclasas; Fil: filosilicatos; Afb: anfibol; Amf: amorfos; Sm: esmectita; I/M: illita/mica; C: caolinita. Contenido relativo: xxx: mayoritario; xx: minoritario; x: accesorio.

Asimismo, en la tabla 2 se presenta la textura de los horizontes<sup>23</sup>. El contenido de arcilla, limo y arena fue analizada por el método hidrométrico de Bouyoucos<sup>24</sup> en la FAUBA.

El estudio mineralógico por difracción de rayos X (difractómetro marca Philips, modelo X'Pert MPD, con tubo de rayos X de cobre, goniómetro vertical theta/2theta, monocromador secundario curvo de grafito) fue realizado por el instituto SEGEMAR (Servicio Geológico Minero Argentino), y también se presenta en la tabla 2. En la composición mineralógica el contenido de filosilicatos dentro de la fracción de roca total es minoritario. La esmectita es un filosilicato que se expande libremente bajo condiciones de hidratación y deshidratación, y su espesor de capa varía de acuerdo al catión de intercambio y al grado de solvatación del espacio entre capas<sup>19</sup>. La illita es dominante en el loess pampeano<sup>27</sup> y el menor contenido de illita/mica en horizontes Bt pudo deberse a la argiluviaación y neoformación de arcilla esmectítica a partir de illita<sup>28</sup>. El escaso contenido de caolinita es propio de suelos de pradera de región templada<sup>28</sup>. El análisis del contenido de Fe y de Al recuperable, que incluye a sus respectivos óxidos amorfos (espectrometría de emisión atómica por plasma inductivo previa digestión débil bajo norma EPA 3050<sup>26</sup>) también fue realizado por el SEGEMAR y se observa en la tabla 2.

#### Ensayo de isotermas de adsorción

Para determinar la capacidad de retención de P del suelo se realizó un ensayo de isotermas de adsorción. Para ello, se analizó la concentración de P en la solución de equilibrio (C) por colorimetría a 680 nm, y se construyeron las isotermas trazando la cantidad de fosfato sorbida (Q) en función de la concentración en el equilibrio (C).

Las isotermas fueron conducidas por una modificación de la técnica estándar propuesta por Nair *et al.* (1984)<sup>29</sup>. Se agitó 1 g de suelo con solución KNO<sub>3</sub> (0,03 M) que contiene fósforo en una concentración definida, en una relación suelo:solución de 1:10. Las concentraciones de P agregadas abarcaron un rango desde 6 hasta 155 mg P.L<sup>-1</sup> como KH<sub>2</sub>PO<sub>4</sub>, considerando que el proceso de adsorción se da a bajas concentraciones<sup>30,31</sup>.

Para mantener la fuerza iónica de la solución de equilibrio se trabajó con solución de KNO<sub>3</sub>. El estado de equilibrio se logró al cabo de 24 hs de agitación. Posteriormente se centrí-

fugó y filtró con filtro de 0,45 µm. En el filtrado se analizó la concentración de P en la solución de equilibrio (C), por colorimetría a 680 nm a partir del método de azul de molibdeno<sup>32</sup>.

Los ensayos fueron conducidos por triplicado manteniendo el valor de pH original del suelo, a 25°C. De esta manera, se contemplaron las principales variables que condicionan la adsorción: tiempo, concentración de P, temperatura y pH del medio<sup>33</sup>; relación suelo:solución, fuerza iónica y catión interviniente, entre otros<sup>29</sup>. No se utilizó cloroformo para inhibir el crecimiento microbiano puesto que al producir la lisis celular puede incrementar la concentración de P disuelto en el sobrenadante, y porque así se representa mejor el ambiente natural<sup>34</sup>.

Las isotermas fueron construidas trazando la cantidad de fosfato sorbida (Q) en función de la concentración en el equilibrio (C) para estratos del suelo de 10 cm de espesor, desde la superficie hasta los 180 cm de profundidad; los ensayos de los estratos 80-90 cm, 150-160 cm y 160-170 cm no se realizaron debido a que no fueron muestreados.

#### Análisis de datos

Los datos fueron analizados utilizando estadística descriptiva e inferencial, mediante el software InfoStat<sup>35</sup>. Para evaluar la presencia de diferencias significativas se realizaron análisis de varianza ( $\alpha=0,05$ ), y la comparación de medias se hizo con el test de Tukey ( $\alpha=0,05$ ).

Se aplicaron modelos matemáticos a los valores experimentales de las isotermas de adsorción, y se utilizó análisis de regresión lineal para evaluar el ajuste de los datos observados sobre los predichos. Para explicar la relación entre los parámetros de los modelos se realizaron análisis de correlación (Pearson) con un nivel de significancia de  $\alpha=0,05$ , previo descarte de aquellas relaciones en las que se detectó presencia de multicolinealidad y de aquellos parámetros que no presentaron diferencias significativas a lo largo del perfil.

Para estimar comportamientos de los parámetros de los modelos de las isotermas se establecieron ecuaciones de regresión lineal múltiple utilizando como variables predictoras las características edáficas relacionadas con la adsorción de P. Las ecuaciones fueron seleccionadas mediante el procedimiento *Stepwise*, con un valor de  $\alpha=0,30$  para ingresar y  $\alpha=0,10$  para retener variables. Se establecieron

así ecuaciones con mínimo cuadrado medio del error, máximo ajuste, mínimo sesgo posible y sin efectos de multicolinealidad.

#### Ajuste a modelos predictivos

Los datos obtenidos mediante las isotermas fueron ajustados a los modelos de Langmuir, Freundlich, Temkin y Dubinin-Radushkevich.

Langmuir<sup>19,34,36,37</sup>:

$$Q = \frac{k_L \cdot C \cdot Q_{max}}{1 + k_L \cdot C} \quad \text{Ec. 1}$$

que se expresa linealmente:

$$\frac{C}{Q} = \frac{1}{k_L \cdot Q_{max}} + \frac{C}{Q_{max}} \quad \text{Ec. 2}$$

donde: C= concentración de P en el equilibrio, después de 24 hs de incubación,  $\mu\text{g.ml}^{-1}$ ; Q= cantidad de fósforo total sorbido por la fase sólida,  $\mu\text{g.g}^{-1}$ ;  $k_L$ = constante relacionada con la fuerza de enlace,  $\text{ml.}\mu\text{g}^{-1}$ ;  $Q_{max}$ = cantidad máxima de P que puede adsorberse,  $\mu\text{g.g}^{-1}$ .

Los supuestos de este modelo (Langmuir<sup>19,34,36,37</sup>) indican que: 1) La energía de adsorción es constante, independientemente del grado de la superficie cubierta (considera una superficie homogénea); 2) La adsorción se produce en sitios específicos, sin interacción entre las moléculas adsorbidas; 3) La máxima adsorción se produce cuando se forma una capa monomolecular completa sobre todas las superficies adsorbentes y reactivas; 4) La adsorción se produce principalmente por quimiosorción. Con los parámetros  $Q_{max}$  y  $k_L$  también se puede calcular la máxima capacidad buffer de fosfatos (MCBP), como estableció Kuo en 1991<sup>38</sup>, cuyas unidades se expresan en  $\text{ml.g}^{-1}$  de P:

$$MCBP = Q_{max} \cdot k_L \quad \text{Ec. 3}$$

y el factor de separación, R, que es la distancia entre la superficie del sorbente y el sorbato, utilizando la concentración inicial de P agregada (C0):

$$R = \frac{1}{1 + (1 + k_L \cdot C_0)} \quad \text{Ec. 4}$$

Freundlich<sup>19,37,39,40</sup>:

$$Q = k_F \cdot C^{1/n} \quad \text{Ec. 5}$$

que se expresa linealmente:

$$\log Q = \frac{1}{n} \cdot \log C + \log k_F \quad \text{Ec. 6}$$

donde: C= concentración de P en el equilibrio, después de 24 hs de incubación,  $\mu\text{g.ml}^{-1}$ ; Q= cantidad de fósforo total sorbido por la fase sólida,  $\mu\text{g.g}^{-1}$ ;  $k_F$ = constante relacionada con la capacidad de retención de P; es la cantidad de P adsorbido por el suelo cuando C= 1,  $\text{ml.g}^{-1}$ ; n= constante relacionada con la afinidad entre el adsorbente y el adsorbato; adimensional.

Los supuestos de este modelo (Freundlich<sup>19,37,39,40</sup>) indican que: 1) La energía de adsorción no es constante, depende del grado de la superficie cubierta (considera una superficie hete-

rogénea); 2) La adsorción se produce en sitios específicos, con interacción entre las moléculas adsorbidas; 3) Se puede aplicar a modelos multicapa.

Temkin<sup>37,39,41-44</sup>:

$$Q = B \cdot \ln(A \cdot C) \quad \text{Ec. 7}$$

que se expresa linealmente:

$$Q = k_T + B \cdot \ln C \quad \text{Ec. 8}$$

$$\text{siendo } k_T = B \cdot \ln A \quad \text{Ec. 9}$$

$$\text{con } B = \frac{R \cdot T}{b} \quad \text{Ec. 10}$$

$$\text{y con } \ln A = \frac{-\Delta G^\circ}{R \cdot T} \quad \text{Ec. 11}$$

donde: C= concentración de P en el equilibrio, después de 24 hs de incubación,  $\mu\text{g.ml}^{-1}$ ; Q= cantidad de fósforo total sorbido por la fase sólida,  $\mu\text{g.g}^{-1}$ ;  $k_T$ = constante de Temkin, es la cantidad de P adsorbido por el suelo cuando C= 1; B= constante relacionada con el calor de adsorción; es la intensidad de la adsorción, es decir, la capacidad de retención del P adsorbido; adimensional; A= constante de unión relacionada a la máxima energía de enlace en el equilibrio,  $\text{ml.}\mu\text{g}^{-1}$ ; R= constante universal de los gases,  $8,314 \text{ J.K}^{-1} \cdot \text{mol}^{-1}$ ; T= temperatura absoluta en grados Kelvin. Condiciones del experimento: 25°C; b= entalpia de adsorción,  $\text{J.mol}^{-1}$ ;  $\Delta G^\circ$ = variación de la energía libre de Gibbs,  $\text{J.mol}^{-1}$ .

Los supuestos de este modelo (Temkin<sup>37,39,41-44</sup>) indican que: 1) La distribución de las energías de enlace es uniforme hasta alcanzar un valor máximo; 2) El calor de adsorción decrece linealmente al aumentar la superficie que se recubre (considera una superficie heterogénea), debido a la repulsión entre el adsorbato y el adsorbente. A partir de los parámetros estimados en el modelo se puede calcular la concentración de P en el equilibrio (C) cuando el P adsorbido Q= 0 (CPE0).

Dubinin-Radushkevich (DR)<sup>36,37,45,46</sup>:

$$Q = Q_{max,DR} \cdot e^{(-k_{DR} \cdot \varepsilon^2)} \quad \text{Ec. 12}$$

que se expresa linealmente:

$$\ln Q = \ln Q_{max,DR} - k_{DR} \cdot \varepsilon^2 \quad \text{Ec. 13}$$

$$\text{siendo } \varepsilon = R \cdot T \cdot \ln(1 + 1 \cdot C^{-1}) \quad \text{Ec. 14}$$

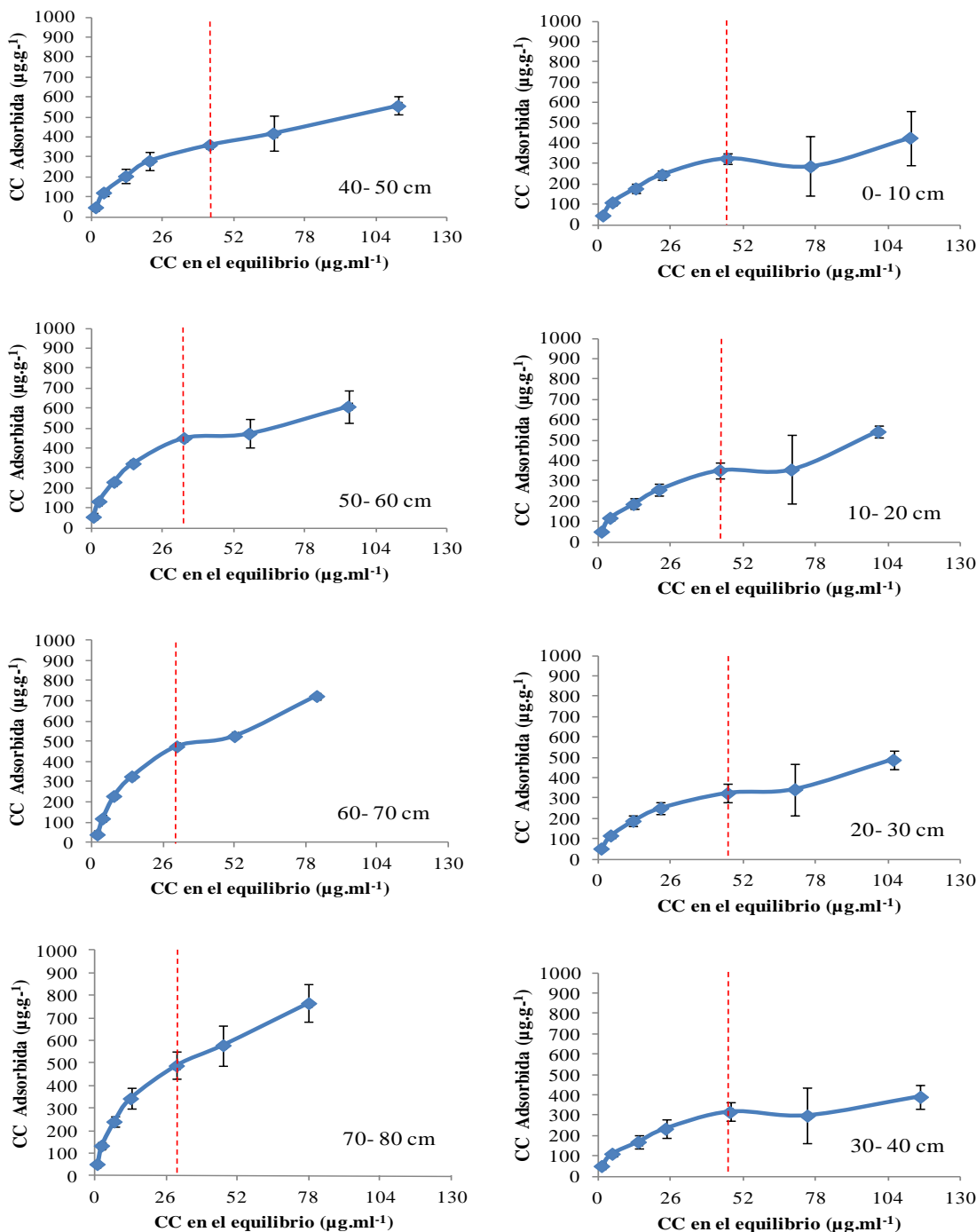
donde: C= concentración de P en el equilibrio, después de 24 hs de incubación,  $\mu\text{g.ml}^{-1}$ ; Q= cantidad de fósforo total sorbido por la fase sólida,  $\mu\text{g.g}^{-1}$ ;  $Q_{max,DR}$ = capacidad de saturación de una monocapa,  $\mu\text{g.g}^{-1}$ ;  $k_{DR}$ = coeficiente de actividad relacionada con la energía de adsorción,  $\text{mol}^2 \cdot \text{J}^{-2}$ ;  $\varepsilon$ = potencial de adsorción para solutos poco solubles en superficies sólidas microporosas de Polanyi; R= constante universal de los gases,  $8,314 \text{ J.K}^{-1} \cdot \text{mol}^{-1}$ ; T= temperatura absoluta en grados Kelvin. Condiciones del experimento: 25°C.

Los supuestos de este modelo (Dubinin-Radushkevich<sup>36,37,45,46</sup>) indican que: 1) La energía de adsorción no es constante (considera una superficie heterogénea); 2) El adsor-

bente tiene una estructura porosa bien desarrollada; los más relevantes son los microporos; 3) La adsorción se produce en multicapas. Este modelo es frecuentemente utilizado para distinguir si el fenómeno de adsorción es físico o químico a través del cálculo de la energía media de adsorción ( $E$ ) por molécula de adsorbato.  $E$  representa la energía liberada cuando se remueve una molécula adsorbida de una ubicación espacial en el adsorbente y se calcula como:

$$E = 1 \cdot (\sqrt{-2k_{DR}})^{-1} \quad \text{Ec. 15}$$

donde:  $k_{DR}$ = constante de la isoterma,  $\text{mol}^2 \cdot \text{J}^{-2}$ ;  $E$ = energía media de adsorción,  $\text{J} \cdot \text{mol}^{-1}$ .



## Resultados y discusión

### Capacidad de adsorción del suelo

A partir del ensayo de adsorción de P se construyeron las isotermas que se observan en las figuras 1 y 1 bis. Puede apreciarse en todos los estratos que la concentración adsorbida tiene un comportamiento ascendente ante el incremento de la concentración en la solución de equilibrio. Asimismo, el cálculo de la derivada de la función en distintos puntos de la curva permitió hallar, en la mayoría de los estratos, que su valor mínimo se alcanzaba cuando la concentración de P en el equilibrio se encontraba entre 30 y 47 µg.ml⁻¹. Ese valor per-

**Fig. 1:** Isotermas de adsorción de P en el suelo. Línea punteada: punto de la curva de mínima pendiente de la recta tangente. CC: Concentración.

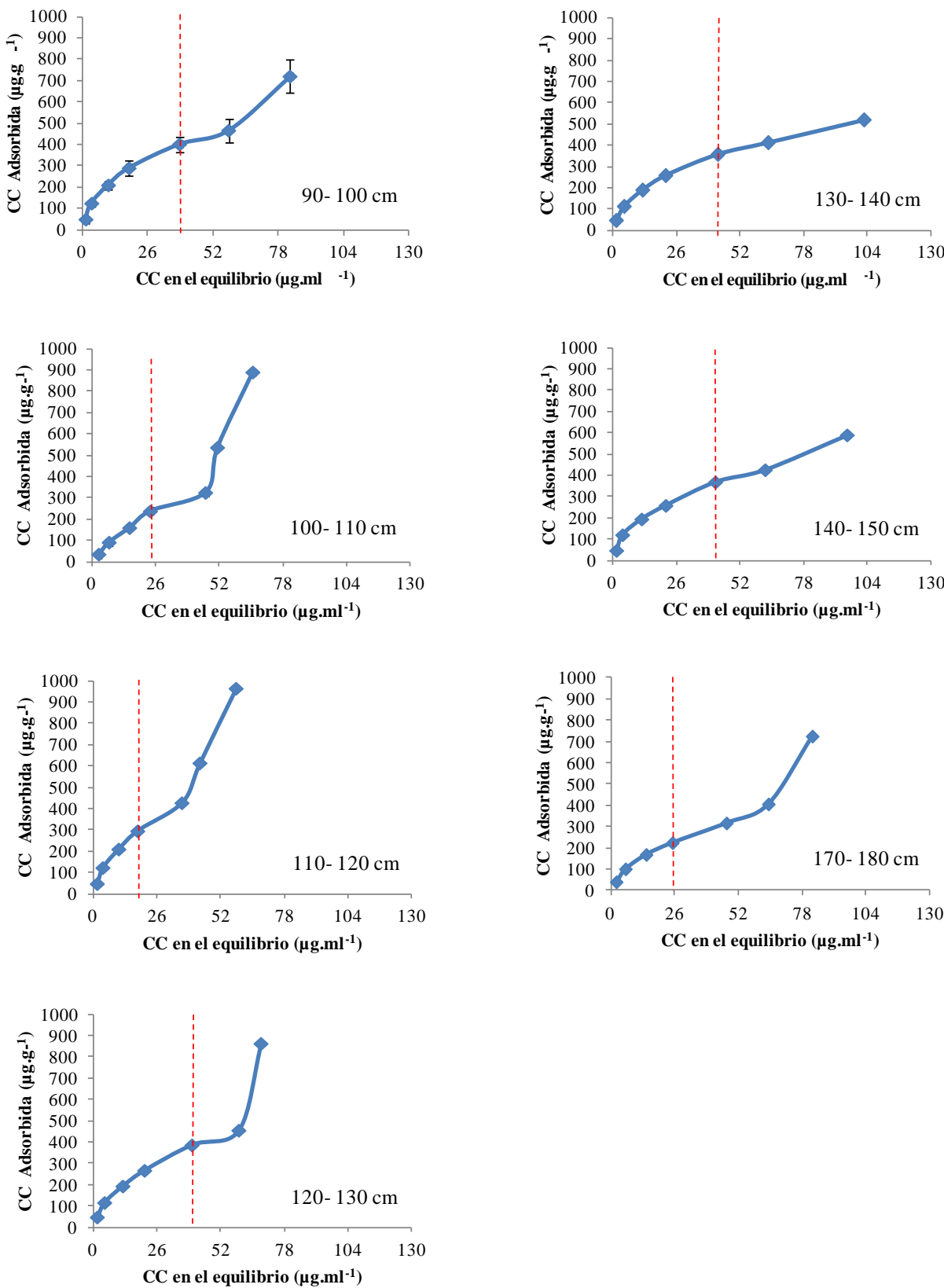


**Fig. 1 bis:** Isotermas de adsorción de P en el suelo. Línea punteada: punto de la curva de mínima pendiente de la recta tangente. CC: Concentración.

mitió delimitar (línea punteada en la figura 1) dos zonas en el gráfico: una previa a la línea donde los datos de la concentración adsorbida se incrementaron logarítmicamente y presentaron menor variabilidad (CV 1-21%); y una posterior a la línea donde los datos se incrementaron exponencialmente, con

mayor variabilidad (CV 5-51%). Según Sui y Thompson (2000)<sup>47</sup> citando a Larsen (1967)<sup>48</sup>, valores iguales o superiores a 20  $\mu\text{g} \cdot \text{ml}^{-1}$  de P en el equilibrio estarían favoreciendo las reacciones de precipitación antes que las de adsorción a la hora de remover el P de la solución, explicando así los dife-

rentes comportamientos observados desde la línea punteada, tanto en contenido como en variabilidad. Al respecto, García *et al.* (2006)<sup>49</sup> en un suelo Argiudol de la región pampeana determinaron que por debajo de 29  $\mu\text{g.ml}^{-1}$  de P en equilibrio, semejante a los hallados en este estudio (30 a 47  $\mu\text{g.ml}^{-1}$ ), se establecen predominantemente los procesos de adsorción.

Los datos experimentales fueron a su vez ajustados a los modelos de Langmuir, Freundlich, Temkin y Dubinin-Radushkevich (DR), cuyos parámetros se sintetizan para cada horizonte del suelo en la tabla 3. Estos parámetros fueron analizados mediante correlaciones; los coeficientes ( $r$ ) y los valores  $p$  asociados se muestran en la tabla 4.

Los resultados evidenciaron que los modelos de Langmuir

( $R^2=0,96-0,99$ ), Freundlich ( $R^2=0,95-0,99$ ) y Temkin ( $R^2=0,89-0,97$ ) ajustaron mejor a los datos observados que el modelo DR ( $R^2=0,33-0,64$ ), indicando que el fenómeno de adsorción puede darse tanto sobre superficies homogéneas como heterogéneas. En general, los modelos de Langmuir y de Freundlich son los que mejor ajustan a las isotermas de adsorción de P, seguidos por el de Temkin<sup>50</sup>, mientras que el de DR, aunque fue citado por Goldberg (2005)<sup>51</sup> en adsorción de fosfatos, es generalmente utilizado para evaluar adsorción de iones metálicos sobre superficies microporosas<sup>27,37,52</sup>.

Los valores medios de los parámetros que caracterizan al modelo de Langmuir mostraron que la máxima capacidad de adsorción de P ( $Q_{max}$ ) alcanzó un valor mínimo de 382  $\mu\text{g.g}^{-1}$

**Tabla 3.** Valores medios de los parámetros de los modelos de adsorción de P en el suelo.

Modelo	Parámetro	Horizontes	A	E	Bt1	Bt2	BCt
		Profundidad (cm)	(0-30)	(30-40)	(40-90)	(90-140)	(140-180)
Langmuir	$Q_{max}$ ( $\mu\text{g.g}^{-1}$ )		418,8 ab	381,8 a	655,5 b	551,1 ab	458,3 ab
	$k_L$ ( $\text{ml.}\mu\text{g}^{-1}$ )		0,089 a	0,082 a	0,096 a	0,060 a	0,044 a
	MCBP ( $\text{ml.g}^{-1}$ )		36,1 ab	32,1 ab	56,3 b	32,4 ab	20,1 a
	$R^2$		0,97*	0,96*	0,98*	0,99*	0,99**
Freundlich	$k_F$ ( $\text{ml.g}^{-1}$ )		50,9 ab	53,6 ab	65,0 b	40,6 ab	25,5 a
	$I/n$		0,49 ab	0,43 a	0,55 ab	0,66 b	0,70 b
	$R^2$		0,95*	0,98*	0,97*	0,95*	0,99**
Temkin	$A$ ( $\text{ml.}\mu\text{g}^{-1}$ )		1,10 a	1,13 a	1,14 a	0,93 a	0,81 a
	$B$		180,3 ab	159,2 a	260,7 c	233,3 bc	200,5 abc
	CPE0 ( $\mu\text{g.ml}^{-1}$ )		0,82 a	0,82 a	0,79 a	0,88 a	0,81 a
	$R^2$		0,91*	0,91*	0,89*	0,94*	0,97**
DR±	$Q_{max_{DR}}$ ( $\mu\text{g.g}^{-1}$ )		267,5 a	247,6 a	350,8 b	299,8 ab	253,6 a
	$k_{DR}$ ( $\text{mol}^2.\text{kJ}^{-2}$ )		-4. $10^{-6}$ a	-4,3. $10^{-6}$ a	-2,5. $10^{-6}$ a	-4. $10^{-6}$ a	-6. $10^{-6}$ a
	$E$ ( $\text{kJ.mol}^{-1}$ )		377,6 ab	358,1 ab	527,9 b	382,6 ab	280,4 a
	$R^2$		0,52*	0,33***	0,46*	0,53*	0,64*
n			9	3	9	7	2

±: En el cálculo de los parámetros se consideraron valores de concentración media. n: número de muestras. Letras diferentes en una misma fila indican diferencias significativas con  $\alpha=0,05$ . \*: Significativo con  $\alpha=0,01$ ; \*\*: Significativo con  $\alpha=0,05$ ; \*\*\*: Significativo con  $\alpha=0,1$ .

**Tabla 4.** Coeficientes de correlación ( $r$ ) y valores  $p$  asociados entre los parámetros de los modelos de adsorción.

	$Q_{max}$	$k_L$	MCBP	$k_F$	$n$	$B$	CPE0	A	$Q_{max_{DR}}$	$k_{DR}$	$E$
$Q_{max}$	1*				1,1. $10^{-3}$				1,2. $10^{-5}$		
$k_L$		1			1,1. $10^{-4}$		0,01			3,3. $10^{-6}$	1,3. $10^{-6}$
MCBP			1		0,02		0,01		5,4. $10^{-5}$		
$k_F$				1	2,2. $10^{-4}$				5,4. $10^{-4}$		
$n$	-0,57	0,65	0,41	0,63	1	2,3. $10^{-4}$		2,2. $10^{-5}$		0,02	
$B$					-0,62	1			2,5. $10^{-7}$		
CPE0		-0,47	-0,46				1	0,01			
A					0,69		-0,49	1	0,04	4. $10^{-7}$	4,1. $10^{-7}$
$Q_{max_{DR}}$	0,71		0,67	0,59		0,79		0,37	1	1,7. $10^{-4}$	9,3. $10^{-6}$
$k_{DR}$		0,74			0,44			0,78	0,63	1	
$E$		0,76						0,78	0,71	1	

\*Por encima de la diagonal: valores  $p$ . Por debajo de la diagonal: coeficientes de correlación ( $r$ ). Sólo se muestran valores significativos con  $\alpha=0,05$ . n=30.

en el horizonte eluvial E y un máximo de  $656 \mu\text{g.g}^{-1}$  en el estrato Bt1 debido a su mayor contenido de arcilla y de óxidos de Fe y Al (tabla 2); partículas que favorecen los procesos de fijación por adsorción específica (intercambio de  $\text{HPO}_4^{2-}/\text{H}_2\text{PO}_4^-$  por  $\text{OH}^-$  de los óxidos de Fe y Al) o no específica (atracción electrostática sobre las láminas de los filosilicatos)<sup>18,19</sup>. De modo similar, el mayor valor de  $Q_{max,DR}$  se obtuvo en el horizonte Bt1 ( $p<0,05$ ), y los menores valores en los estratos A, E y BCt. Aunque los parámetros  $Q_{max}$  y  $Q_{max,DR}$  se relacionan significativamente ( $r=0,71$ ,  $p<0,05$ ; tabla 4), se define a  $Q_{max}$  de Langmuir como la cantidad máxima de P que puede adsorberse en una capa monomolecular completa dado que este modelo alcanzó un mejor ajuste a los datos que el de DR. De esta manera, según la clasificación de Juo y Fox (1977)<sup>53</sup>, el suelo posee una capacidad media de adsorción ( $100-500 \mu\text{g.g}^{-1}$ ) con una tendencia hacia valores superiores ( $500-1000 \mu\text{g.g}^{-1}$ ) en los horizontes Bt. Sharpley (1982)<sup>54</sup> evaluó la capacidad de sorción en superficie de 20 suelos y encontró valores de  $Q_{max}$  muy similares a los de este estudio. En cuanto a los estratos más profundos del perfil, García *et al.* (2006)<sup>49</sup> determinaron un valor de  $Q_{max}$  de  $740 \mu\text{g.g}^{-1}$  en un suelo Argiudol de la región Pampeana, semejante al alcanzado en este trabajo para el horizonte Bt1.

Las constantes relativas a la energía de enlace ( $k_L$ , A, y  $k_{DR}$ ) no presentaron diferencias significativas entre horizontes ( $p>0,05$ ; tabla 3). El parámetro E calculado a través de la ecuación de DR evidenció valores de energía media de adsorción entre 280 y 528  $\text{kJ.mol}^{-1}$ , con datos superiores en el horizonte Bt1 e inferiores en el BCt ( $p<0,05$ ). Valores de E entre 40 y 800  $\text{kJ.mol}^{-1}$  de  $\text{P-PO}_4^{3-}$  ubican a este tipo de adsorción como quimisorción, caracterizada por ser sitio-específica, producirse generalmente en una monocapa, y ser poco reversible<sup>55</sup>. Los altos valores del horizonte Bt1 se corresponden con la acumulación de arcilla y de Fe y Al que caracterizan a ese estrato (tabla 2).

La constante asociada con el calor de adsorción, B, mostró un valor medio en el horizonte Bt1 superior ( $p<0,05$ ) al de los horizontes A y E. Dicha constante indica que cuando su valor es mayor, a temperatura constante, menor es la entalpía de adsorción (Ec. 10), evidenciando un bajo costo energético para retener fosfatos. Valores semejantes de B (tabla 3) se hallaron en los trabajos de Mendoza (1986)<sup>39</sup>, Afsar *et al.* (2012b)<sup>56</sup> y Afsar y Hossain (2012)<sup>57</sup> en suelos con porcentajes de arcilla entre 17 y 47%. Por otra parte, el cálculo de la variación de la energía libre de Gibbs (Ec. 11) indica que la adsorción se produce espontáneamente ( $\Delta G<0$ ) sólo en los tres primeros horizontes de este suelo.

El  $k_F$  del modelo de Freundlich, que se define como la capacidad de adsorción cuando la concentración en el equilibrio es de  $1 \mu\text{g P.ml}^{-1}$ , fue superior ( $p<0,05$ ) en el horizonte Bt1 e inferior en el estrato profundo (140-180 cm). Esto coincide precisamente con la mayor y menor capacidad de saturación dado por  $Q_{max,DR}$  ( $r=0,59$ ) y con la energía media de adsorción E ( $r=0,90$ ) de cada estrato. Los valores  $k_F$  de este trabajo fueron similares a los determinados por López Camelio *et al.*

(1984)<sup>58</sup>, Mendoza (1986)<sup>39</sup> y Zamuner y Culot (1999)<sup>59</sup> en suelos Molisoles y Vertisoles.

Por otra parte, el CPE0 (Temkin), que indica la concentración de P en el equilibrio cuando la cantidad de P adsorbido es 0, presentó valores que oscilaron entre  $0,79$  y  $0,88 \mu\text{g.P.ml}^{-1}$ . Pose *et al.* (2013)<sup>60</sup> también hallaron una concentración inferior a la unidad en un suelo Molisol de Buenos Aires no afectado por estiércol, de  $0,24 \mu\text{g.P.ml}^{-1}$ . No obstante, analizando el CPE0 del sitio afectado por estiércol (corral de engorde), los autores informaron que dicha concentración se incrementaba a  $19 \mu\text{g.P.ml}^{-1}$ , sugiriendo así que el suelo puede presentar mayor riesgo de pérdida de P por escurrimiento que el sitio no afectado<sup>60</sup>. Considerando entonces que el CPE0 del suelo no impactado con estiércol ( $0,79-0,88 \mu\text{g.P.ml}^{-1}$ ), supera el valor de concentración de P total en agua para protección de la vida acuática (entre  $0,035$  y  $0,1 \mu\text{g.ml}^{-1}$ )<sup>3</sup>, podría ocurrir que ante determinados eventos lluviosos este nutriente se movilice y alcance los cuerpos de agua cercanos. Situación que se agravaría en un suelo de un EEC impactado con estiércol, presentando un mayor riesgo de pérdida del nutriente al ambiente.

En la figura 2 se observa el factor de separación, R, que entre la superficie del sorbente (partículas de arcilla, óxidos e hidróxidos, MO) y el sorbato ( $\text{P-PO}_4^{3-}$ ) disminuye a medida que se incrementa la concentración de P agregada, dado que se van ocupando cada vez más los sitios de adsorción. También se aprecia que los tres horizontes superiores (A, E, Bt1) siguen el mismo comportamiento. Valores de R entre 0 y 1 demarcen una adsorción favorable sobre la superficie de las partículas de suelo<sup>37</sup>. Por otra parte, la inversa de la afinidad ( $1.n^{-1}$ ) entre el adsorbente y el adsorbato mostró una tendencia hacia valores más bajos en los horizontes superiores. Por consiguiente, si bien la adsorción es favorable en todo el perfil, los estratos superiores son los que presentan sitios con mayor afinidad ( $n$ ) y mayor energía de enlace ( $k_L$ ) por lo que el factor R tiende a ser menor (horizontes A, E, Bt1, figura 2); posiblemente esto es debido a la tendencia hacia mayores

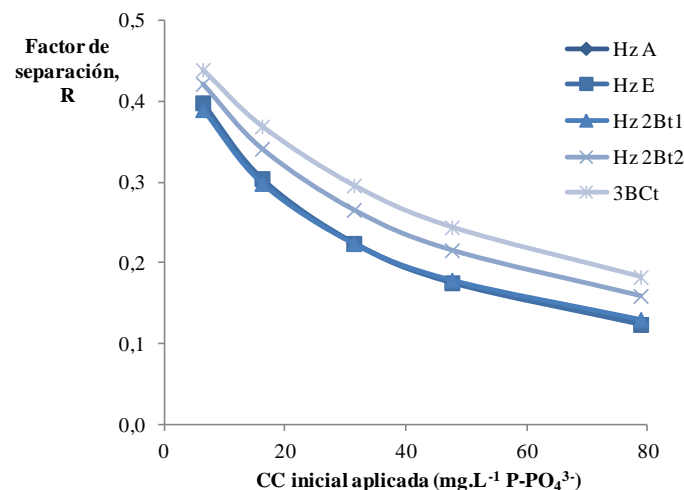


**Fig. 2:** Factor R medio para cada horizonte en función de las concentraciones aplicadas de P. Hz.: Horizonte.  $n_{Hz\ A}=45$ ;  $n_{Hz\ E}=15$ ;  $n_{Hz\ Bt1}=45$ ;  $n_{Hz\ Bt2}=35$ ;  $n_{Hz\ BCt}=10$ .

contenidos de CO respecto de los horizontes inferiores, lo que a su vez determina una adsorción espontánea ( $\Delta G < 0$ ) de P en esos sitios. López Cameló *et al.* (1984)<sup>58</sup>, Mendoza (1986)<sup>39</sup> y Zamuner y Culot (1999)<sup>59</sup> también hallaron valores entre 0,4 y 0,9 para la constante  $1.n^{-1}$  en suelos Molisoles de Argentina.

En relación a la máxima capacidad *buffer* de fosfatos (MCBP) se ha establecido que cuando dicho parámetro aumenta, también se incrementa la capacidad para resistir los cambios de la concentración de P en la solución del suelo<sup>62</sup>. Por consiguiente, este parámetro permite caracterizar al perfil general del suelo con una capacidad *buffer* muy baja (10-50 ml.g<sup>-1</sup>), excepto el estrato Bt1 con una MCBP baja (50-100 ml.g<sup>-1</sup>), de acuerdo a la clasificación de Moody y Bolland (1999)<sup>61</sup>. El valor medio de MCBP en la superficie de este suelo fue similar al determinado por Mendoza (1991)<sup>63</sup> en suelos Argialboles, de 36 ml.g<sup>-1</sup>, y se encontró dentro del rango publicado por Bolaño de Daniel (1984)<sup>64</sup>, entre 23 y 50 ml.g<sup>-1</sup>. Asimismo, el valor medio del horizonte Bt1 se relaciona con su contenido de filosilicatos y de óxidos de Fe y Al (tablas 1 y 2). Dado que horizontes con diferentes características físicas y químicas (tablas 1 y 2) pueden tener la misma MCBP (por ejemplo, los horizontes E y Bt2, tabla 3), cuando se analizan las reacciones de adsorción es necesario considerar, además de la cantidad de sitios disponibles, la energía con que dichos sitios pueden retener al nutriente. Relaciones significativas de MCBP con  $Q_{max,DR}$  y  $E$  ( $r=0,67$ ,  $r=0,94$ ) sustentan este concepto.

De acuerdo a la tabla 4, hay horizontes con gran cantidad de sitios de adsorción ( $Q_{max}$ ) pero de baja afinidad ( $n$ ,  $r=0,54$ ),

y por ende, de bajo calor intercambiado con el ambiente ( $b$ ) para adsorber fosfatos ( $r=0,94$ ). Estas características son las que definen a los horizontes profundos. Así, el fosfato proveniente de aplicaciones de estiércol al suelo que migre en el perfil y no llegue a ser retenido por el horizonte Bt1 (horizonte que presentó la mayor MCBP de los estratos del suelo bajo estudio) continuará desplazándose verticalmente, dado que los horizontes subsiguientes poseen menor cantidad de sitios de sorción y de baja energía de enlace (tabla 3).

#### *Relación entre la capacidad de adsorción de P y las características edáficas*

Con el propósito de comprender qué factores edáficos están involucrados en la retención del elemento, se establecieron ecuaciones matemáticas que permiten estimar los parámetros de los modelos de adsorción a partir de ellos. Dichas ecuaciones se presentan en la tabla 5 y allí se puede observar que sólo aquellas que estiman los parámetros  $Q_{max,DR}$  y  $B$  alcanzaron un ajuste a los datos superior al 60%, mientras todas las demás ajustaron por debajo de ese valor.

La máxima capacidad de adsorción de P puede ser explicada casi en un 70% por el contenido de MO (representada por el NKj) y de arcilla según la ecuación que estima  $Q_{max}$  de DR (Ec. 24). Ambos participan contribuyendo significativamente ( $p<0,05$ ) con una gran superficie específica donde pueden sorberse los iones fosfato. Asimismo, la MO a través de sus diversos grupos funcionales también influye en la disponibilidad de esos sitios, ya que puede ocuparlos por reacciones de adsorción o bien por reacciones de intercambio de ligando con el fosfato<sup>64</sup>.

**Tabla 5.** Ecuaciones matemáticas que explican los parámetros de los modelos a partir de las características edáficas del perfil del suelo.

Parámetros de los modelos estimados	n	R <sup>2</sup>	p-valor*	Ec.
<b>Langmuir</b>				
$Q_{max} = 120,18 + 11,17 \cdot Arcilla + 95,12 \cdot CO$	28	0,43	0,0008; 0,1029	16
$k_L = 0,11 + 0,01 \cdot K^+ + 1,1 \cdot 10^{-3} \cdot Arcilla - 2,3 \cdot 10^{-4} \cdot CE$	29	0,46	0,0246; 0,1190; 0,0023	17
$MCBP = 22,70 + 7,48 \cdot K^+$	29	0,38	0,0004	18
<b>Freundlich</b>				
$k_F = 36,77 + 6,47 \cdot K^+$	29	0,32	0,0013	19
$1/n = 0,26 + 0,01 \cdot Ca^{2+} - 0,03 \cdot K^+ + 6,0 \cdot 10^{-4} \cdot CE$	29	0,51	0,1279; 0,0347; 0,0001	20
<b>Temkin</b>				
$B = 52,92 + 13,78 \cdot Al + 19,66 \cdot CO + 0,13 \cdot CE$	29	0,65	0,0027; 0,0983; 0,0550	21
$A = 0,95 + 1,91 \cdot NKj + 0,02 \cdot Arcilla - 1,6 \cdot 10^{-3} \cdot CE$	29	0,46	0,0257; 0,0006; 0,0003	22
$CPE0 = 0,72 + 0,01 \cdot CaCO_3 Eq - 0,01 \cdot Ca^{2+} - 0,10 \cdot Na^+ + 3,8 \cdot 10^{-4} \cdot CE$	29	0,42	0,0704; 0,0230; 0,0182; 0,0359	23
<b>DR</b>				
$Q_{max,DR} = 149,03 + 417,14 \cdot NKj + 4,16 \cdot Arcilla$	29	0,69	0,0013; <0,0001	24
$k_{DR} = -5,2 \cdot 10^{-6} + 6,5 \cdot 10^{-7} \cdot K^+$	29	0,30	0,0022	25
$E = 343,62 + 40,39 \cdot K^+ + 4,77 \cdot Arcilla - 0,41 \cdot CE$	29	0,56	0,0021; 0,0193; 0,0416	26

Unidades: NKj, Arcilla, Al, CO, CaCO<sub>3</sub>Eq en %; CE en  $\mu\text{S} \cdot \text{cm}^{-1}$ ; Na<sup>+</sup>, K<sup>+</sup> y Ca<sup>2+</sup> en meq.100g<sup>-1</sup>. \*Valores p de cada variable.

La ecuación que estima la constante  $B$  de Temkin alcanzó un ajuste a los datos del 65% (Ec. 21), e indica que dicha constante se incrementa significativamente ( $p<0,05$ ) con el contenido de Al, pero también con el aporte de MO (representada por el CO) y de sales ( $p<0,1$ ). Dentro del suelo, el Al se encuentra formando iones complejos con ácidos orgánicos<sup>65</sup>, y

formando óxidos e hidróxidos cuya carga superficial es pH dependiente<sup>19</sup>, entre otros compuestos. Estos óxidos e hidróxidos libres de Al y el borde los silicatos laminares se caracterizan por presentar un punto de carga cero (PCC) elevado (por ej.: PCC gibbsita= 9,8)<sup>66</sup>. Si bien en el suelo estos compuestos de Al se presentan muchas veces asociados a

silicatos laminares, reduciendo su PCC por compensación de cargas<sup>67</sup>, en el rango de pH estudiado se caracterizan por presentar una densidad de cargas positivas en superficie que facilitan la adsorción de fosfatos. Así, los horizontes con mayor proporción de compuestos de aluminio y de MO requieren una menor entalpía de adsorción (*b*) de fosfatos (*B* se relaciona inversamente con *b*) dado que poseen mayor cantidad de sitios ( $r_{Qmax}=0,94$ ,  $r_{QmaxDR}=0,79$ ,  $p<0,05$ ; tabla 4) favorables a la sorción de los mismos. La presencia de sales también reduce la entalpía de adsorción, posiblemente debido al aumento de la fuerza iónica de la solución<sup>65,68</sup>.

En este suelo, cuyo pH osciló entre 5,8 y 7,6 (tabla 1), se destaca que los iones también intervienen en la adsorción del nutriente (Ec. 17-20, 23, 25-26). Particularmente, el catión potasio podría actuar como un intermediario del proceso, favoreciendo significativamente ( $p<0,05$ ) la formación de enlaces de mayor energía y afinidad (*n*) que inciden a su vez en la capacidad *buffer* del mismo (Ec. 17-20, 25-26). La concentración de este ion en la solución del suelo o fijado electrostáticamente sobre la superficie coloidal contribuye a la reducción del potencial eléctrico negativo, facilitando así la adsorción de P<sup>65</sup>. Se destaca asimismo que los feldespatos potásicos (tabla 2) forman parte de la mineralogía de este suelo.

Los cationes calcio y sodio, de radios iónicos inferiores al potasio, parecen incidir reduciendo significativamente ( $p < 0,05$ ) el CPE0 (Ec. 23); posiblemente también se comporten como intermediarios del proceso, habilitando nuevos sitios de unión, aunque de menor afinidad que con el K<sup>+</sup> (Ec. 20). Por el contrario, el CaCO<sub>3</sub> no reduciría el CPE0 (Ec. 23) dentro de las concentraciones de P ensayadas en este suelo, dado que en las isotermas a muy bajas concentraciones se favorecen las reacciones reversibles de adsorción<sup>30</sup> mientras que las de precipitación y coprecipitación, en las que estaría involucrado el CaCO<sub>3</sub>, se producen a mayores concentraciones.

Asimismo, las sales al incrementar la fuerza iónica de la solución reducen ( $p<0,05$ ) la energía de enlace (Ec. 17, 22, 26) y la afinidad (Ec. 20) por lo que podrían generar enlaces débiles entre el sorbato y el sorbente favoreciendo la concentración del nutriente en la solución de equilibrio (Ec. 23), y así una mayor posibilidad de pérdida hacia el ambiente.

## Conclusiones

A partir de este trabajo se ha podido estimar la máxima capacidad de adsorción de un suelo Argialbol de la Pampa Ondulada argentina, cuya función es la de sostén de un EEC. Los resultados indicaron que si bien la adsorción de P es favorable en todo el perfil, los estratos superiores (A, E, Bt1) son los que presentaron partículas con sitios de mayor afinidad y energía de enlace que las de los horizontes profundos. La MO y las partículas de tamaño arcilla intervienen este resultado proveyendo los sitios de adsorción de P, mientras que los cationes como el K<sup>+</sup> podrían actuar como intermediarios de la reacción. Por consiguiente, el fosfato proveniente del estiércol que ingrese al suelo, si no llega a ser retenido por el primer

horizonte Bt (mayor capacidad *buffer*), continuará desplazándose verticalmente, pudiendo salir del sistema al llegar a la napa. Además, dado que los valores del CPE0 superaron a los valores guías de P total en agua para protección de la vida acuática, es posible que el suelo del EEC efectivamente impactado con estiércol presente mayor riesgo de pérdida de P al ambiente.

## Agradecimientos

Esta investigación fue realizada con subsidio del estado nacional, otorgado por medio de un proyecto UBA bajo la dirección de la Dra. Ana R. García (FAUBA). Se agradece a todo su equipo de investigación y a la Cátedra de Química Inorgánica y Analítica (FAUBA) por su colaboración en este trabajo. Se destaca al Lic. Guillermo Cozzi y a su equipo del Servicio Geológico Minero Argentino (SEGEMAR) quienes llevaron adelante el análisis de roca total y de filosilicatos por difracción de rayos X. Asimismo se agradece al EEC por abrir sus puertas y colaborar en todo con esta investigación.

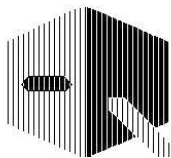
## Referencias bibliográficas

1. Autoridad del Agua (ADA). Resolución 336/2003. Disponible en: <http://www.ada.gba.gov.ar/sites/default/files/2019-04/Resoluci%C3%B3n%20336-03%20ADA%20parametros%20de%20descarga%20adminisble.pdf> Consultado: octubre 2021
2. National Water Quality Management Strategy (NWQMS). Australian and New Zealand Guidelines for Fresh and Marine Water Quality. Paper N° 4. Volume 1: The Guidelines (2000). Disponible en: <https://www.waterrquality.gov.au/sites/default/files/documents/anzecc-armcanz-2000-guidelines-vol1.pdf> Consultado: octubre 2021
3. Canadian Council of Ministers of the Environment (CCME). Water Quality Guidelines for the Protection of Aquatic Life (2004). Disponible en: <http://st-ts.ccme.ca/en/index.html?chems=all&chapters=1> Consultado: octubre 2021
4. AN Sharpley, I Sisak. Differential availability of manure and inorganic sources of phosphorus in soil. **Soil Sci. Soc. Am. J.**, **61**, 1503-1508 (1997).
5. A García, AF de Iorio. Phosphorus distribution in sediments of Morales Stream (tributary of the Matanza-Riachuelo River, Argentina). The influence of organic point source contamination. **Hidrobiología**, **492**, 129-138 (2003).
6. A García, AF de Iorio. Incidencia de la descarga de efluentes de un feedlot en la calidad de agua del arroyo Morales, Buenos Aires-Argentina. **Rev. Facultad de Agronomía UBA**, **25**(2), 167-176 (2005).
7. MA Elrashidi, MD Mays, TJ Zimmer. Changes in release characteristics and runoff phosphorus for soils amended with manure. **Commun. Soil Sci. Plant Anal.**, **36**(13-14), 1851-1873 (2005).
8. CI Chagas, MV Piazza, M De Siervi, OJ Santanatoglia, J Morettón, M Paz, *et al.* Overland run-off water quality in extensive and intensive farming systems of Argentina. **Agrochimica**, **51**(2-3), 130-136 (2007).

9. T Borda, L Celi, L Zavattaro, D Sacco, E Barberis. Effect of agronomic management on risk of suspended solids and phosphorus losses from soil to waters. **J. Soils Sediments**, **11**, 440–451 (2011).
10. PM Haygarth, AN Sharpley. Terminology for phosphorus transfer. **J. Environ. Qual.**, **29**, 10-15 (2000).
11. WJ Gburek, E Barberis, PM Haygarth, B Kronvang, C Stamm. Phosphorus mobility in the landscape. En: *Phosphorus: agriculture and the environment*. Eds. JT Sims y AN Sharpley. Agronomy Series N°46. American Society of Agronomy, Inc.; Crop Science Society of America, Inc.; Soil Science Society of America, Inc. Madison, Wisconsin, US (2005).
12. GM Pierzynski, RW McDowell, JT Sims. Chemistry, cycling, and potential movement of inorganic phosphorus in soils. En: *Phosphorus: agriculture and the environment*. Eds. JT Sims y AN Sharpley. Agronomy Series N°46. American Society of Agronomy, Inc.; Crop Science Society of America, Inc.; Soil Science Society of America, Inc. Madison, Wisconsin, US (2005).
13. JT Sims, GM Pierzynski. Chemistry of phosphorus in soils. En: *Chemical processes in soils*. Eds. MA Tabatabai y DL Sparks. Soil Science Society of America Book Series N°8. Soil Science Society of America, Inc. Madison, Wisconsin, US (2005).
14. F Djordic. Displacement of phosphorus in structured soils. Doctoral thesis. Swedish University of Agricultural Sciences. Uppsala, Suecia (2001). Disponible en: <http://pub.epsilon.slu.se/21/91-576-5826-9.fulltext.pdf> Consultado: octubre 2021
15. MJ Cabello, FH Gutiérrez Boem, CE Quintero, G Rubio. Soil characteristics involved in phosphorus sorption in Mollisols. **Soil Sci. Soc. Am. J.**, **80**, 1585-1590 (2016).
16. WJ Chardon, OF Schoumans. Solubilization of phosphorus: Concepts and process description of chemical mechanisms. En: *Phosphorus losses from agricultural soils: Processes at the field scale*. Eds. WJ Chardon y OF Schoumans. COST Action 832. Alterra, Wageningen, Holanda, 42-52 (2002).
17. BS Sekhon. Modeling of soil phosphorus sorption and control of phosphorus pollution with acid mine drainage floc. Dissertation submitted in partial fulfillment of the requirements for the degree of Doctor of Philosophy in Plant and Soil Sciences. Davis College of Agriculture, Forestry, and Consumer Sciences. West Virginia University. Virginia, US (2002). Disponible en: <https://researchrepository.wvu.edu/etd/1713/> Consultado: octubre 2021
18. AR García. Actividades de engorde a corral (feedlot): retención y movilización de nitrógeno y fósforo en un suelo Hapludol éntico, y su potencial impacto en el ambiente. Tesis para obtener el grado de Magister de la Universidad de Buenos Aires, área Ciencias del Suelo. Escuela para Graduados. Facultad de Agronomía. UBA (2009).
19. H Bohn, B Mc Neal, G O'Connor. Química del Suelo. Ed. Limusa S.A. Grupo Noriega Editores. México DF (1993).
20. OS Heredia. Fósforo. En: *Principios de edafología con énfasis en suelos argentinos*. Coord. M Conti. 2º ed. Editorial Facultad de Agronomía – UBA. Buenos Aires, Argentina (2000).
21. A Andriulo (Coord.). Guía de buenas prácticas para el manejo de nutrientes (N y P) en la Pampa Ondulada. Desarrollo de Índices de Riesgo de contaminación por N y P. Grupo Medio Ambiente. Estación Experimental INTA Pergamino. Buenos Aires, Argentina (2010).
22. Servicio Meteorológico Nacional (SMN). Ministerio de Defensa, Presidencia de la Nación. Disponible en: <https://www.smn.gob.ar/> Consultado: noviembre 2021
23. Instituto Nacional de Tecnología Agropecuaria (INTA). Instituto de Suelos. Carta de suelos de la República Argentina. Ed. INTA. Disponible en: <http://anterior.inta.gob.ar/suelos/cartas/index.htm> Consultado: noviembre 2021
24. J Dewis, F Freitas. Métodos físicos y químicos de análisis de suelos y aguas. Organización de las Naciones Unidas para la Alimentación y la Agricultura. Roma (1970).
25. AL Page, RH Miller, DR Keeney. Methods of soil analysis. Part 2. Chemical and microbiological properties. 2º ed. Agron. 9, ASA and SSSA, Madison, Wisconsin (1982).
26. US Environmental Protection Agency (USEPA). Method 3050B. Acid digestion of sediments, sludges, and soils. Revision 2. En: *Test methods for evaluating solid wastes. Physical/chemical methods*. SW-846, Vol. 1, Section A, Part I, Chapter 3. USEPA. Washington DC, US (1996).
27. AF de Iorio. Capacidad de sorción de Cu y Zn en Natracuoles de la Pampa Deprimida (Argentina). Relación con las distintas fases geoquímicas. Memoria para optar al grado de Doctora de la Universidad de Vigo. Vigo, España (2010).
28. M Orgeira, C Vásquez, R Compagnucci, I Raposo, F Pereyra. Magnetismo de rocas en suelos actuales de la Pampa Ondulada, provincia de Buenos Aires, Argentina: Vinculación del clima con el comportamiento magnético. **Rev. Mex. Cienc. Geol.**, **26**(1), 65-78 (2009).
29. P Nair, T Logan, A Sharpley, L Sommers, M Tabatabai, T Yuan. Interlaboratory comparison of a standardized phosphorus adsorption procedure. **J. Environ. Qual.**, **13**, 591-595 (1984).
30. A Lindsay. Chemical equilibria in soils. Wiley and Sons. New York (1979).
31. W Lindsay, P Vlek, S Chien. 1989. Phosphate minerals. En: *Minerals in Soil Environment* Eds. J Dixon y S Weed, 2º ed. Soil Science Society of America, Inc. Madison, Wisconsin, US, 1089–1130 (1989).
32. J Murphy, H Riley. A modified single solution method for the determination of phosphate in natural waters. **Anal. Chim. Acta**, **27**, 31-36 (1962).
33. F Cabrera Capitán. Estudio de la adsorción isoterma de aniones ortofosfato por óxidos metálicos existentes en la naturaleza. Resumen de Tesis Doctoral. Facultad de Ciencias, Universidad de Sevilla (1975). Disponible en: <https://digital.csic.es/handle/10261/78057> Consultado: octubre 2021
34. D Graetz, V Nair. Phosphorus sorption isotherm determination. En: *Methods of phosphorus analysis for soils, sediments, residuals and waters*. Ed. G Pierzynski. SERA-IEG 17 (Southern Extension/Research Activity - Information Exchange Group). Virginia Tech University, Virginia, US, 33-37 (2000).

35. J Di Rienzo, F Casanoves, M Balzarini, L Gonzalez, M Tablada, C Robledo. InfoStat. Grupo InfoStat, FCA, Universidad Nacional de Córdoba. Córdoba. Argentina (2008).
36. A Dąbrowski. Adsorption - from theory to practice. **Advances in Colloid and Interface Science**, **93**, 135-224 (2001).
37. A Dada, A Olalekan, A Olatunya, O Dada. Langmuir, Freundlich, Temkin and Dubinin–Radushkevich isotherms studies of equilibrium sorption of  $Zn^{2+}$  unto phosphoric acid modified rice husk. **IOSR Journal of Applied Chemistry**, **3(1)**, 38-45 (2012).
38. S Kuo. Phosphate buffering and availability in soils. **Trends in Soil Sci.**, **1**, 203-213 (1991).
39. RE Mendoza. Isotermas de adsorción de fósforo en suelos argentinos: I. Métodos de ajuste y comparación entre ecuaciones. **Ciencia del Suelo**, **2**, 107-116 (1986).
40. NA Mórtola. Comportamiento de las formas de fósforo en un Ultisol con diferentes manejos de implantación forestal. Tesis presentada para optar al título de Magister de la UBA, Área Ciencias del Suelo. Escuela para Graduados. Facultad de Agro-nomía. UBA (2013).
41. MF Ahmed, IR Kennedy, ATMA Choudhury, ML Kecske's, R Deaker. Phosphorus adsorption in some Australian soils and influence of bacteria on the desorption of phosphorus. **Communications in Soil Science and Plant Analysis**, **39**, 1269–1294 (2008).
42. MM Areco. Métodos alternativos para el tratamiento de la contaminación ambiental por metales pesados. Tesis para optar al título de Doctor de la UBA, área Ciencias Biológicas. Facultad de Ciencias Exactas y Naturales, UBA (2011).
43. MZ Afsar, S Hoque, KT Osman. A comparison of the Langmuir, Freundlich and Temkin equations to describe phosphate sorption characteristics of some representative soils of Bangladesh. **Int. J. Soil Sci.**, **7(3)**, 91-99 (2012a).
44. F Obiri-Nyarko, J Kwiatkowska-Malina, G Malina, T Kasela. Removal of lead and benzene from groundwater by zeolite and brown coal: isotherm and kinetic studies. En: *Proceedings of the 4th International Conference on Environmental Pollution and Remediation*. Prague, Czech Republic, 2013.
45. F Granados-Correa, J Bonifacio Martínez, J Serrano Gómez. Estudio cinético y termodinámico de la adsorción de Cr (VI) presente en solución acuosa sobre fosfato de calcio sintético. **Rev. Soc. Quím. Perú**, **75(2)**, 201-212 (2009).
46. AF Chamorro, RA Sánchez Andica. Estudio de la adsorción de plomo en suelos de la región minera en el distrito de Buenos Aires en el departamento del Cauca, Colombia. **Revista de Ciencias. Facultad de Ciencias Naturales y Exactas, Universidad del Valle**, **16**, 145-160 (2012).
47. Y Sui, ML Thompson. Phosphorus sorption, desorption, and buffering capacity in a biosolids-amended Mollisol. **Soil Sci. Soc. Am. J.**, **64**, 164-169 (2000).
48. S Larsen. Soil phosphorus. **Advances in Agronomy**, **19**, 151-210 (1967).
49. A García, C Weigandt, V Rodríguez, I Ciapparelli, M Navarro, AF de Iorio Sorción-desorción de P en un suelo calcáreo y su potencial impacto sobre la calidad de agua. En: *XX Congreso Argentino de la Ciencia del Suelo, I Reunión de Suelos de la Región Andina*. Salta, Argentina, 2006.
50. I Dubus. La rétention du phosphore dans les sols: principes d'étude, modélisation, mécanismes et comportements du sol impliqués. ORSTOM Nouméa, Doc. Sci. Tech. III3 (1997).
51. S Goldberg. Equations and models describing adsorption process in soils. En: *Chemical Processes in Soils*. Eds. MA Tabatabai y DL Sparks. SSSA Book Series no. 8, Soil Science Society of America Inc. Madison, Wisconsin, US (2005).
52. C de Santiago. La fisisorción de nitrógeno. Fundamentos físicos, normativa, descripción del equipo y procedimiento experimental. Ministerio De Fomento, Ministerio De Medio Ambiente y Medio Rural y Marino, Centro De Estudios y Experimentación De Obras Públicas (2012). Disponible en: <https://es.scribd.com/doc/86917380/FISISORCIÓN-NITROGENO> Consultado: octubre 2021
53. ASR Juo, RL Fox. Phosphate sorption characteristics of some benchmark soils of West Africa. **Soil Science**, **124(6)**, 370-376 (1977).
54. AN Sharpley. Prediction of water extractable phosphorus content of soil following a phosphorus addition. **J. Environ. Qual.**, **11(2)**, 166-170 (1982).
55. AR Moreno Marenco. Estudio de diferentes bioadsorbentes como posibles retenedores de fosfatos en aguas. Tesis para obtener el título de Magister en Ciencias Químicas. Facultad de Ciencias. Universidad Nacional de Colombia. Bogotá, Colombia (2013). Disponible en: <https://repositorio.unal.edu.co/bit-stream/handle/unal/49446/52978683.2013.pdf?sequence=1&isAllowed=y> Consultado: octubre 2021
56. MZ Afsar, S Hoque, KT Osman. Phosphate desorption characteristics of some representative soils of Bangladesh: effect of exchangeable anions, water molecules and solution to soil ratios. **Open Journal of Soil Science**, **2(3)**, 234-241 (2012b).
57. MZ Afsar, ME Hossain. Characterization of some representative calcareous soils of Bangladesh with respect to soil phosphorus requirements. **Int. J. Agric. Res.**, **7(8)**, 388-397 (2012).
58. LG de López Cameló, OS Heredia, A Nervi, ZMM de Sese. Adsorción de fósforo en algunos suelos argentinos. I - Condiciones experimentales e isotermas de adsorción. **Rev. Facultad de Agronomía**, **5(3)**, 165-174 (1984).
59. E Zamuner, JP Culot. Efecto de la fertilización en la capacidad de sorción de fósforo. **Invest. Agr.: Prod. Prot. Veg.**, **14(1-2)**, 107-116 (1999).
60. N Pose, E Zamuner, G Eyherabide, L Picone, C Videla, N Macreira. Características de sorción de fósforo del suelo en un sistema de engorde intensivo a corral y en una pastura natural. **Chilean J. Agric. Anim. Sci., ex Agro-Ciencia**, **29(1)**, 35-44 (2013).
61. PW Moody, MDA Bolland. Phosphorus. En: *Soil analysis: an interpretation manual*. Eds. KI Peverill, LA Sparrow y DJ Reuter. CSIRO. Melbourne, Australia, 187–220 (1999).
62. P Ehler, C Morel, M Fotyma, J-P Destain. Potential role of phosphate buffering capacity of soils in fertilizer management

- strategies fitted to environmental goals. **Z. Pflanzenernähr. Bodenk.**, **166**, 409-415 (2003).
63. RE Mendoza. Efecto del fósforo nativo adsorbido en el suelo sobre la media de la capacidad “buffer” de fosfato. **Turrialba**, **41(3)**, 350-358 (1991).
64. AAB de Daniel. Determinación de la capacidad reguladora y concentración ajustada de fósforo, en suelos de la región Pampeana. **Ciencia del Suelo**, **2(1)**, 99-106 (1984).
65. E Oburger, DL Jones, WW Wenzel. Phosphorus saturation and pH differentially regulate the efficiency of organic acid anion-mediated P solubilization mechanisms in soil. **Plant Soil**, **341**, 363–382 (2011).
66. DG Strawn, HL Bohn, G O'Connor. Soil Chemistry. 4° ed. Wiley Blackwell. New York (2015).
67. M Arias, MT Barral, F Díaz Fierros. Hidróxidos de aluminio sintéticos y agregación en muestras de caolinita y cuarzo. **Suelo y planta**, **2**, 395-410 (1992).
68. NJ Barrow. Modelling the effects of pH on phosphate sorption by soils. **Journal of Soil Science**, **35**, 283-297 (1984).



## Phytochemical study and *in vitro* biological activities of *Chlorella vulgaris*, *Chlorella pyrenoidosa* and *Chlorella minutissima* extracts

Antonio Menezes-Filho<sup>1\*</sup>, Matheus Ventura<sup>1</sup>, Hellen Batista-Ventura<sup>1</sup>, Carlos Castro<sup>2</sup>, Celiana Triches<sup>3</sup>, Cinthia Porfiro<sup>3</sup>, Jacqueline Guimarães<sup>3</sup>, Marconi Teixeira<sup>1</sup>, Frederico Soares<sup>1</sup>, Aparecida Taques<sup>4</sup>.

<sup>1)</sup> Department of Agrarian Sciences, Doctorate in Agrarian Sciences,  
Goiânia Federal Institute, Campus Rio Verde, Goiás, Brazil.

<sup>2)</sup> Department of Agrochemistry, Master in Agrochemistry,  
Goiânia Federal Institute, Campus Rio Verde, Goiás, Brazil.

<sup>3)</sup> Department of Pharmacy, UniBRAS College, Campus Rio Verde, Goiás, Brazil.

<sup>4)</sup> Department of Engineering, Mato Grosso Federal Institute, Campus Bela Vista, Mato Grosso, Brazil.

(\*) [antonio.menezes@estudante.ifgoiano.edu.br](mailto:antonio.menezes@estudante.ifgoiano.edu.br); [astronomoamadorgoias@gmail.com](mailto:astronomoamadorgoias@gmail.com)

Recibido: 30/11/2021

Revisado: 24/12/2021

Aceptado: 30/12/2021

### Resumo

**Estudo fitoquímico e atividades biológicas *in vitro* dos extratos de *Chlorella vulgaris*, *Chlorella pyrenoidosa* e *Chlorella minutissima*.** O estudo teve como objetivo a triagem de compostos fitoquímicos e avaliação das atividades biológicas dos extratos de *Chlorella vulgaris*, *Chlorella pyrenoidosa* e *Chlorella minutissima* (aqueoso e hidroetanólico). Foi realizado fitoquímica, varredura em espectrofotometria, fenólicos e flavonoides totais, eliminação do radical DPPH e a atividade antioxidante total, atividade antibacteriana foi realizada sobre *Staphylococcus aureus*, *Escherichia coli*, *Salmonella* serovar Enteritidis e *Thyphymurium* e citotóxica sobre *Artemia salina*. Os extratos exibiram a presença de diversos grupos fitoquímicos, alto conteúdo de flavonoides e fenólicos totais, expressivas atividades redutoras para DPPH e %AA. A inibição foi positiva para cepas bacterianas e baixa atividade citotóxica.

**Palavras-chave:** Atividade antioxidante; Compostos fenólicos, Clorofitas; *Escherichia coli*; *Staphylococcus aureus*.

### Abstract

The study aimed to screen phytochemicals and evaluate the biological activities of *Chlorella vulgaris*, *Chlorella pyrenoidosa* and *Chlorella minutissima* extracts (aqueous and hydroethanolic). Phytochemistry, spectrophotometric scanning, total phenolics and flavonoids, DPPH radical scavenging and total antioxidant activity were performed, antibacterial activity was performed on *Staphylococcus aureus*, *Escherichia coli*, *Salmonella* serovar Enteritidis and *Thyphymurium* and cytotoxic on *Artemia salina*. The extracts showed the presence of several phytochemical groups, high content of flavonoids and total phenolics, expressive reducing activities for DPPH and %AA. Inhibition was positive for bacterial strains and low cytotoxic activity.

**Keywords:** Antioxidant activity; Chlorophylls; *Escherichia coli*; Phenol compounds; *Staphylococcus aureus*.

### Introducción

*Chlorella* Beijerinck is a genus of eukaryotic green unicellular microalgae that shows spherical shape  $\approx$  2 to 10  $\mu\text{m}$  (diameter) with high photosynthesis capacity, fast reproduction requiring only sunlight, CO<sub>2</sub>, water and a small amount of nutrients<sup>1,2</sup>. According by Huss *et al.*<sup>3</sup> the lack of obvious morphological characters combined with an exclusively asexual reproductive cycle by means of autospores has caused considerable problems in the taxonomic description and identification of *Chlorella* species. Currently, this diverse genus presents remarkable phylogenetic studies that support the morphological characteristics of the species of green microalgae included in *Chlorella*. According by Andrade *et al.*<sup>1</sup> the name *Chlorella* derived from the Greek “chloros” and from the Latin “ella”, which mean green and small. *Chlorella* mi-

croalgae have been present on earth since the pre-Cambrian period around 2.5 billion years ago. Japan is currently the world leader in *Chlorella* microalgae consumption.

*Chlorella* species live in freshwater and marine ecosystems having bioactive compounds such as proteins, vitamins, chlorophyllian pigments, polyunsaturated fatty acids, sterols and especially polyphenolics being represented by phloroglucinol, *p*-coumaric acid, ferulic acid and apigenin<sup>4</sup>, which makes this genus very interesting from a health-beneficial point of view, being used as forage, in medicine and as food additives<sup>1,5</sup>.

The different species of this genus such as *Chlorella vulgaris*, *Chlorella pyrenoidosa* and *Chlorella minutissima* have a very diversified chemical constitution, although they share in common several polysaccharide molecules, involved in bio-

logical activities such as antioxidants, antifungals, antibacterials, antivirals, antitumor, cytotoxic and anti-radiation agent<sup>6,7</sup>. In addition to the countless biological activities, this group of green microalgae are nutritional sources of proteins, lipids (palmitoleic, oleic, linoleic,  $\alpha$ -linoleic,  $\gamma$ -linoleic, and homo  $\gamma$ -linoleic), chlorophylls (*a*, *b* and *c*),  $\beta$ -carotene, soluble vitamins, choline, dietary fiber and mineral salts such as iron, calcium, potassium, magnesium and phosphorous<sup>8,9</sup>.

The green microalgae *Chlorella* have experienced a strong surge in their applications last years, but are still not fully exploited as source resource in medical, biological, biotechnological process, and agricultural science. This growing knowledge generates a large number of considerable studies, however, little is known about the numerous and potential biological activities with photo-protective action, antioxidant for numerous free radicals, especially reactive oxygen species such as singlet, antibacterial and cytotoxic oxygen<sup>7,9-11</sup>.

The present research work was planned to examine the phytochemical and bioactive compounds of *C. vulgaris*, *C. pyrenoidosa* and *C. minutissima* marine algae extracts.

## Material and methods

The reagents used were ethanol (LSchemicals, Brazil), iodine (Synth, Brazil), mercury II sulfate (Synth, Brazil), petroleum ether (Neon, Brazil), acetone (Neon, Brazil), Folin-Ciocalteu reagent (Sigma Aldrich, Singapore), ferric chloride (Neon, India), aluminum chloride (Neon, China), quercetin (Gemini, India), 2,2-diphenyl-1-picrylhydrazyl (Sigma Aldrich, Singapore), linoleic acid (Vetec, Brazil), sodium chloride (Neon, India), count plate agar (Kasvi, U.S.A), chlorophyll *a* (Sigma Aldrich, China), chlorophyll *b* (Sigma Aldrich, China), chlorophyll *c* (Sigma Aldrich, China), xanthophyll (Sigma Aldrich, Singapore),  $\beta$ -carotene (Sigma Aldrich, Singapore), sodium carbonate (Neon, China), gallic acid (Sigma Aldrich, Singapore), sodium nitrate (Neon, China), sodium hydroxide (Neon, Brazil), 3,5-di-tert-4-butylhydroxytoluene (Sigma Aldrich, Singapore), potassium phosphate (Neon, India), azithromycin, cephalexin and tigecycline (CenterLab, Brazil) and Tween 20 (Sigma Aldrich, U.S.A).

The three Chlorella algae species were supplied in the form of lyophilized powder: *C. vulgaris* by Qingdao Fraken International Trading Co. Ltd. (China); *C. pyrenoidosa* by Qingdao Hilda-Jingyi Trading Co. Ltd (China) and *C. minutissima* by Xi'an Tongze Biotech Co. Ltd (China). The identification of Chlorella species was carried out using a dichotomous key for the Chlorella genus, HPLC and UV, and certification rules the ISO, FDA, HACCP and Kosher. Initially, they were dried in an oven  $50 \pm 2$  °C and crushed in a mill (7lab, Mod. Micro910, Brazil). The powder obtained was stored in an amber bottle in a refrigerator at -12 °C. 150 g of powdered samples were separately extracted by reflux using distilled water and 70% ethanol as the solvents for 12 h. The aqueous extract was reduced in a hot bath at  $80 \pm 5$  °C, and the hydroethanolic extract was reduced in a rotary evaporator with reduced pres-

sure. Then, the extracts were frozen and lyophilized until constant mass according by Sembiring *et al.*<sup>12</sup>.

Phytochemical tests were carried out on the aqueous and hydroethanolic extracts for qualitative determination according to Sembiring *et al.*<sup>12</sup>, Madike *et al.*<sup>13</sup>, and Mehdi *et al.*<sup>14</sup>. The three algae materials were tested for groups of alkaloid, flavonoid, tannin, saponin, quinone, terpenoid and steroids, reducing sugars and non-reducing sugars, resins, amino acids, coumarins, glycosides, purines, organic acids, aromatic and aliphatic, phenolics, xanthoproteins, leucoanthocianins, polysaccharides, phlobatannins, carboxylic acids and oxylates.

Analysis by thin-layer chromatography (TLC) was performed on chromatoplates (Xtra SIL G/UV<sub>254</sub>). Five (5  $\mu$ L) of the algae extract was added 1 cm from the lower edge of the chromatoplate. Then, the plate was transferred to a vat for chromatography. The chromatographic run was stopped when the mixture reached 1 cm from the upper edge of the chromatoplate. The development system consists of a mixture of ethanol: petroleum ether: acetone in a 1:1:1 volume ratio. After development, the plate is air dried, marked the center of the pigment point, measured the distance traveled by the solvent front and the distance traveled by each pigment. The Retardation factors (*R*'s) are then calculated. Chlorophyll (*a*), chlorophyll (*b*), Chlorophyll (*c*), xanthophyll and  $\beta$ -carotene standards were used for *R*'s comparison<sup>15</sup>.

The total phenolic contents were determined according to colorimetric Folin-Ciocalteu method as described by Labiad *et al.*<sup>16</sup> (modified). Aliquot containing 0.5 mL of sample solution was mixed with 2.5 mL of Folin-Ciocalteu reagent diluted with distilled water (1:9, v/v), followed by the addition of 5 mL of sodium carbonate (7.5%, w/v). The solution was stored in a dark room for 60 min., and the absorbance (Abs) was measured at 765 nm using a UV-Vis spectrophotometer (Bel-Photonics, Mod. M-51, Italy) and a glass cuvette (5 mL). The standard curve of gallic acid is obtained under the same conditions as above using solutions with a range of concentrations between 0-500 mg.L<sup>-1</sup>, which were prepared in 96% ethanol, and *R*<sup>2</sup> = 0.9997. The total phenolic content was measured as gallic acid equivalents (mg GAE g<sup>-1</sup> dry extract algae).

Flavonoid contents were measured using a modified colorimetric method described by Labiad *et al.*<sup>16</sup>. Aliquot containing 0.25 mL of algae extract solution was added to a test tube containing 1.25 mL of distilled water. Then, 0.075 mL of an aqueous sodium nitrite solution (5%, w/v) was added to the mixture and maintained for 5 min. Then, 0.15 mL of an aluminum chloride solution (10%, w/v) was added and homogenized for 1 min. After 6 min., 0.5 mL of 1 M sodium hydroxide was finally added. The solution was diluted with 0.275 mL of distilled water, and homogenized for 5 min. The absorbance (Abs) of the final solution was measured at 510 nm; the standard curve of quercetin was obtained under the same conditions as above, using solutions with a range of concentrations between 0-650 mg L<sup>-1</sup>, prepared in 96% ethanol and *R*<sup>2</sup> = 0.9991. The total flavonoid content is expressed as mg quercetin equivalent (QE g<sup>-1</sup> of dry extract algae).

2,2-Diphenyl-1-picrylhydrazyl (DPPH) scavenging ability assay was used to evaluate the antioxidant activity of each algae extract. Test was conducted in a 96-well plate according to Sembiring *et al.*<sup>12</sup> (modified). 20 µL stock solution for each algae extract was prepared at different concentrations (between 5-2.000 ppm, v/v) and 180 µL of DPPH solution 0.147 mmol.mL<sup>-1</sup> were added to each well. After 60 min incubation at room temperature in dark room, absorbance was read at 517 nm using the micro-plate reader of UV-Vis spectrophotometer. Hydroethanol solution was used as blank. The scavenging ability (%) was calculated according to equation (1), and ascorbic acid and 3,5-di-*tert*-4-butylhydroxy-toluene (BHT) was used as positive standards.

$$\text{% reduction} = \frac{(\text{Abs standard} - \text{Abs crude extract})}{\text{Abs standard}} * 100 \quad \text{Eq. 1}$$

All tests were performed in triplicate. Concentrations of algae extract samples resulting in 50% inhibition on DPPH ( $\text{IC}_{50}$  value, expressed in µg.mL<sup>-1</sup>) were calculated.

The antioxidant activity (%AA) of *Chlorella* algae extracts was determined according to the thiocyanate method proposed of Mitsuda *et al.*<sup>17</sup> and described by Gulçin *et al.*<sup>18</sup> 10 mg of lyophilized water extracts were dissolved in 10 mL water. 10 mg of each algae hydroethanolic extract were dissolved in 10 mL hydroethanolic solution (between 5-100 µg.mL<sup>-1</sup>) or standard samples in 2.5 mL of potassium phosphate solution buffer (0.04 M, pH 7.0), was added to 2.5 mL linoleic acid emulsion. The 50 mL linoleic acid emulsion consists of 175 µg Tween 20, 155 µL linoleic acid, and 0.04 M potassium phosphate buffer. 50 mL control contains 25 mL linoleic acid emulsion and 25 mL potassium phosphate buffer. The solution was incubated at 37 ± 2 °C in tubes assay in the dark room. After, the solution was stirred for 3 min., the peroxide value was determined by reading the Abs at 500 nm in a spectrophotometer UV-Vis. Therefore, high Abs indicates high linoleic acid oxidation. Solutions without added extracts or standards were used as control. All data are the average of quadruplicate analyses. The inhibition percentage of lipid peroxidation was calculated by following equation 2:

$$\text{% Inhibition} = \frac{(\text{A}_0 - \text{A}_1)/\text{A}_0}{100} * 100 \quad \text{Eq. 2}$$

where:  $\text{A}_0$  = Abs of the control reaction;  $\text{A}_1$  = Abs in the presence of the samples.

Antibacterial activity was determined according to Tuama and Mohammed<sup>19</sup> (modified). The antibacterial assay was investigated applying the standard agar well diffusion. The assay pathogens *S. aureus* (ATCC 25923), *E. coli* (ATCC 25922), *S. serovar Enteritidis* (ATCC 13076) and *S. serovar Thyphimurium* (ATCC 14028) were uniformly homogenized on count plate agar (CPA) using sterile Drigalski-spreader, then, five wells of 9 mm diameter were made using sterile well tip. 50 µL of different concentrations were added to each well (25, 50, 75, and 100 µg.mL<sup>-1</sup>). Then, the plates were incubated at 36 ± 2 °C for 36 h for the bacterial strains; after incubation the zones of inhibition were recorded. A minimum 5 mm antibi-

osis halo was determined using a digital caliper (Eda, Mod. 8", China).

The photo-protection activity was adopted as the methodology described by Medeiros *et al.*<sup>20</sup> (modified). The critical wavelength scan was obtained scanning from 250 to 400 nm in a UV-Vis spectrophotometer, using a 1 cm single-field quartz cuvette. *Artemia salina* cytotoxic assay was conducted in according to Silva *et al.*<sup>21</sup>, as proposed by Meyer *et al.*<sup>22</sup> (modified). Each algae extract (20 mg) was dissolved in 2 mL of hydroethanolic solution (45%, v/v) and samples of this solution (500, 375, 250, 125, 50 and 25 µL) were transferred, in triplicate, to the 5 mL vials. After total removal of the solvent, 5 mL of a saline solution (NaCl, 0.38 g.L<sup>-1</sup>), was added in each of the bottles, resulting in final concentrations of 1.000, 750, 500, 250, 100 and 50 µg.mL<sup>-1</sup>. Larvae of *A. salina* nauplii type (10 per vials) were added and after of 12 h contact, the survivors were counted. As a negative control, saline aqueous solution (0.38 g.L<sup>-1</sup>) was used. The lethal concentration  $\text{LC}_{50}$  (expressed in µg.mL<sup>-1</sup>) was derived from the best fit line obtained by linear regression analysis.

Assays for total phenolics and flavonoids, DPPH free radical reduction and total antioxidant activity (%AA) and antibacterial activity were performed in quadruplicate. When significant differences were observed, they were analyzed using the Duncan's test ( $p < 5\%$ ) using the Statistica software (SPSS).

## Results and discussion

In this study, aqueous and hydroethanolic extracts of three algae of the *Chlorella* genus exhibited a rich and varied complexity of positive phytochemical groups that are involved in several biological activities of therapeutic use such as alkaloids, flavonoids, tannins, saponins, reducing sugars, amino acids, glycosides, organic acids, aromatics, phenolics, xanthoproteins and polysaccharides (Table 1). The aqueous extracts of *Chlorella* exhibited the highest number of positive phytochemical groups.

Kannan *et al.*<sup>23</sup> studied the seaweed genera *Gracilaria* (*G. corticata*) and *Spirulina* (*S. platensis*) where also through TLC they found positive results for alkaloids, flavonoids, glycosides, phenols and saponins similar to this study with the genus *Chlorella*. Phytochemical screening of *Caulerpa racemosa* exposed the presence of alkaloids, phenolics, flavonoids and steroids in the study by Srivastav *et al.*<sup>24</sup>. Algae in several families and genera share relatively common phytochemical groups, which are important both for these organisms and for food and medicinal use.

Several phytochemical groups of special metabolism in algae have important biological activities, such as cytotoxic agents (tannins), analgesic and anti inflammatory (terpenoids), anti inflammatory, estrogenic, antimicrobial, antiallergic, antioxidant, vascular and cytotoxic antitumor (flavonoids), congestive heart failure and cardiac arrhythmia (glycosides), and antibacterial and antifungal saponins<sup>25</sup>.

*Chlorella* algae extracts were tested for the presence of chlo-

**Table 1.** The phytochemical of aqueous and hydroethanolic of *C. vulgaris*, *C. pyrenoidosa* and *C. minutissima* extracts.

Phytochemical	Type extract					
	Aqueous			Hydroethanolic		
	1	2	3	1	2	3
Alkaloids	+	+	+	-	-	-
Flavonoids	+	+	+	+	+	+
Tannins*	+	+	+	-	-	-
Saponins	+	+	+	-	-	-
Quinones	-	-	-	-	-	-
Terpenoids and Steroids	+	+	+	+	+	+
Reducing sugars	+	+	+	-	-	-
Non-reducing sugars	-	+	+	+	+	-
Resins	+	+	+	+	+	-
Amino acids	+	+	+	-	-	-
Coumarins	-	+	-	-	-	-
Glycosides	-	+	+	+	+	+
Purines	-	-	-	-	-	-
Organic acids	+	+	+	+	+	+
Aromatics and Aliphatics**	+	+	+	+	+	+
Phenolics	+	+	+	+	+	+
Xanthoproteins	+	+	+	-	-	-
Leucoanthocyanins	-	-	-	-	-	-
Polysaccharides	+	+	+	-	-	-
Phlobatannins	-	-	-	-	-	-
Carboxylic acids	-	-	-	-	-	-
Oxylates	-	-	-	-	-	-

Notes: *C. vulgaris* (1). *C. pyrenoidosa* (2). *C. minutissima* (3).

\*Tannins (Green). \*\*Positive result for aliphatic substances. (-) absent. (+) presence. Source: Authors, 2021.

rophyll *a*, chlorophyll *b*, chlorophyll *c* xanthophyll and β-carotene using the TLC technique. Table 2 shows the *R<sub>f</sub>s* obtained, which indicate high separation efficiency by method used. It is suggested that the mobile phase constituted by ethanol, petroleum ether and acetone played an important role in this step of separation of compounds for *Chlorella*. Similar effects to this study were reported during the separation of pigments and other important groups of molecules performed by Jeffrey<sup>26</sup> for several species of seaweed using classical planar chromatography (paper) and mobile phases acetone, ethyl ether, ethanol, pyridine and carbon disulphide.

Pigment separation occurred exhibiting the following pattern for chlorophyll *a* (blue spots), chlorophyll *b* (greenish yellow), chlorophyll *c* (light green), xanthophyll (yellow spots), chlorophyll degradation products (grey spots) and β-carotene at the highest point, being similar when compared to the standards. According by Kannan *et al.*<sup>23</sup>, Mendiola *et al.*<sup>27</sup> and Kannan *et al.*<sup>28</sup>, a lot phytomolecules have been recognized in algae extracts equivalent to various carotenoids formerly known in *S. platensis* microalgae along with numerous degradation products.

The pigments observed in the three *Chlorella* samples in this study corroborate the research by Mello *et al.*<sup>29</sup>, where researchers discuss the purpose of these pigments such as chlo-

**Table 2.** *R<sub>f</sub>s* values for separation on TLC, the monodimensional method of aqueous and hydroethanolic of *C. vulgaris*, *C. pyrenoidosa* and *C. minutissima* extracts.

Identified component	R <sub>f</sub> s values of algae extracts*					
	Aqueous extract			Hydroethanolic extract		
	1	2	3	1	2	3
Chlorophyll <i>a</i>	2.01	2.09	2.13	1.96	1.90	1.99
Chlorophyll <i>b</i>	1.83	1.86	1.82	1.80	1.78	1.85
Chlorophyll <i>c</i>	0.55	0.91	0.77	0.69	0.60	0.72
Xanthophile	5.53	5.60	5.49	5.40	5.55	5.60
β-carotene	7.30	7.21	7.34	7.28	7.26	7.31

Notes: \**R<sub>f</sub>s* values are dimensionless. (1) *C. vulgaris*, (2) *C. pyrenoidosa*, (3) *C. minutissima*. Source: Authors, 2021.

rophylls, xanthophylls and carotenoids that, in addition to being large and complex molecules, also participate in the absorption of electromagnetic radiation, playing an important role in the conversion of solar energy into chemical energy.

The aqueous extracts of *Chlorella* in this study showed similarity although at different band intensities in the UV-Vis spectrophotometric analysis (Figure 1-A). In Figure 1-B, a similar behavior can be observed both for the extracts of *C. vulgaris* and *C. pyrenoidosa* and different for *C. minutissima*, which showed similarity with the aqueous extracts. Although extracts showed differences in UV-Vis bands (with both extracting solvents), all of them showed absorption bands related to groups composed of chlorophylls *a* (600-700 ~10 nm), *b* (400-500 ~10 nm) and *c* (450-500 ~10 nm), xanthophylls (400-700 ~10 nm) and β-carotene (300-500 ~50 nm) corroborating the TLC analysis.

It is noteworthy that the index on the quantitative or qualitative rate of chlorophylls varies according to the absorption of light by the alga, and that the bands with higher intensities generally occur between 645 to 663 nm, where still in Figure 1 (A and B) it is possible to see such statement proposed by Tamburic *et al.*<sup>30</sup>. Also in the study by Tamburic *et al.*<sup>30</sup> and Oliveira *et al.*<sup>31</sup>, bands with medium to high intensities tell about the health of these organisms, where bands with low and no intensity between this UV-Vis range are highly indicative of damage to cell culture due to discoloration. Thus, this study demonstrates that the three *Chlorella* species analyzed have a high degree of pigmentation, thus, exhibiting excellent quality in the health of these marine organisms.

Hydroethanolic extracts are the best option for obtaining β-carotene, due to its molecular conformation and the mixture of non-toxic solvents. In Figure 1 (B) UV-Vis spectra show homogeneity and absorption between 300-550 ~50 nm in *C. pyrenoidosa*, *C. minutissima* and *C. vulgaris* (superimposed on *C. pyrenoidosa* as described above). As discussed by Hornero-Méndez and Britton<sup>32</sup>, β-carotene is an important source of vitamin A, in addition to presenting high photoprotective activity against harmful damage from energizing radiation emitted in UV wavelengths (A, B and C) both for algae and

for humans using photoprotective emulsions, preventing these energy sources from damaging several biomolecules, including promoting the appearance of skin cancers and premature aging. According Silva *et al.*<sup>21</sup> the carotenoids identified in these microalgae are astaxanthin, zeaxanthin, violaxanthin, and lutein which are already industrially produced synthetically for use in a variety of food products and cosmetics.

This has been also discussed by Rinawati *et al.*<sup>33</sup>, who also analyzed by UV-Vis spectrophotometry the content of chlorophylls and carotenoids in algae. The chlorophyll content in microalgae in the logarithmic phase was: *C. vulgaris* 200-1.500 mg.L<sup>-1</sup>, *Nannochloropsis* sp. 100-500 g.L<sup>-1</sup>, *Porphyridium cruentum* 500-800 g.L<sup>-1</sup> and *Spirulina platensis* 1.000-3.500 mg.L<sup>-1</sup> and for stationary phases microalgae *C. vulgaris* 100-1.000 mg.L<sup>-1</sup>, *Nannochloropsis* sp. 200-500 g.L<sup>-1</sup>, *P. cruentum* 900-2.000 mg.L<sup>-1</sup> and *S. platensis* 2.000-6.000 mg.L<sup>-1</sup>. While the carotenoid content of microalgae in the logarithmic phase of *C. vulgaris* 10-40 g.L<sup>-1</sup>, *Nannochloropsis* sp.

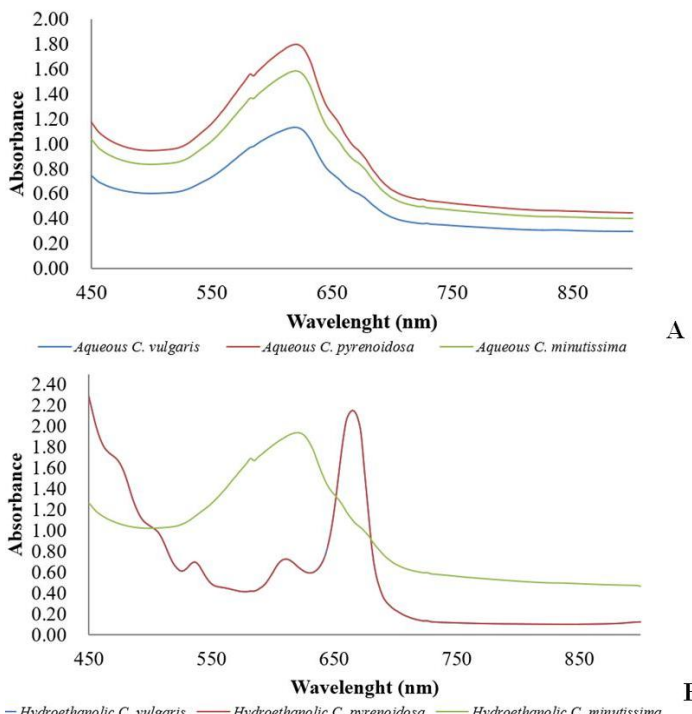


**Fig. 1:** UV-Vis spectra between 450-900 nm of the aqueous (A) and hydroethanolic (B) extracts of *C. vulgaris*, *C. pyrenoidosa* and *C. minutissima*. The *C. vulgaris* scan line is superimposed on the *C. pyrenoidosa* line in (B). Source: Authors, 2021.

10-60 g.L<sup>-1</sup>, *P. cruentum* 10-60 ug.L<sup>-1</sup> and *S. platensis* 20-40 ug.L<sup>-1</sup> and for stationary phases microalgae *C. vulgaris* 10-50 g.L<sup>-1</sup>, *Nannochloropsis* sp. 10-70 g.L<sup>-1</sup>, *P. cruentum* 70-130 ug.L<sup>-1</sup> and *S. platensis* 20-1.100 mg.L<sup>-1</sup>.

All *Chlorella* extracts in both extracting solvents showed remarkable extraction of total phenolic compounds (Table 3). Among the samples of aqueous extracts of *C. vulgaris* and *C. minutissima* there was no significant difference according to Duncan's test, although they showed higher values compared to the other extracts. Similar extraction results were also observed for total flavonoids, however, the hydroethanolic extract of *C. minutissima* had a higher flavonoid content compared to the other extracts, showing a statistically significant difference. Again, it is observed in this study that water as an extracting solvent proves to be the best option for obtaining these groups of compounds with notable antioxidant activities.

Our values for phenolic compounds were higher than those obtained by Miranda *et al.*<sup>34</sup> evaluating the methanol extract of *C. vulgaris* with a value of 24.95 mg in 100 g<sup>-1</sup> of dry alga matter, and 0.65 to 3.17 mg GAE 100 g<sup>-1</sup> by the study in *C. vulgaris* extracts<sup>7</sup>. Results similar to those of this study were obtained by Siddhanta *et al.*<sup>35</sup> investigating the extract of the seaweed *Himanthalia elongata* with high levels of phenolic compounds of 151.3 mg GAE 100 g<sup>-1</sup> and flavonoids of 42.5 mg QE 100 g<sup>-1</sup> of dry extract.

Potential DPPH free radical reducing activity was also verified for all aqueous and hydroethanolic extracts of *Chlorella*. Among the other extracts, the *C. pyrenoidosa* extract showed greater reduction capacity, which could be due to the numerous phytochemical classes (Table 1) verified in the qualitative test. The algae aqueous and hydroethanolic extracts showed high antioxidant activity but some lesser than the antioxidant ascorbic acid and BHT ( $IC_{50}$  1.97 ± 0.06 and 3.14 ± 0.09  $\mu\text{g.mL}^{-1}$ ). Similar results were obtained by Miranda *et al.*<sup>34</sup> for the methanolic extract of *C. vulgaris* cultivated at 30 °C, which presented higher antioxidant activity = 85%, quite similar to BHT = 86%. By the Rancimat test (lipid medium) two fractions of methanolic extracts showed much higher antioxidant activity with induction times > 37.50 h at 60 °C and 11.5 h at 100 °C. According to the researchers, salicylic, transcinnamic, synaptic, chlorogenic, and caffeine phenolic compounds found in the methanolic extract of *Chlorella* may be responsible for its greater antioxidant activity.

**Table 3.** Total phenolic content, flavonoid content, DPPH radical reduction and antioxidant activity found for the studied algae.

Assay	Results					
	Aqueous extract			Hydroethanolic extracts		
	1	2	3	1	2	3
TPC (mg GAE.g <sup>-1</sup> )	187.32±0.63a	133.18±0.21b	182.09±0.33a	117.11±0.39c	100±0.93cd	121±0.15c
TFC (mg QE.g <sup>-1</sup> )	56.66±0.21b	51.72±0.19b	62.27±0.60c	61.15±0.95c	53.09±1.02b	72.04±1.07a
DPPH ( $IC_{50}$ $\mu\text{g.mL}^{-1}$ )	99.15±0.26c	87.77±0.98b	94.18±0.19c	178.09±0.18e	190.44±1.00f	156.01±0.93d
% AA (%AA)	81.17±1.26d	86.09±1.60c	83.20±2.09d	90.56±1.97b	97.90±1.99a	90.18±2.84b

**Notes:** TPC = Total phenolic compounds. TFC = Total flavonoid compounds. DPPH = Free radical reduction expressed as 50% Inhibition Concentration. % AA = Percentage of antioxidant activity. (1) *C. vulgaris*. (2) *C. pyrenoidosa*. (3) *C. minutissima*. Equal letters on the same line do not differ significantly by Duncan's test ( $p < 5\%$ ). Source: Authors, 2021.

Among the studies that corroborate our results we can mention the study by Yu *et al.*<sup>6</sup> with *C. vulgaris*, where it was observed a high DPPH reducing activity ranging from 60.01 to 65.1%. Song *et al.*<sup>36</sup> also studied algae extracts of the *Chlorella* sp., attributing the antioxidant potential on polysaccharide compounds with removal of 49.10% of the DPPH radical, 56.60% for the hydroxyl radical and 32.10% for the superoxide radical. Hu *et al.*<sup>37</sup> also found potential DPPH radical reduction activity on *C. pyrenoidosa* extracts with a reduction between 29.67 to 54.16%. These studies corroborate our results, demonstrating the formidable antioxidant activity of the algae *C. vulgaris*, *C. pyrenoidosa* and *C. minutissima* extracts obtained in different organic solvents.

Important antioxidant activities are reported for several seaweed extracts, Kannan *et al.*<sup>23</sup> were also successful for methanolic extracts of the algae *G. corticata* and *S. platensis* with significant reduction using the free radical method by Fenton reagent, with reduction values equal to 50% and 94.4%, respectively. Also by these authors, an important reduction value over the DPPH free radical was observed between 53.8-70.4% and 51.8-64.7% for the methanol extracts of the algae *G. corticata* and *S. platensis*, respectively, resulting in values similar to those obtained in this study for the three *Chlorella* species. It is suggested that numerous phytochemical groups are involved in the antioxidant activity, which is also proposed by Premalatha *et al.*<sup>38</sup> who evaluated the extracts of the algae *Ulva fasciata* and *Chaetomorpha antenniana* as potential reducing agents in the DPPH assay, and the same was reported for the extract of *H. elongata* by Siddhanta *et al.*<sup>35</sup> with  $IC_{50} = 0.125 \mu\text{g.mL}^{-1}$ .

When evaluating extracts in determining their capacities to reduce free radicals, it should always be verified in more than one method, therefore, this study verified this biological activity in the %AA assay where *Chlorella* extracts presented a reduction rate higher than 81%. It was observed through Duncan's test that the hydroethanolic extract of *C. pyrenoidosa* 97% presented the highest antioxidant activity for this model (%AA). Additionally the numerous species of algae capable of reducing free radicals present protective barriers characteristics against oxidative stress by reactive species in the environment and in the cellular production in living organisms.

The oxidative stress, which in turn result in oxidative damage of cellular components in the form of lipid peroxidation, protein denaturation or DNA conjugation finally cell death<sup>7</sup>. Furthermore, oxidative stress has been associated with many diseases such as neural degeneration, Parkinson's and Alzheimer disease, AIDS, and aging and cardiovascular diseases, and cancer<sup>7</sup>.

*Chlorella* aqueous and hydroethanolic extracts showed potential capacity to inhibit *S. aureus* and *E. coli* strains at the highest concentrations 75-100  $\mu\text{g.mL}^{-1}$  which proved to be dose-dependent (Table 4). For the hydroethanolic extracts of *C. vulgaris* and *C. pyrenoidosa*, a slight inhibition activity on *S. serovar Enteritidis* was observed, although no statistically significant difference was observed in both extracts and concentrations 75-100  $\mu\text{g.mL}^{-1}$  by Duncan's test. Although *Chlorella* extracts have shown potential values as natural antibacterial agents, the synthetic antibacterial references azithromycin, cephalexin and Tigecycline are still the best options in combating these bacteria of interest to health, according to manufacturers (CenterLab, Brazil).

Uma *et al.*<sup>39</sup> found antibacterial activity superior than this study for *S. aureus* between 6-25 mm, *E. coli* between 9-21.4 mm; high sensitivity was also verified on strains of *Klebsiella pneumoniae*, *Pseudomonas*, *Vibrio cholerae* and *Streptococcus pyogenes*, in extracts of *C. vulgaris* from different extracting solvents. Algae extracts act in different ways, as it is a natural product obtained in different parts of the world. Possibly the difference between the results of antibiosis on the tested bacteria has an influence on colony health, biological activities and environmental variation. Pratt *et al.*<sup>40</sup> attributes high sensitization activity to chlorellin against a large and complex group of potentially pathological microorganisms, especially Gram-positives and Gram-negatives bacteria: *S. aureus*, *S. pyogenes*, *Bacillus subtilis*, *Bacterium coli* and *Pseudomonas pyocyanea* (*P. aeruginosa*).

Marine algae are potential source organisms with important special functions that can symbolize functional clues in the development of new pharmaceutical drugs, as well as potential improvements over their use in the form of herbal medicines. According Dhargalkar and Verlecar<sup>41</sup> the marine algae

**Table 4.** Antibacterial activity on *Staphylococcus aureus*, *Escherichia coli*, *Salmonella serovar Enteritidis* and *Salmonella serovar Thyphimurium* by aqueous and hydroethanolic of *C. vulgaris*, *C. pyrenoidosa* and *C. minutissima* extracts.

Microorganisms	Inhibition zone (mm)					
	Aqueous extracts			Hydroethanolic extracts		
	25, 50, 75, and 100 $\mu\text{g.mL}^{-1}$			25, 50, 75, and 100 $\mu\text{g.mL}^{-1}$		
	1	1	2	1	2	3
<sup>a</sup> <i>S. aureus</i>	0c/0c/0c/10b	0c/0c/8b/11b	0c/0c/9b/11b	0c/0c/8b/11b	0c/0c/9b/11b	0c/0c/8b/10b
<sup>b</sup> <i>E. coli</i>	0d/0d/6c/8c	0c/0c/0c/7b	0c/0c/8b/10b	0c/0c/0c/7b	0c/0c/8b/10b	0c/0c/0c/0c
<sup>c</sup> <i>S. serovar Enteritidis</i>	0b/0b/0b/0b	0c/0c/0c/6b	0c/0c/7b/9b	0c/0c/0c/6b	0c/0c/7b/9b	0c/0c/0c/0c
<sup>c</sup> <i>S. serovar Thyphimurium</i>	0b/0b/0b/0b	0b/0b/0b/0b	0b/0b/0b/0b	0b/0b/0b/0b	0b/0b/0b/0b	0b/0b/0b/0b

**Note:** (1) *C. vulgaris*. (2) *C. pyrenoidosa*. (3) *C. minutissima*. <sup>a</sup>Azithromycin, <sup>b</sup>Cephalexin and <sup>c</sup>Tigecycline. Antibiotics: *S. aureus* 23a mm, *E. coli* 28a mm, *S. serovar* Thyphimurium 28a mm, *S. serovar* Enteritidis 27a mm. Equal letters on the same line do not differ statistically by Duncan's test ( $p < 5\%$ ). Source: Authors, 2021.

products like fibers execute a diverse array of functions such as antioxidant agents, anticoagulant, antimutagenic and anti-tumor.

According by Siddhanta *et al.*<sup>35</sup> and Kannan *et al.*<sup>23</sup> many bioactive and pharmacologically important compounds such as alginate, carrageen and agar are obtained from marine algae and treatment used in herbal medicine and pharmacy, and microbiology studies.

According to Bobin *et al.*<sup>42</sup> and Violante *et al.*<sup>43</sup> one of the factors that determine the photoprotection activity and effectiveness of a natural product is directly involved in terms of its chemical composition, consecutively its activity in absorbing high energy waves such as UV, in addition to the molar extinction coefficient and solubility. The UV critical wave assay is an *in vitro* test that in numerous studies has shown to be a pleasant option due to its simplicity and speed when compared to *in vivo* assays. In this essay Mansur *et al.*<sup>44</sup>, Ferrari<sup>45</sup> and Violante *et al.*<sup>43</sup> address the correlation of absorption of a certain compound, isolated or not, on the erythematogenous effect caused by UV radiation.

The aqueous extracts exhibited bands of medium intensity in the scan between the critical wavelengths in the UVC, where *C. vulgaris* presented two bands, a broad one at 259 nm and a smaller one at 268 nm, still at 259 nm *C. pyrenoidosa* and *C. minutissima* showed similar bands, although at different absorption intensities (Figure 2). Hydroethanolic extracts behaved heterogeneously when compared to aqueous extracts, where *C. minutissima* exhibited a strong and broad band with maximum absorption at 268 nm, followed by hydroethanolic extract of *C. vulgaris* with maximum absorption at 259 nm and *C. pyrenoidosa* at 268 nm.

Synthetic chemical filters show maximum absorption in regions other than UV, for UVC between 100-290 nm, for UVB the range comprises between 290-320 nm, UVA between 320-400 nm<sup>43,46</sup>. Algae have a special absorption capacity in the ultraviolet region due to their constitution on photosynthetic pigments. Furthermore, the photoprotection activity is not exclusively on pigments, an important portion involves groups of phytomolecules such as flavonoids, tannins, anthraquinones, alkaloids and polyphenols<sup>43,47</sup>.

The topical photoprotective activity using emulsions conjugated with extracts proven to act as a temporary barrier on the dermis, reduces the incidence of certain types of cancers such as non-melanoma and melanoma<sup>48</sup>. The melanoma type originates from cells responsible for melanin synthesis and the non-melanin type is found in sun-exposed areas of the body, such as the neck, arms, ears and face<sup>49</sup>.

*Chlorella* aqueous extracts exhibited higher median lethal concentration activity ( $LC_{50}$ ) with values of 931.50; 929.26 and 838.07  $\mu\text{g.mL}^{-1}$  for *C. vulgaris*, *C. pyrenoidosa* and *C. minutissima*, respectively. The hydroethanolic extracts exhibited a low median lethal concentration ( $LC_{50}$ ) with values of 1.177; 1.213 and 1.158  $\mu\text{g.mL}^{-1}$ , respectively for *C. vulgaris*, *C. pyrenoidosa* and *C. minutissima*.

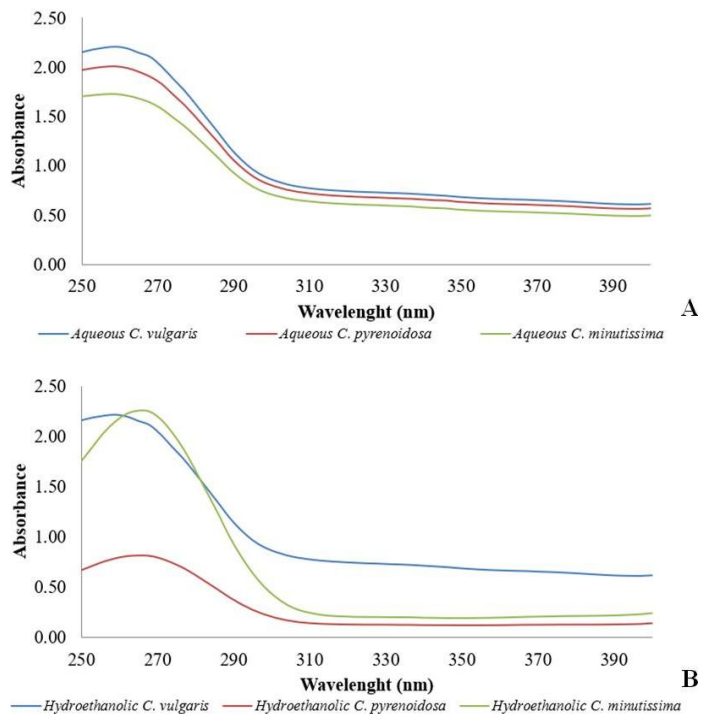


**Fig. 2:** UV 250 to 400 nm scanning spectrum critical for aqueous (A) and hydroethanolic (B) extracts of *C. vulgaris*, *C. pyrenoidosa* and *C. minutissima*. Source: Authors, 2021.

According to Calazans *et al.*<sup>50</sup> and Meyer *et al.*<sup>22</sup> natural extracts that present  $LC_{50}$  values higher than 1.000  $\mu\text{g.mL}^{-1}$  are considered non-toxic, and values lower than 1.000  $\mu\text{g.mL}^{-1}$  are considered potentially toxic. Thus, it is observed that all aqueous extracts exhibited weak, although positive lethal cytotoxicity against *A. salina*. The hydroethanolic extracts, on the other hand, presented values higher than the recommended 1.000  $\mu\text{g.mL}^{-1}$  and were considered non-toxic.

It is worth noting that there is little literature on toxicity of eukaryotic microalgae on cell lines and *A. salina*, while a larger number of papers deal with cyanobacteria. Nicolai *et al.*<sup>51</sup> evaluated several algae extracts, and among them commercial strains of *C. vulgaris* were considered non-toxic and suitable for feeding in studies in the European Union, in addition, of these *in vitro* studies they did not demonstrate toxicity neither for fibroblasts nor for *A. salina*. Although our study showed values below 1.000  $\mu\text{g.mL}^{-1}$ , the extracts are safe for food use due to very low toxicity.

## Conclusions

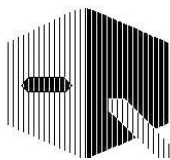
In this study aqueous and hydroethanolic extracts of green microalgae *Chlorella vulgaris*, *Chlorella pyrenoidosa* and *Chlorella minutissima* showed a great variety of special bioactive compounds, especially alkaloids, flavonoids, terpenoids and steroids, organic acids and phenols. Furthermore, these extracts showed variation in their antioxidant potential (DPPH and %AA), especially in hydroethanolic extracts. This antioxidant capacity was significantly correlated with their quantitative of total phenolic and flavonoid contents. Results of the UV-Vis supercritical wave test and the low cytotoxic activity shown in the biological test with *A. salina* indicate that Chlo-

rella extracts have high potential as a photoprotective materials and transmitting confidence for their possible use in various industrial segments such as the food, pharmaceutical and biological. However, future studies are needed to evaluate the feasibility of *C. vulgaris*, *C. pyrenoidosa* and *C. minutissima* extracts for developing potent antioxidant, photoprotective, antibacterial and cytotoxic drugs.

## References

1. CJ Andrade, LM Andrade. An overview on the application of genus *Chlorella* in biotechnological processes. **J. Adv. Res. Biotechnol.**, **2**, 1-9 (2017).
2. FRG Silva, TMS Matias, LIO Souza, TJ Matos-Rocha, AS Fonseca, KC Mousinho, AF Santos. Phytochemical screening and *in vitro* antibacterial, antifungal, antioxidant and antitumor activities of the red propolis Alagoas. **Braz. J. Biol.**, **79**, 452-459 (2019).
3. VAR Huss, C Frank, EC Hartmann, M Hirmer, A Kloboucek, BM Seidel, E Kessler. Biochemical taxonomy and molecular phylogeny of the genus *Chlorella* *Sensu Lato* (Chlorophyta). **J. Phycol.**, **35**, 587-598 (1999).
4. K Goiris, K Muylaert, S Voorspoels, B Noten, DD Paepe. Detection of flavonoids in microalgae from different evolutionary lineages. **J. Phycol.**, **50**, 485-492 (2014).
5. EV Tretiakova, PG Beliaeva, AI Saralov. Substantiation of using *Chlorella* genus microalgae as a raw material for preparation of chemopreventive substances. **I. J. P.**, **5**, 774-780 (2018).
6. M Yu, M Chen, J Gui, S Huang, Y Liu, H Shentu, J He, Z Fang, W Wang, Y Zhang. Preparation of *Chlorella vulgaris* polysaccharides and their antioxidant activity *in vitro* and *in vivo*. **In. J. Biol. Macromol.**, **137**, 139-150 (2019).
7. OH Abdel-Karim, SF Gheda, GA Ismail, AM Abo-Shady. Phytochemical screening and antioxidant activity of **Chlorella vulgaris**. **D. J. S.**, **41**, 81-91 (2020).
8. MLS Queiroz, MC Rocha, CO Torello, J Souza Queiroz, C Bincoletto, MA Morgano, AK Calgarotto. *Chlorella vulgaris* restores bone marrow cellularity and cytokine production in lead-exposed mice. **Food Chem. Toxicol.**, **49**, 2934-2941 (2011).
9. J Matos, CL Cardoso, P Falé, CM Afonso, NM Bandarra. Investigation of nutraceutical potential of the microalgae *Chlorella vulgaris* and *Arthrospira platensis*. **I. J. Food Science Technol.**, **55**, 303-312 (2020).
10. LM Andrade, CJ Andrade, M Dias, CAO Nascimento, MA Mendes. *Chlorella* and *Spirulina* microalgae as sources of functional foods, nutraceuticals, and food supplements; an overview. **MOJ Food Process Technol.**, **6**, (2018).
11. HJ Hussein, SS Naji, NMS Al-Khafaji. Antibacterial properties of the *Chlorella vulgaris* isolated from polluted water in Iraq. **J. Pharm. Res.**, **10**, 2457-2460 (2018).
12. EM Sembiring, B Elya, R Sauriasari. Phytochemical screening, total flavonoid and total phenolic content and antioxidant activity of different parts of *Caesalpinia bonduc* (L.) Roxb. **Pharmacogn. J.**, **10**, 123-127 (2018).
13. LN Madike, S Takaïdza, M Pillay. Preliminary Phytochemical screening of crude extracts from the leaves, stems, and roots of *Tulbaghia violacea*. **In. J. Pharmacogn. Phyto. Res.**, **9**, 1300-1308 (2017).
14. MAH Mehdi, FYS Alarabi, M Farooqui, V Pradhan. Phytochemical screening and antiamebic studies of *Tamarindus indica* of leaves extract. **Asian J. Pharm. Clin. Res.**, **12**, 507-512 (2019).
15. E Torres-Rodríguez, YA Núñez-Romero, Y Mojena-Guerra, Y Fung-Boix, Y Fonseca-Turruella. Análisis fitoquímico de partes aéreas de *Sida pyramidata* Cav. Yerba de aura. **Rev. Cub Quími.**, **33**, 401-414 (2021).
16. MH Labiad, H Harhar, A Ghanimi, M Tabyaoui. Phytochemical screening and antioxidant activity of Moroccan *Thymus satu-reioïdes* extracts. **J. Material Environ. Sc.**, **8**, 2132-2139 (2017).
17. H Mitsuda, K Yuasumoto, K Iwami. Antioxidation action of indole compounds during the autoxidation of linoleic acid. **Eijo Shokuryo**, **19**, 210-214 (1996).
18. İ Gülcin, I Güngor Sat, Ş Beydemir, M Elmastaş, Ö İrfan Küfrevoğlu, Comparision of antioxidant activity of clove (*Eu-geenia caryophylata* Thunb) buds and lavender (*Lavandula stoe-chas* L.). **Food Chemistry**, **87**, 393-400 (2004).
19. AA Tuama, AA Mohammed. Phytochemical screening and *in vitro* antibacterial and anticancer activities of the aqueous extract of *Cucumis sativus*. **Saudi J. Biol. Scien.**, **26**, 600-604 (2019).
20. MAC Medeiros, B Santos, FMC Marques, MFMS Leite, MM Simões, RM Anjos, L Brito Júnior, GLA Maia, MASG Alves, AP Sousa, AA Oliveira Filho. Avaliação da atividade fotoprotetora do extrato aquoso de *Rhaphiodon echinus* (Nees & Mart.) Schauer. **Sci Plen.**, **17**, 1-5 (2021).
21. J Silva, C Alves, S Pinteus, J Reboleira, R Pedrosa, S Bernardino. **Chlorella. Nonvit. Nonm. Nutri. Suppl.**, 187-193 (2019).
22. BN Meyer, NR Ferrigni, JE Putnam, LB Jacobsen, DE Nichols, JL McLaughlin. Brine shrimp: a convenient general bioassay for active plant constituents. **Planta Med.**, **45**, 41-34 (1982).
23. M Kannan, A Pushparaj, B Dheeba, K Nageshwari, K Kannan. Phytochemical screening and antioxidant activity of marine algae *Gracilaria corticata* and *Spirulina platensis*. **J. Chem. Pharm. Res.**, **6**, 312-318 (2014).
24. N Srivastav, K Saurav, V Mohanasrinivasan, K Kannabiran, M Singh. **British J. Pharmacol. Toxicol.**, **1**, 72-76 (2010).
25. M Sonam, RP Singh, S Pooja. Phytochemical screening and TLC profiling of various extracts of *Reinwardtia indica*. **Int. J. Pharmacog. Phytochem. Res.**, **9**, 523-527 (2017).
26. SW Jeffrey. Paper-chromatographic separation of chlorophylls and carotenoids from marine algae. **Biochem. J.**, **80**, 336-342 (1961).
27. JA Mendiola, S Santoyo, A Cifuentes, G Reglero, E Ibáñez, FJ Señoráns. Antimicrobial activity of sub-supercritical CO<sub>2</sub> extracts of the green alga *Dunaliella salina*. **J. Food Prot.**, **71**, 2138-2143 (2008).
28. M Kannan, AJA Ranjit Singh, M Narayanan. Phytochemistry and immunopharmacological investigation of *Rubia cordifolia* Liin. (Rubiaceae). **Pharmacologyonline**, **3**, 653-662 (2009).
29. AJM Melo, EM Saito, B Schulze, SC Sticca. Expressão de pigmentos em algas pardas (*Canistrocarpus cervicornis* e *Padina*

- gymnospora)*: uma abordagem químicoecológica. Estudos ecológicos da Ilha de Santa Catarina, 2011.
30. B Tamburic, FW Zemichael, GC Maitland, K Hellgardt. Parameters affecting the growth and hydrogen production of the green alga *Chlamydomonas reinhardtii*. **Int. J. Hydrogen Energy**, **36**, 7872-7876 (2011).
  31. FS Oliveira, MC Soares, RL Costa, FRX Batista. Padronização do procedimento de determinação da clorofila utilizado como parâmetro para a estimativa da viabilidade celular em algas verdes. In: XIX Jornada em Engenharia Química, de 3 a 8 de Março de 2014.
  32. D Hornero-Méndez, G Britton. Involvement of NADPH in the cyclization reation of carotenoid biosynthesis. **FEBS Letters**, **515**, 133-136 (2002).
  33. M Rinawati, LA Sari, KT Pursetyo. Chlorophyll and carotnoids analysis spectrophotometer using method on microalgae. IOP Conference Series: Earth and Environmental Science, 441, 2<sup>nd</sup> **Int. Conf. Fisheries Marine Sc.**, 26 September, 2019, Surabaya, Indonesia, p. 1-21.
  34. MS Miranda, S Sato, J Mancini-Filho. Antioxidant activity of the microalga *Chlorella vulgaris* cultered on special conditions. **Bullett. Chimi. Farm.**, **140**, 165-168 (2001).
  35. AK Siddhanta, KH Mody, BK Ramavat, VD Chauhan, HS Garg, AK Goel, MJ Doss, MN Srivastava, GK Patnaik, VP Kamboj. Bioactivity of marine organisms: Part VIII-Screening of some marine flora of western coast of India. **Indian J. Exp. Biol.**, **36**, 638-643 (1997).
  36. H Song, M He, C Gu, D Wei, Y Liang, J Yan, C Wang. Extration optimization, purification, antioxidant activity, and preliminary structural characterization of crude polysaccharide from an artic *Chlorella* sp. **Polymers**, **10**, (2018).
  37. Q Hu, B Pan, J Xu, J Sheng, Y Shi. Effects of supercritical carbon dioxide extraction conditions on yields and antioxidant activity of *Chlorella pyrenoidosa* extracts. **J. Food Eng.**, **80**, 997-1001 (2007).
  38. M Premalatha, P Dhasarathan, P Theriappan. Phytochemical characterization and antimicrobial efficiency of seaweed samples, *Ulva fasciata* and *Chaetomorpha antennina*. **Int. J. Pharm Bio Sci.**, **12**, 2-16 (2011).
  39. R Uma, V Sivasubramanian, S Niranjali Devaraj. Preliminary phytochemical analysis and in vitro antibacterial screening of green micro algae, *Desmococcus olivaceus*, *Chlorococcum humicola* and *Chlorella vulgaris*. **J. Algal Bio. Util.**, **2**, 74-81 (2011).
  40. R Pratt, TC Daniels, JJ Eiler, JB Gunnison, WD Kumler, JF Oneto, LA Strait, HA Spoehr, GJ Hardin. Chlorellin, an antibacterial substance from *Chlorella*. **Science**, **99**, 351-352 (1944).
  41. VK Dhargalkar, XN Verlecar. Southern ocean seaweeds: a resource for exploration in food and drugs. **Aquaculture**, **287**, 229-242 (2009).
  42. MF Bobin, M Raymond, MC Martini. UVA/UVB absorption properties of natural products. **Cosmet Toiletries**, **109**, 63-78 (1994).
  43. IMP Violante, IM Souza, CL Venturini, AFS Ramalho, RAN Santos, M Ferrari. Avaliação *in vitro* da atividade fotoprotetora de extratos vegetais do cerrado de Mato Grosso. **Rev. Bras. Farmacog.**, **19**, 452-457 (2009).
  44. JS Mansur, MVR Breder, MCA Mansur, RD Azulay. Correlação entre a determinação do fator de proteção solar em seres humanos e por espectrofotometria. **An. Bras. Dermatol.**, **61**, 167-172 (1986).
  45. MM Costa, APA Farias, CAB Oliveira. Importância dos fotoprotetores na minimização de danos a pele causados pela radiação solar. **Braz. J. Devel.**, **7**, 101855-101867 (2021).
  46. AM Fernandes, SMC Siqueira, ML Furtado, AEQR Campos, AFV Pinheiro. Avaliação das atividades antioxidante e fotoprotetora da espécie *Syzygium cumini* (L.) Skeels. **Braz. J. Devel.**, **6**, 64719-64725 (2020).
  47. ML Furtado, SMC Siqueira, AM Fernandes, RA Montes, AO Alcântara, DP Oliveira, NAP Pinheiro, AFV Amorim. Avaliação *in vitro* da atividade fotoprotetora e antioxidante de extratos vegetais de *citrullus lanatus* (Thunb.) Matsum. & Nakai. **Braz. J. Devel.**, **7**, 6793-6812 (2021).
  48. M Ferrari, MSC Oliveira, AK Nakano, PA Rocha-Filho. Determinação do fator de proteção solar (FPS) *in vitro* e *in vivo* de emulsões com óleo de andiroba (*Carapa guianensis*). **Rev. Bras. Farmacogn.**, **17**, 626- 630 (2002).
  49. MCMR Souza, TG Horta, ES Melo, FDB Rocha. Câncer de pele: hábitos de exposição solar e alterações cutâneas entre agentes de saúde em um município de Minas Gerais. **Rev. Enf. Cen. Oes. Mineiro**, **6**, 1945-1956 (2016).
  50. RSP Calazans, LO Bulian, LO Alves, JO Salvi. Estudo fitoquímico e avaliação da citotoxicidade aguda frente à *Artemia salina* (Leach) de plantas comercializadas em feira-livre. **Rev. Uni. Vale Rio Verde**, **17**, 1-10 (2019).
  51. A Niccolai, E Bigagli, N Biondi, L Rodolfi, L Cinci, C Luceri, MR Tredici. *In vitro* toxicity of microalgal and cyanobacterial strains of interest as food source. **J. Appl. Phycol.**, **29**, 199-209 (2017).



## Cell encapsulation using chitosan: chemical aspects and applications

Maura Rojas Pirela<sup>1,2</sup>, Verónica Rojas<sup>2</sup>, Elizabeth Pérez Pérez<sup>1</sup>, Cristóbal Lárez Velásquez<sup>3\*</sup>

<sup>1)</sup> Laboratorio de Análisis Biotecnológico y Molecular (ANBIOMOL) "Prof. Guillermo López Corcuera"

Facultad de Farmacia y Bioanálisis, Universidad de Los Andes. Mérida 5101, Venezuela.

<sup>2)</sup> Instituto de Biología, Facultad de Ciencias, Pontificia Universidad Católica de Valparaíso, Valparaíso, Chile.

<sup>3)</sup> Laboratorio de Polímeros, Departamento de Química, Universidad de Los Andes, Mérida 5101, Venezuela

(\*) [clarez@ula.ve](mailto:clarez@ula.ve); [larezcristobal@gmail.com](mailto:larezcristobal@gmail.com)

Recibido: 07/10/2021

Revisado: 14/11/2021

Aceptado: 03/12/2021

### Abstract

In this work, the main approaches for the preparation of encapsulating matrices using chitosan-containing formulations have been reviewed. Various methodologies have been considered, such as physical intermolecular bonds and chemical cross-linking reactions, including the click reactions which have become novel in the cross-linking of systems containing this biopolymer. Likewise, the formation of different macroscopic assemblies such as spheroids, vesicles, layer by layer polycomplexes, etc., has been addressed. In the final part of the work, the main achievements reported with these matrices in the encapsulation of cells, both eukaryotic and prokaryotic, are discussed, emphasizing their potential applications and perspectives in different fields as medicine (treatment of traumatic diseases, diabetes, venous diseases, tissue regeneration, transplantation and tolerance); food (administration of probiotics); industrial applications (bioethanol production); etc.

**Keywords:** Cell encapsulating matrices; Click reaction; chemical crosslinking; ionotropic gelation

### Resumen

**Encapsulación de células usando quitosano: aspectos químicos y aplicaciones.** En este trabajo se han revisado los principales enfoques para la preparación de matrices encapsulantes utilizando formulaciones que contienen quitosano. Se han considerado diversas metodologías, como las uniones intermoleculares físicas y las reacciones químicas de entrecruzamiento, incluidas las reacciones *click*, las cuales se han vuelto una novedad en la reticulación de sistemas que contienen este biopolímero. Asimismo, se ha abordado la formación de diferentes ensamblajes macroscópicos como esferoides, vesículas, policomplejos capa a capa, etc. En la parte final del trabajo se discuten los principales logros reportados con estas matrices en el encapsulado de células, tanto eucariotas como procariotas, enfatizando sus potenciales aplicaciones y perspectivas en diferentes campos como la medicina (tratamiento de enfermedades traumáticas, diabetes, enfermedades venosas, regeneración de tejidos, trasplante y tolerancia); en la industria alimentaria (administración de probióticos); aplicaciones industriales (producción de bioetanol); etc.

**Palabras claves:** Matrices encapsulantes de células; reacción *click*; reacciones de entrecruzamiento; gelación inotrópica

### Introduction

Cell encapsulation basically consists of confining living cells within non-living matrices in order to protect their physical integrity, preserving also their normal metabolic activities, for their subsequent transit or use in risky environments for them. The method was proposed for the first time by Chang in the 60s of the previous century, showing different experimental approaches that allow it to be achieved<sup>1</sup>.

One of the main reasons for the encapsulation of cells is the protection that the encapsulating coating gives them, which is usually formed by a partially permeable polymeric membrane artificially created. Thus, in the case of transplanted cells,

encapsulation could prevent their rejection if it manages to "hide" them from the host's immune system (a process known as immunoisolation), without the need to use immunosuppressants<sup>2</sup>.

Research on new systems for cell encapsulation, or the improvement of already known systems, will always be very topical because the results are potentially applicable in the treatment of disorders associated with various diseases such as diabetes, neurological degeneration, hemophilia, cancer, kidney failure, etc.<sup>3-5</sup>. In a broader sense, the search for new matrices for the encapsulation of proteins, peptides, DNA, cells, and even microorganisms, has been oriented towards

the use of biomaterials such as polysaccharides, i.e., alginates<sup>6</sup>, agarose<sup>7</sup>, chitosan<sup>8</sup> (see chemical structures in figure 1); proteins, i.e., gelatin<sup>9</sup>, collagen<sup>10</sup>, silk fiber<sup>11</sup>; polynucleotides (RNA and DNA<sup>12</sup>) and some biodegradable polymers such as polylactic and polyglycolic acids and their copolymers<sup>13</sup> and polyhydroxyalcanoates<sup>14</sup> (see chemical structures in figure 2). Among the current most important reasons for the preference of these materials is their biodegradability, since it is intended that they not only be able to transport cells but also allow the design of controlled release systems towards well pre-established therapeutic targets.

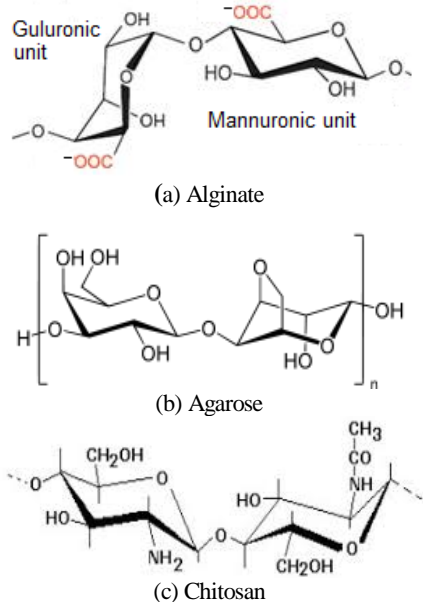


**Fig. 1:** Chemical structure of some polysaccharides employed in the cell encapsulation.

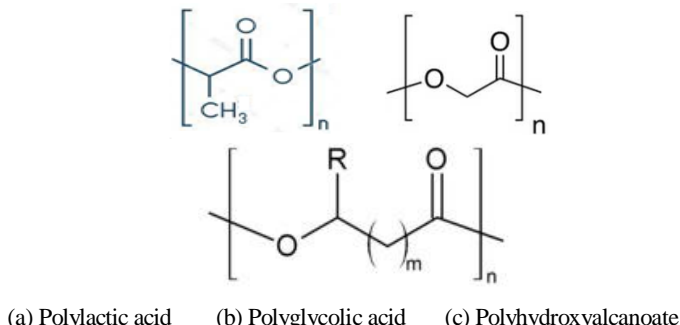


**Fig. 2:** Chemical structure of some biodegradable polymers employed in the cell encapsulation.

In this work, the main approaches using chitosan-containing formulations for the encapsulation of cells are reviewed. Different methodologies have been considered for the formation of the encapsulating matrix, such as physical and chemical cross-linking reactions, including click reactions. Likewise, the formation of different macroscopic structures such as spheroids, vesicles, layer-by-layer polycomplexes, etc., has been addressed. On the other hand, a brief discussion of the main achievements reported for the chitosan-containing matrices obtained during encapsulation of both, eukaryotic and

prokaryotic cells, is also presented, emphasizing their potential applications.

### Chemical aspects of the encapsulation of cells using chitosan

Chitosan is a highly versatile polysaccharide which is usually obtained by deacetylation of chitin, a relatively inexpensive material routinely extracted from industrial crustacean processing wastes. However, for applications in the health field, in recent years there has been a tendency to produce it from fungi to minimize the intoxication risks associated to marine product derivatives<sup>15</sup>. It is considered a prominent candidate for the encapsulation of a diversity of materials<sup>16</sup>, including cells, to be used in living systems because it has adequate properties for these purposes, such as its non-toxicity, biodegradability, and biocompatibility<sup>17,18</sup>. However, it is essential to consider that for such uses it is necessary to work with materials of high degrees of purity.

From a chemical point of view, some relevant chitosan-characteristic reactions can be established in this kind of applications. Thus, encapsulation of materials within envelopes or matrices containing chitosan in their composition can be achieved using various experimental approaches, such as:

- Formation of three-dimensional networks generated by intermolecular crosslinking due to physical interactions, which can be of various nature (hydrophobic<sup>19</sup>, hydrogen bonds<sup>19</sup>, molecular entanglement<sup>20</sup>, ionic interactions<sup>21</sup>, etc.).
- Three-dimensional networks formation caused by covalent bonds linking different polymer chains, which can be achieved through chemical reactions that do not include crosslinking agents<sup>22</sup> or that require their presence, whether they are low or high molecular weight<sup>23</sup>. Among these reactions have recently been included the so-called “click reactions”, also known as orthogonal reactions<sup>24</sup>, based on chitosan derivatives which are specially prepared for such purposes.

One of the most exploited characteristics of chitosan for this type of application is its cationic nature in aqueous acidic medium, which is enhanced in some derivatives such as quaternary ammonium salts in a wide pH range. This cationic character allows its electrostatic interaction with materials carrying anionic residues, as it has been shown in the preparation of microspheres encapsulating solutions of an anionic polyelectrolyte obtained by oxidation of the polysaccharide scleroglucan (generating pendant carboxylate residues along its chain) within a skin formed by the chitosan/scleroglucan polyelectrolyte complex<sup>25</sup>. Spheres are formed by simply dropping a polyanion solution into a chitosan solution in an acid medium. Similarly, the encapsulation of chitosan solutions within the skin formed by the polyelectrolyte complex of both biopolymers is also possible. An idealized picture of this type of sphere is shown in figure 3.

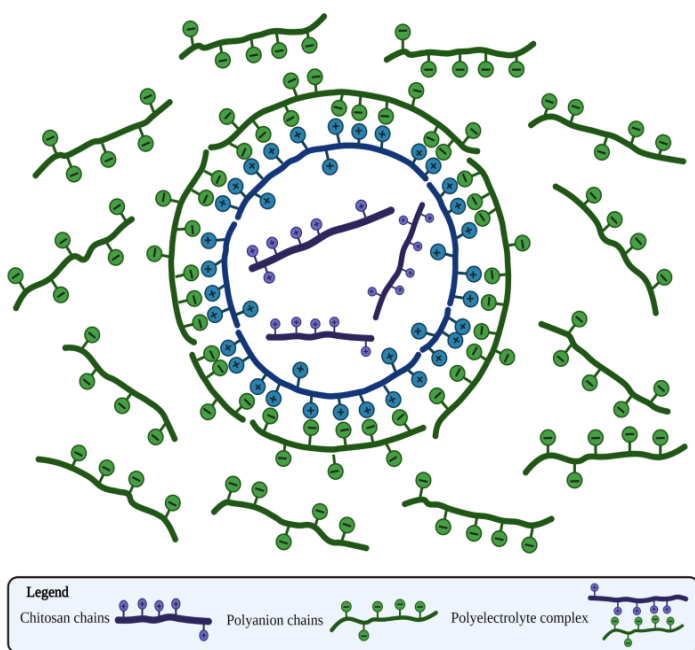


**Fig. 3:** Idealized structure of a sphere formed by interfacial polycomplexation of chitosan and a polyanion when a drop of chitosan solution is dropped into the polyanion solution.

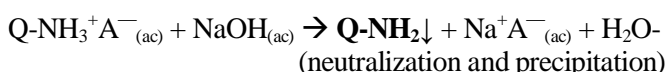
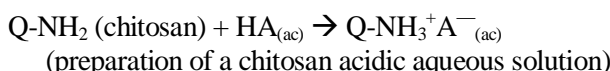
Some of the most common experimental methods of encapsulation that have been reported using containing-chitosan formulations are: spheres formation by ionotropic crosslinking, i.e., a suspension of cells in a aqueous chitosan solution is dropped over an aqueous solution of sodium tripolyphosphate (STPP) under agitation<sup>26</sup>; cell assemblies confined between layers of chitosan (built layer by layer)<sup>27</sup>; preparation of the gelling mixture containing the cells and its subsequent covalent crosslinking by various chemical routes, i.e., polymerization reactions with thermal initiation<sup>28</sup>; bioorthogonal reactions, in which the experimental conditions must be refined in order to achieve functional materials (considering the complex biological mixtures employed and the presence of living cells)<sup>29</sup>; etc.

#### *Chitosan cross-linking processes in the formation of encapsulating matrices*

A great variety of cross-linking processes using chitosan-containing formulations have been reported in the formation of encapsulating matrices. A summary of the most common ones is presented in the following sections.

#### Cross-linking by physical interactions:

- Precipitation due to pH change: neutralization of an acidic aqueous solution of chitosan ( $\text{Q}-\text{NH}_3^+ \text{A}^-_{(\text{ac})}$ ) with a base ( $\text{NaOH}$ ) leads to decreasing of chitosan cationic groups, favoring hydrogen bonding and/or hydrophobic interactions and causing its precipitation according to the following reactions:



- Aggregation by changing the solvent properties: addition of a miscible solvent (but less polar than water such as 1,2-propanediol) to an aqueous solution of chitosan, in acid medium, causes changes in the properties of the solvent, whose dielectric constant becomes lower<sup>19</sup>, unfailingly leading to gelation if right conditions are reached. As in the previous case, hydrogen bonding and hydrophobic interactions will be favored under the new conditions.

- Aggregation due to temperature changes: when the temperature of aqueous solutions of specific chitosan derivatives is increased, hydrophobic aggregates are formed due to the occurrence of a conformational transition which causes gelling of the system, i.e., aqueous solutions of poly(isopropyl-acrylamide)-grafted chitosan undergo gelling around 29.5 °C<sup>30</sup>.

- Ionotropic cross-linking: neutralization of the cationic charges of chitosan with low molecular weight polyanions, such as STPP, generates spherically assembled hydrogels with controllable size. The occurrence of this kind of process has also been reported with other similar polyanions, i.e., adenosine triphosphate (ATP), trisodium citrate, and sodium sulfate<sup>31</sup> (see structures in figure 4).

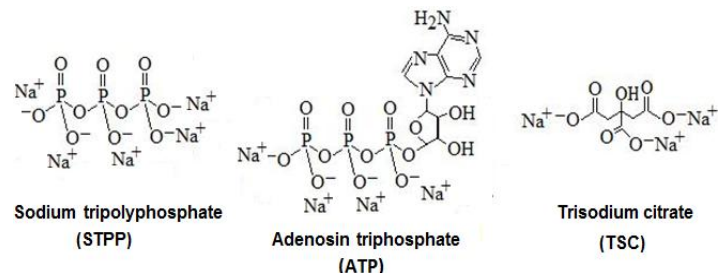


**Fig. 4:** Chemical structure of some low molecular weight polyanions used as crosslinking agents in ionotropic hydrogelation.

- Formation of polyelectrolyte complexes (PEC): neutralization of electrical charges of opposite sign (positive in chitosan and negative in polyanions) generates composite materials known as chitosan-based polyelectrolyte complexes<sup>32,33</sup>, which are also denominated as “chitoplexes”<sup>34</sup>. An important group of these materials, mainly due to their natural origin, are the so-called polyplexes, in which the polyanionic part would be made up of nucleic acids, i.e., plasmidic DNA<sup>35</sup>.

#### Chitosan chemical cross-linking:

- Through hydroxyl groups: a specific example of this type of reaction is its cross-linking with epichlorohydrin<sup>36</sup>; however, it is important to consider that to achieve the selective reaction of the -OH groups in chitosan, usually the primary hydroxyls of the C6 carbon, the amine groups must be previously protected by reactions such as phthaloylation<sup>37</sup> and formation of Schiff bases with aryl-aldehydes<sup>38</sup>, which allow their subsequent regeneration. The use of methanesulfonic acid as a solvent has also been reported as a method of protecting amine groups<sup>39</sup>. Other reactions that can lead to cross-linking through the -OH groups, after protection of the amine groups, are reactions with diacyl halides, i.e., adipoyl chloride<sup>39</sup>.

- Through amine groups: the most frequently reported covalent cross-linking reaction of chitosan, through the amine groups present on carbon C2, is the formation of Schiff bases with dialdehydes. In this regard, cross-linking using glutaraldehyde has been one of the most studied reactions (see simplified scheme in figure 5), although it has not yet been fully understood due to the complexity involved in this multifactorial process<sup>40</sup>. Although other dialdehydes have also been used for this purpose, such as glyoxal (figure 6a)<sup>41</sup>, the current emphasis has been moving to some related compounds, especially those of natural origin, such as genipin (figure 6b)<sup>42</sup> and vanillin (figure 6c)<sup>43</sup>, seeking to reduce toxic effects of aldehydes, among other things; nevertheless, it should be noted that cross-linking with this kind of compounds also proceeds through complex mechanisms. Macromolecular dialdehydes has also been assayed to chemical cross-linking of chitosan, i.e., scleroglucan-dialdehyde (figure 6d) obtained by the Malaprade reaction of scleroglucan (oxidation with potassium periodate of the polysaccharide produced by fungi of the genus Sclerotium)<sup>25</sup>. Similarly, a very interesting cross-linking reaction has been achieved using a chitosan-dialdehyde (figure 6e) generated by this same reaction to obtain a cross-linking material containing only chitosan and its dialdehyde derivative<sup>44</sup>.

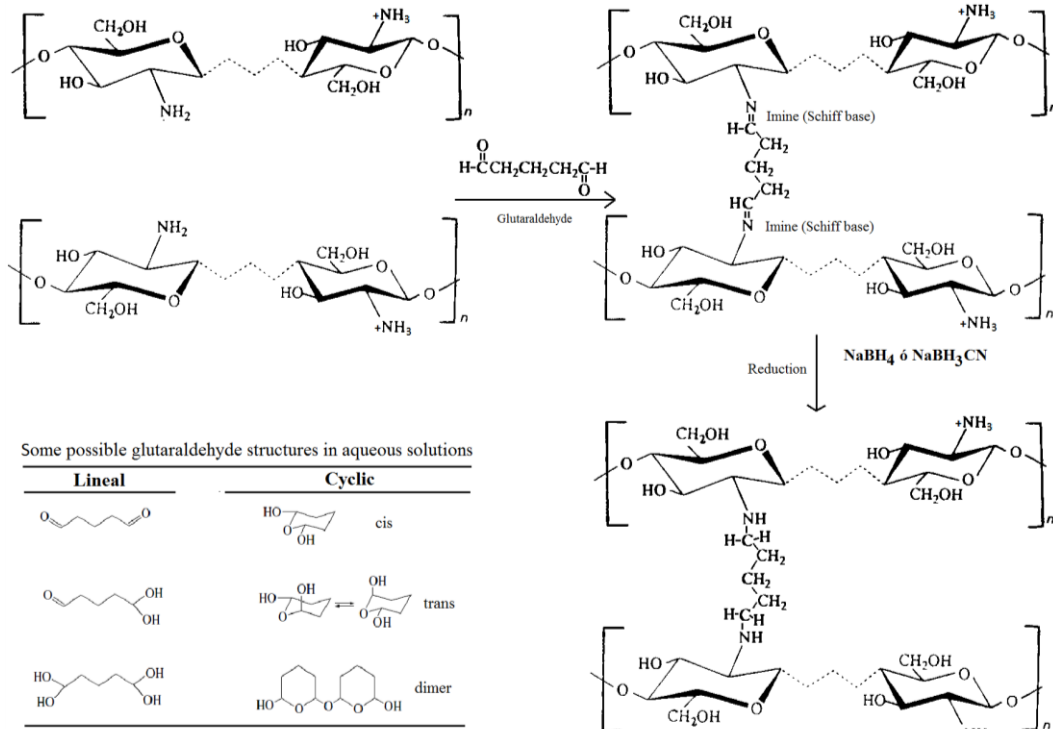


**Fig. 5:** Simplified scheme of the cross-linking reaction of chitosan with glutaraldehyde via Schiff base formation. The subsequent reduction of the imines and glutaraldehyde structures that can coexist in aqueous solutions are also shown.

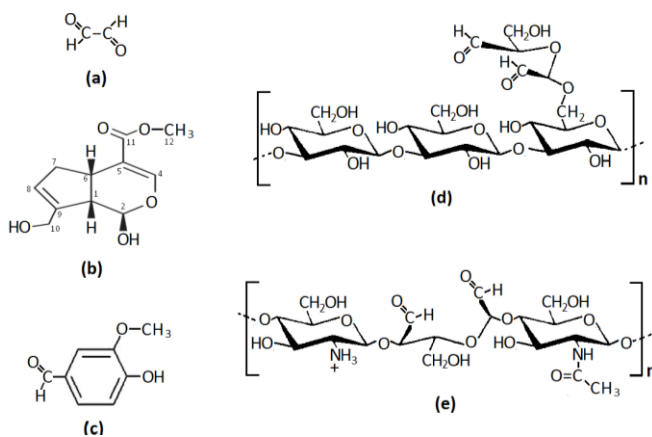


**Fig. 6:** Chemical structure of some compounds used in the chemical cross-linking of chitosan through the amine group at the C2 carbon: (a) glyoxal, (b) genipin and (c) vanillin, (d) scleroglucan-dialdehyde and (e) chitosan-dialdehyde.

- Through pendant groups added by derivatization: addition of

new pendant groups to the chitosan polymer chain can lead to new cross-linking reactions, which allow to obtain novel materials and open new horizons to the versatility of chitosan as a material for use in bioapplications. Generation of these pendant groups can be achieved through a wide variety of chitosan modification reactions, many of which can already be considered routine reactions, through both: amine group at the C2 carbon (acylation, alkylation, quaternization, phosphorylation, sulfation, etc.) as well as hydroxyl groups at C3 and C6 carbons (acylation, alkylation, silylation, halogenation, azidation, etc.)<sup>45</sup>. These derivatives can be subsequently manipulated to establish new processes for cell encapsulation, i.e., coupling of the derivative from 5-azido pentanoic acid and chitosan with ethoxylated glycerol tripropionate through a click reaction (figure 7), whose product has been assayed with good results in mesenchymal cell encapsulation<sup>24</sup>. Thus, click reactions have increased the prospects for chitosan as promising materials for such applications<sup>29,46</sup>.

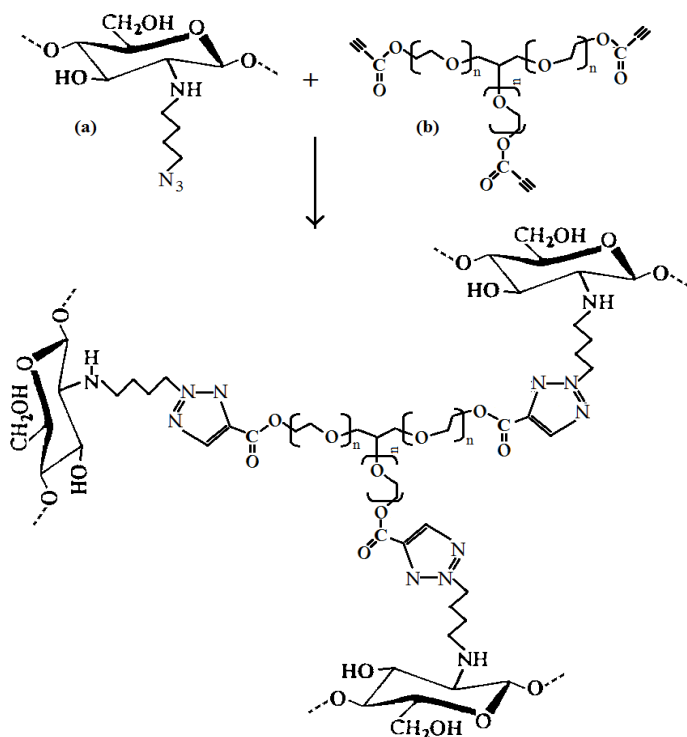


**Fig. 7:** Chemical cross-linking via click reaction between the derivative from 5-azido pentanoic acid/chitosan (a) and the ethoxylated glycerol tripropionate (b).

### Cell encapsulation using chitosan

Chitosan derivatives, and their combinations with other natu-

ral and synthetic polymers, are among the most studied polymeric materials for cell encapsulation<sup>47-52</sup>. Various types of eukaryotic and prokaryotic cells have been used in numerous studies of cell encapsulation with these biopolymers (figures 8-10). Encapsulation of some eukaryotic cells such as chondrocytes<sup>53,54</sup>, fibroblasts<sup>47,55</sup>, stem cells<sup>56</sup>, mesenchymal cells<sup>57</sup>, hepatocytes<sup>58</sup>, erythrocytes<sup>59</sup>, pancreatic  $\beta$ -cells<sup>60</sup>, cardiomyocytes<sup>61</sup>, etc., have served as the basis for studies focused on cell therapy for the treatment of certain pathologies<sup>48,49,62-65</sup>, transplantation and immune tolerance<sup>50,59,65-68</sup>, tissue regeneration<sup>47,68</sup> and industrial applications<sup>69</sup>. On the other hand, the encapsulation of bacteria<sup>70-76</sup> has been focused mainly on the oral administration of probiotics<sup>70</sup> and the treatment of some diseases<sup>53</sup>. Each of these topics will be briefly discussed in the following sections.

#### Eukaryote cells encapsulation

**Pathology treatments:** chitosan has been used as encapsulating material for mesenchymal stem cells (MSCs) in the treatment of traumatic diseases in which a traumatic injury has occurred, i.e., in the spinal cord (figure 8A); chitosan not only maintains the cellular viability of MSCs but also allows these cells to release vesicles and extracellular trophic factors (growth factors, chemokines, and cytokines), as well as maintain their antioxidant characteristics<sup>48</sup>. MSCs appear to exert a paracrine action that can therapeutically enhance spinal cord regeneration, limiting glial cicatrization<sup>76</sup>, reducing cell death at the injured site<sup>77</sup>, and acting as

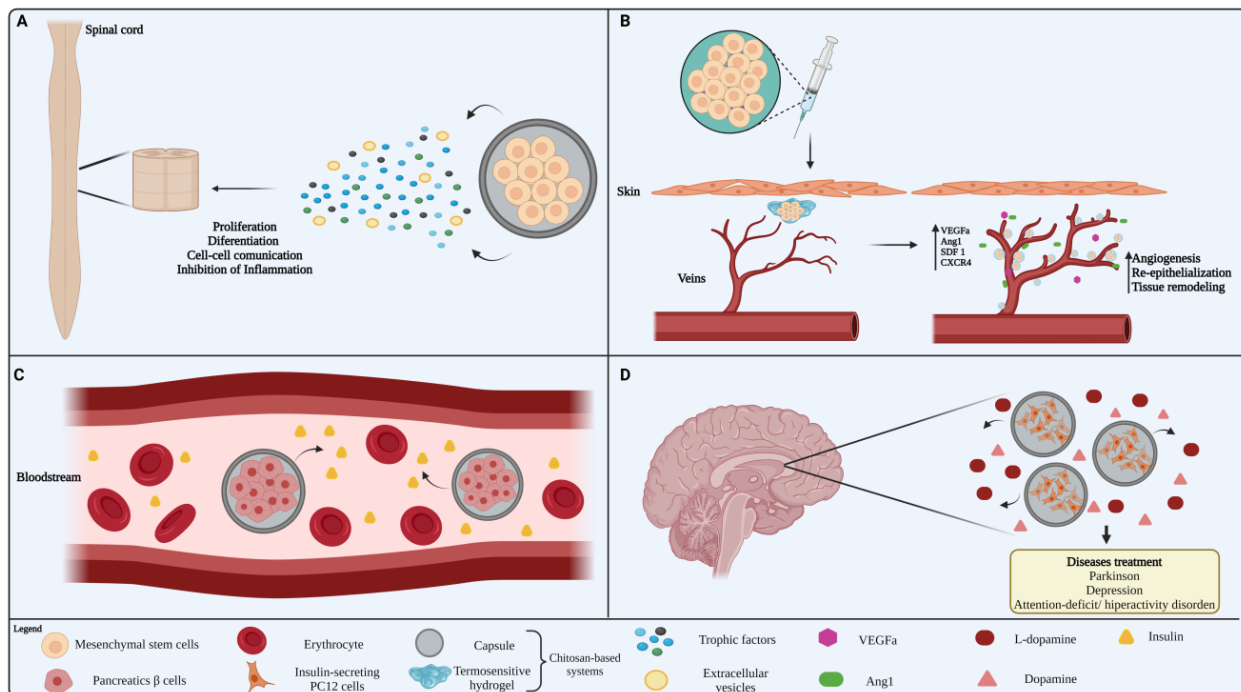


**Fig. 8:** Encapsulation of eukaryotic cells in chitosan-based systems for treatment of some pathologies. **A.** Traumatic diseases: the release of trophic factors and extracellular vesicles by MSCs promotes the regeneration of the nervous tissue; **B.** Venous diseases: encapsulated MSCs release paracrine factors that modulate inflammation, angiogenesis, and tissue remodeling; **C.** Metabolic diseases such as diabetes: encapsulated pancreatic  $\beta$ -cells could be used as a controlled insulin delivery system for the control of blood glucose; **D.** Neurodegenerative diseases: encapsulation of some neurotransmitter-secreting cells, such as PC12 cells, would be used as a strategy for the treatment of diseases associated with neurotransmitter deficiency or secretory cell dysfunction.

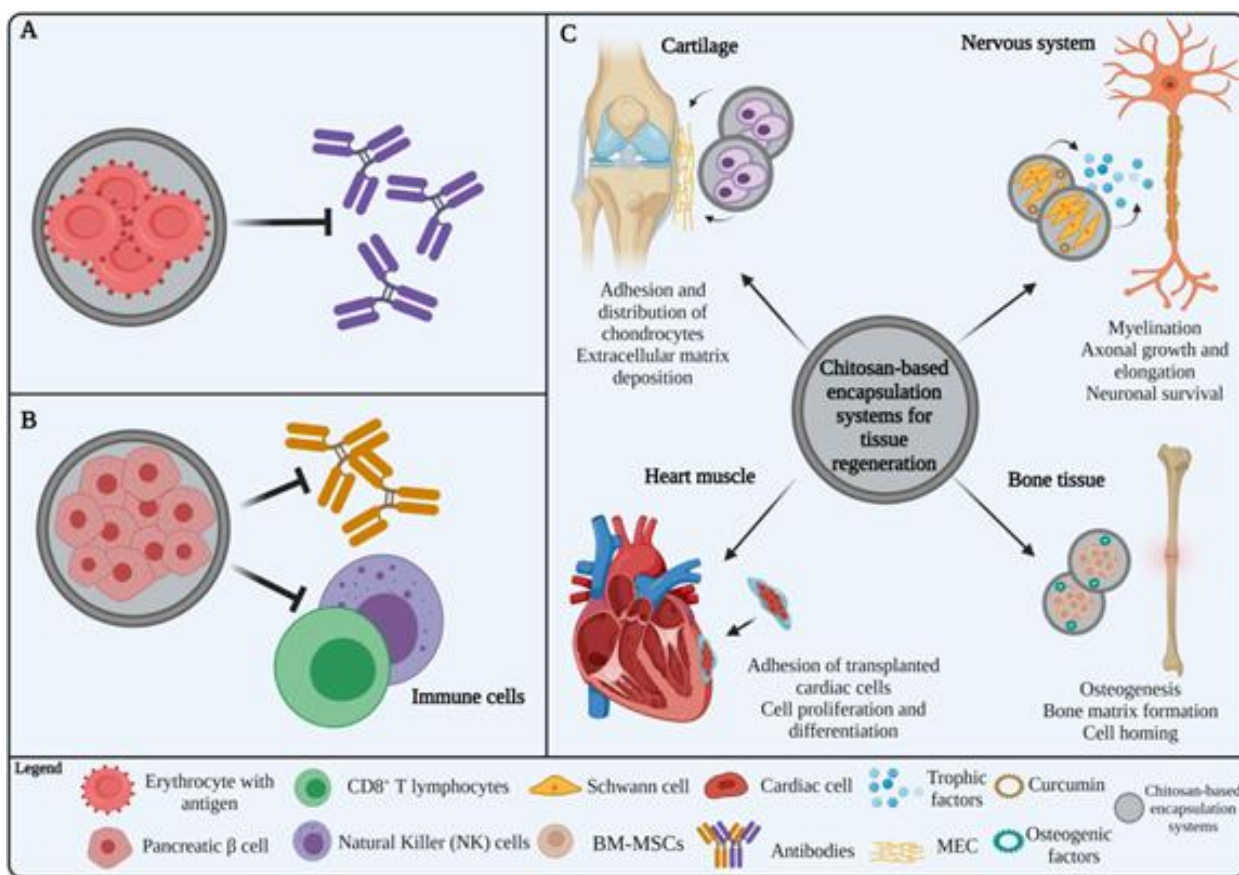


**Fig. 9:** Encapsulation of eukaryotic cells in chitosan-based systems for tissue transplantation and regeneration: **A.** Erythrocyte transfusion: encapsulation of erythrocytes expressing surface antigens could prevent the antibodies binding to them and, consequently, attenuate recognition of the system host immune; **B.** Pancreatic cell implantation: encapsulation of  $\beta$ -cells would inhibit the adhesion of antibodies to these cells, preventing cytotoxicity mediated by natural killer (NK) and CD8<sup>+</sup> T cells; **C.** Tissue regeneration: the encapsulation of different types of cells could be a strategy for the regeneration of various tissues (cartilage, nervous system, bone, heart muscle, etc.).

a carrier of signal molecules that regulate cell-to-cell and cell-extracellular matrix communications<sup>48</sup>. Together with MSCs, chitosan could orchestrate the modulation of inflammation, promoting the establishment of a less hostile environment after traumatic injury and, subsequently, the survival of transplanted cells<sup>48</sup>.

In other cases, such as diabetes and venous diseases, the injection of heat-sensitive hydrogels of chitosan/collagen/ $\beta$ -glycerophosphate ( $\beta$ -GP) containing three-dimensional spheroidal mesenchymal stem cells (3D MSC) has been studied to accelerate the healing of chronic wounds<sup>62</sup> (figure 8B). The combination of these polymers promotes a conducive environment for encapsulated MSCs, especially accelerating the adhesion, proliferation, secretion, and expression of paracrine factors, such as vascular endothelial growth factor A (VEGFA), angiopoietin 1 (Ang1), factor 1 derived from stromal cells (SDF1) and its chemokine receptor 4 with CXC motif (CXCR4) which, in addition, to reduce inflammation, also promote angiogenesis, re-epithelialization and tissue remodeling in the wound<sup>78</sup>.

Besides being proposed for the treatment of venous insufficiency linked to diabetes, encapsulation of pancreatic  $\beta$ -cells in microcapsules of alginate/chitosan (AC) and algi-

nate/chitosan/PEG (ACPEG) could be used as a delivery system for insulin-controlled release for blood glucose control (figure 8C)<sup>49</sup>. These materials could represent a suitable system for pancreatic cell support and insulin secretion. Its permeable-selective nature allows the diffusion of nutrients and the production and release of insulin<sup>49</sup>, offering a therapeutic alternative to traditional treatments of insulin injections and diet. Encapsulation of PC12 cells with chitosan has been evaluated (figure 8D) as a therapeutic strategy for neurodegenerative diseases associated with the loss of dopamine in the cerebral striatum, i.e., Parkinson's disease<sup>79</sup>. PC12 is a dopamine-secreting cell line of great interest in studies of neuroprotective models for Parkinson's disease<sup>80,81</sup>. Besides promoting the viability of PC12 cells, its encapsulation with chitosan stimulates them to produce and release catecholamines and their precursors, such as L-dopa and dopamine, even four weeks after encapsulation<sup>80</sup>. The difference in the secretory capacities of these encapsulated cells is attributed to a possible chitosan interaction with some adhesion molecules present on the cell surface<sup>80</sup>. Therefore, the use of dopamine-secreting cells can be considered as a strategy for treatments of Parkinson's and other diseases associated with dopamine deficiency or secretory cell dysfunction<sup>82,83</sup>. Transplantation and tolerance: microencapsulation is considered a very

promising tool for immuno-isolation in transplantation and immune tolerance studies<sup>84</sup>. In addition to re-presenting an alternative to the chronic suppression of the patient's immune system, which makes these patients vulnerable to other diseases, the encapsulation of living cells serves as an immuno-permeable barrier, increasing cell viability after transplantation. Additionally, these encapsulation systems act as selectively permeable barriers, allowing the free diffusion of nutrients and metabolic waste, and improving cell survival<sup>84</sup>.

Some studies have suggested that cell encapsulation with this polymer is a novel and effective strategy in tissue engineering<sup>50,59,65-68,79</sup> (figure 9). Cell transplantation has been proposed as a strategy for the immuno-camouflage of living and functional red blood cells<sup>69</sup>. Encapsulation of erythrocytes in ACPEG capsules could be used to prevent the binding of antibodies to red blood cells and, consequently, to attenuate the recognition of the host's immune system<sup>69</sup> (figure 9A) This strategy would be a great advance in transfusion therapies, since it would allow the production of universal red blood cells, without the use of specific enzymes for the elimination of surface antigens<sup>85,86</sup>. Furthermore, it would be a great advantage in transfusion therapies, especially for rare blood groups<sup>86</sup> or in regions where the frequency of certain blood groups is very low<sup>11</sup>. Transplantation of encapsulated pancreatic  $\beta$ -cells in chitosan-based systems in the treatment of diabetes, additionally to being an alternative for the production of insulin, would function as a barrier minimizing the damage induced by the inflammatory responses to the transplanted cells<sup>49</sup> (figure 9A), contributing to longer life and function during a xenogeneic transplantation<sup>53</sup>. A similar situation can occur for Parkinson's disease, where encapsulation of cells such as PC12 will not only allow the controlled release of dopamine but would also be a method to safely confine these tumor cells and isolate them from the immune system<sup>79</sup>.

It should be noted that the immuno-isolating capacity of chitosan microencapsulation is not only attributed to the ability to inhibit the adhesion of antibodies (including IgG) to the transplanted cells<sup>55</sup>, but also to the prevention of cytotoxicity mediated by natural T killer cells (NK) and CD8<sup>+50</sup> (figure 9B). These cells are crucial in the vertebrate immune system because they act as regulatory agents of the alloimmune response in transplanted patients<sup>89-91</sup>. Notably, CD8<sup>+</sup> cells can escape to the immunosuppressive effects of drugs such as cyclosporin and rapamycin<sup>91</sup>, whereby cell encapsulation with polymers such as chitosan could be an alternative for immune suppression therapy in transplanted patients because of an attenuating effect on immune cells escaping of immunosuppressive drugs effects could be additionally obtained.

**Tissue regeneration:** due to its biological properties, chitosan has been widely studied as a very promising material in regenerative medicine, being used as scaffolds or platforms

for the repair and/or regeneration of various tissues, including skin, bone, liver, cartilage, nerves, and muscle<sup>81</sup> (figure 8C).

**Cartilage regeneration:** encapsulation of chondrocytes with chitosan-containing systems is considered a great tool in tissue engineering and orthopedics<sup>53,92-95</sup>. The covering obtained with chitosan/hyaluronic acid (HA) fulfilling a temporary function of extracellular matrix (ECM) and creates a favorable chondrogenic microenvironment due to the promotion of deposition of cartilaginous extracellular matrix (CCEM) components by encapsulated chondrocytes<sup>93</sup>, facilitating adhesion and uniform distribution of chondrocytes at the implant site<sup>53,94</sup> (figure 9C.1). Furthermore, proliferative activity and differentiation of chondrocytes are stimulated by the presence of these polymers<sup>93</sup>. It should be noted that the encapsulation of adipose tissue-derived stromal cells (ADSC) with chitosan/ $\beta$ -glycerophosphate/starch has been considered as an alternative for the regeneration of cartilage tissue; encapsulation of these cells with these polymers promotes chondrocytic differentiation and CEM accumulation<sup>95</sup>.

**Nervous system regeneration:** several studies have evaluated the encapsulation of neuronal stem cells (NMCs) with chitosan derivatives as a strategy for the repair of nervous tissue<sup>96,97</sup> (figure 9C.1). In murine nerve cells encapsulation studies and injection of neural progenitors-spheroid-type aggregates with self-healing hydrogels (SH-H) of glycol-chitosan and benzaldehyde-difunctionalized PEG, at both ends (DF-PEG), induced proliferation and differentiation to neuron-like cells was observed. In addition, cells encapsulated with SH-Hs had the ability to regenerate and rescue neural function in the central nervous system (CNS) of a zebrafish embryo neural injury model (*Danio rerio*), caused by exposure to ethanol<sup>96</sup>. Similarly, the SH-Hs treatment loaded with spheroid neural stem cells (NSCs), additionally to restoring neuronal functions, had a positive influence on the development and hatching rate of treated embryos. The advantage of these neural progenitors encapsulated with SH-Hs could be attributed to their ability to fill physical spaces associated with injuries<sup>97</sup> and facilitate metabolism, oxygen availability, migration and cell-cell communication, creating an adequate microenvironment for the proliferation of encapsulated NSCs<sup>96,97</sup>. On the other hand, the encapsulation of Schwann cells (SCs) with chitosan has also been studied<sup>98</sup> (figure 9C.1). SCs are glial cells that play an important role in the regeneration of the injured peripheral nervous system (PNS)<sup>99</sup>. In this study, the sciatic nerve regeneration was evaluated *in vivo* using artificial neural guide channels of poly-L-lactic acid contained with SCs and curcumin encapsulated in chitosan nanoparticles<sup>98</sup>. Treatment with these nanoparticles induced a significant increase in the number of axons in the injured sciatic nerve, as well as a restoration of motor and sensory function<sup>99</sup>.

In these systems, SCs would play an important role in nerve regeneration through the release of neurotrophic factors, i.e., neurotrophic factor derived from the glial cell line (GDNF)<sup>100</sup> and growth factors such as nerve growth factor (NGF)<sup>101</sup>, which contribute to the myelination process, promotion of growth and axonal elongation, as well as survival of neurons<sup>100,101</sup> (figure 9C.1). On the other hand, curcumin would act as a factor to decrease apoptosis<sup>98</sup> and stimulate the proliferation of SCs<sup>102</sup> and, consequently, improve the regeneration and functional recovery of injured nerve. Encapsulation and transplantation of SCs together with compounds that facilitate their activity could have a great influence on the therapeutic activity of these cells, notably improving neuronal regeneration therapy.

**Bone regeneration:** the encapsulation of osteoblasts with chitosan hydrogels has been proposed as a method to transport osteoblast cells in bone disorders treatments<sup>103</sup> (figure C.3). A greater adhesion, proliferation, and expression of type 1 collagen (collagen more abundant in the vertebrate ECM) was achieved through the manufacture of a 3D tracing system to make tissue scaffolds based on pure chitosan and chitosan cross-linked with pectin and genipin, as well as a higher mineralization activity in osteoblast cells *in vitro*<sup>103</sup>. Likewise, some reports based on the encapsulation of stromal MSCs derived from human bone marrow (BM-MSCs), which can self-renew and differentiate into multiple cell lines, demonstrated that its encapsulation in chitosan/dextran hydrogels not only maintained their viability but could also differentiate into adipocytes and osteocytes<sup>104</sup>. Similarly, encapsulation of BM-MSCs together with osteogenic factors, such as bone morphogenic protein-2 (BMP2), in chitosan/poly ( $\epsilon$ -caprolactone) heat-sensitive gels have a positive effect on osteogenesis and bone matrix formation<sup>105</sup> (figure 9C.3). More importantly, the encapsulation of these MSCs not only influences their proliferation and differentiation, but they could also serve as an alternative to take advantage of some signaling pathway, such as the stromal cell-derived factor-1 (SDF-1)/CXC receptor 4 (CXCR4) route, very important in the process of mobilization and relocation or "homing" of MSCs<sup>106,107</sup>. Studies focused on MSCs derived from human adipose tissue (hASCs) revealed that after being injected and promoted the over-expression of their chemokine receptor CXC type 4 (CXCR4) these cells had the ability to respond and migrate towards the derived stromal cell factor (SDF-1a), which was released from a injectable thermosensitive hydrogels of chitosan/ glycerolphosphate/ hydroxylethylcellulose (CH/GP/ HEC)<sup>107</sup>. The expression of CXCR4 in cells and the concomitant release of its ligand SDF-1a from CH/GP/HEC hydrogels led to increased localization/retention of hASCs<sup>107</sup>. In addition to the massive infiltration of hASCs, in response to SDF-1a, a process of close vascularization was observed, which could indicate that these hydrogels would act as optimal supports for the migration of endogenous cells, which could facilitate repair and regeneration of tissues.

**Regeneration of cardiac muscle tissue:** options for the treatment of myocardial infarction are very limited<sup>62</sup> due to the inability of the mature myocardium to regenerate<sup>109</sup>. However, encapsulation of cardiac cells (cardiomyocytes and myoblasts) in photo-crosslinkable hydrogels, obtained from azidobenzoic acid-chitosan- and acryloyl-poly(ethylene glycol)-RGDS (Az-chitosan/Acr-PEG-RGDS), was evaluated as an alternative for regeneration of cardiac tissue (figure 9C.4), obtaining evidence of adhesion, proliferation and differentiation of encapsulated C2C12 myoblasts<sup>62</sup>. Likewise, a high viability of neonatal rat cardiomyocytes encapsulated in these photo-crosslinkable hydrogels was observed. Importantly, when adhesion of these hydrogels in the cardiac tissue was evaluated, it was evident that they remained adhered in the different parts of the heart where were applied, both on the surface (epicardium) and within the ventricle, a relevant fact for the treatment of myocardial infarction<sup>62</sup>.

**Other applications:** chitosan microencapsulation of some yeasts has also been studied for therapeutic and industrial purposes<sup>76,110,111</sup>. Encapsulation of the probiotic *Saccharomyces boulardii* in alginate/chitosan (AC) microspheres showed to have positive effects on its survival, protecting it from acid degradation and accelerating its transit through the gastrointestinal tract<sup>76</sup>; the use of this yeast with similar microencapsulation systems could be of great application not only for the therapies of inflammatory bowel diseases<sup>112</sup> but also for infectious enteritis<sup>113</sup> and enterocolopathies associated with *Clostridium difficile*<sup>114</sup>. On the other hand, the use of alginate/chitosan/alginate (ACA) and genipin/alginate/chitosan (GAC) has been proposed for industrial applications as an attractive method for the encapsulation of yeasts in the production of bioethanol<sup>111</sup>; these systems would improve the stability of the cells and the tolerance to the inhibitors, increasing the amount of biomass inside the reactor and decreasing the cost of recovery, as well as recycling and subsequent processing of the cells. Apparently, encapsulation with systems such as ACA and GAC attenuates the effect of ethanol concentration on yeast growth, which would imply a protective action related to tolerance to stress conditions in the culture.

#### *Encapsulation of bacteria*

**Administration of probiotics:** one of the main challenges in supplementing food with probiotics is that these can remain active in different environmental conditions. In addition to resisting oxygen exposure while functional food products are in storage, probiotics must face up to the host's harsh gastrointestinal conditions (such as gastric pH, bile salts, and enzymes) once ingested<sup>115,116</sup>. Thus, microencapsulation is classified as one of the main solutions for the preservation of probiotics, especially that based on some polymers such as chitosan<sup>71,116-119</sup>. Chitosan has been used in the protection of probiotic cells mainly as a coating/covering, and not as the capsule itself<sup>72,73,120</sup>. Some studies carried out with different bacterial strains have shown that the use of alginate microcapsules

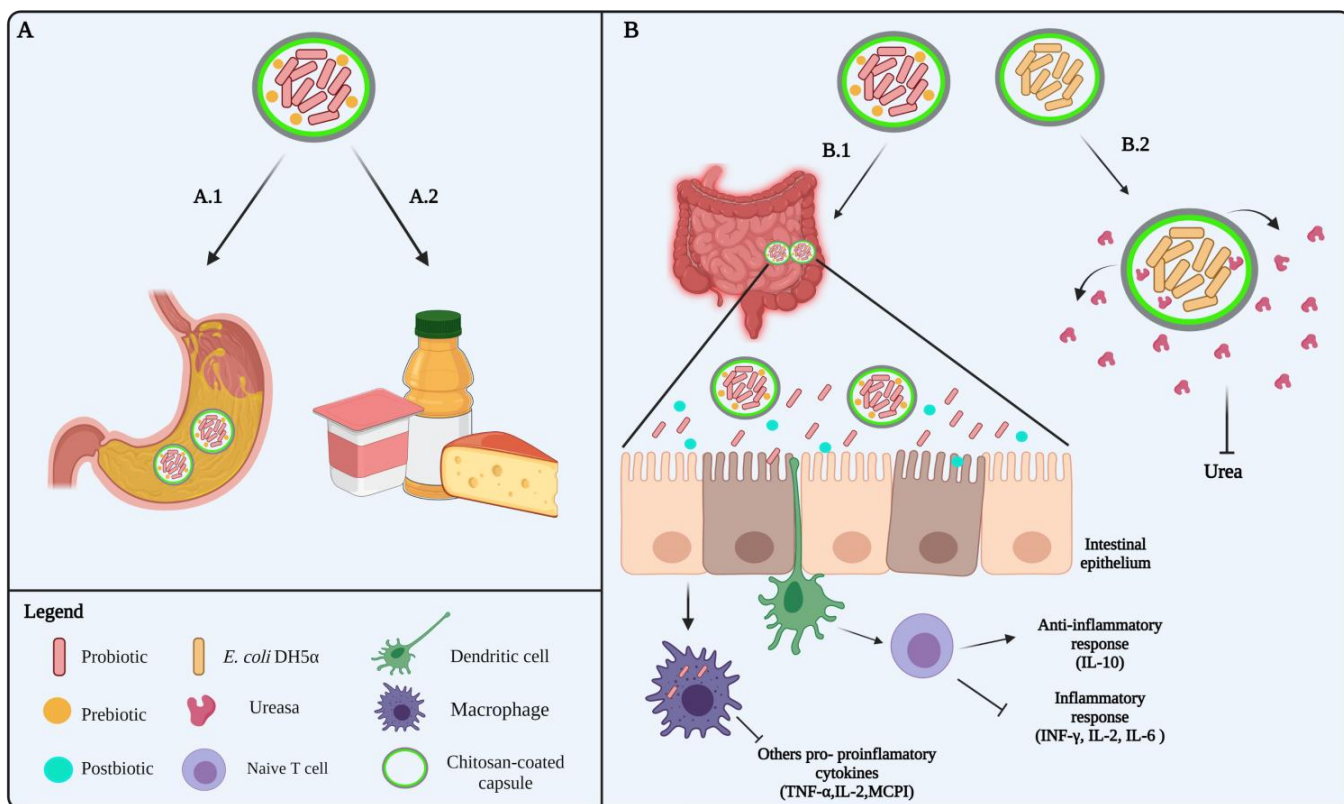


**Fig. 10:** Encapsulation of prokaryotic cells in systems containing chitosan. **A.** Probiotic protection would allow the storage and protection of the organism in different environmental conditions: **A.1** Efficient protection of probiotics in extreme conditions of stomach pH, bile and digestive enzymes, resulting in a greater number of viable cells in the intestine, **A.2** Confinement of probiotics could contribute to the stability of the microorganism in food matrices; **B.** Encapsulation of probiotics could be used in the treatment of some pathologies such as: **B.1** Bowel inflammatory diseases taking advantage of its anti-inflammatory effect, **B.2** Disorders associated with chronic kidney diseases, i.e., uremia, through overexpression and release of recombinant urease in genetically modified bacteria.

coated with chitosan is the best option for the storage and protection of probiotic bacteria, such as *Lactobacillus* and *Bifidobacterium* spp., under different experimental conditions<sup>64,65,67</sup>. Furthermore, chitosan-coated pectin capsules have been reported to efficiently protect *Lactobacillus casei* CIMB 30185 from extreme stomach pH conditions, resulting in increased numbers of viable cells in the intestine<sup>68</sup>.

In addition to protecting or improving the efficiency of the probiotic, some symbiotic encapsulation systems based on chitosan have been developed<sup>71</sup>. In these systems, contrary to others, a prebiotic or a specific carbon source of this is added<sup>120</sup> (figures 10A and 10B) which, in addition to serving as a substrate, can contribute to the stability and survival of the probiotic. A study using symbiotic systems based on AC/*L. casei*/selenium-enriched green tea (TVS) showed that the presence of TVS increases the probiotic survival at a storage temperature of 4 °C, under experimentally simulated gastric and bile solution conditions<sup>71</sup>. Similarly, the co-encapsulation of anthocyanins with *L. casei*, in addition to having a positive effect on the survival of the probiotic in simulated gastric conditions, improves the stability of the microorganism in food matrices such as yogurt<sup>121</sup>. Fur-

thermore, the use of other prebiotics such as inulin and starch has been reported in the co-encapsulation of lactic bacteria such as *Lactobacillus acidophilus*<sup>122,123</sup>. Comprehensively considered, these studies prompt that chitosan encapsulation and/or coating systems can lead to remarkable advances in the development of food and nutraceutical ingredients with markedly improved functionalities.

**Treatment of diseases:** the encapsulation of bacterial cells in AC gels has been proposed as an oral therapy strategy for some disorders such as inflammatory bowel diseases (Crohn's disease and ulcerative colitis) and uremia<sup>63,64</sup> (figures 10B.1 and 10B.2, respectively). Encapsulation of bacteria such as *Escherichia coli* strain Nissle 1917 (EcN), an organism with probiotic properties, was shown to have an anti-inflammatory and immunomodulatory effect in a colitis rat model<sup>64</sup>. The anti-inflammatory effect of probiotics is attributed to the modulation of the immune system in the intestinal micro-environment<sup>124</sup>, specifically through the modulation of the function of some immune cells, such as dendritic cells (DCs) and macrophages, and intestinal epithelial cells, mediating the activation of pattern recognition receptors (PRR) such as Toll-like receptors (TLR) expressed on cell surfaces<sup>125</sup>. Probiotic binding to some of the

TLRs, i.e., TLR2, can inhibit the secretion of cytokines and pro-inflammatory mediators, such as monocyte chemoattractant protein 1 (MCP1), tumor necrosis factor-alpha (TNF- $\alpha$ ), interleukins (IL-6, IL-2), but in turn promotes an increased expression of anti-inflammatory cytokines (IL-10)<sup>64,125,126</sup> (figure 10B.1) through the regulation of some signaling pathways, such as the NF- $\kappa$ B pathway and others such as that one triggered by mitogen-activated protein kinases (MAP kinases)<sup>127</sup>. Furthermore, some molecules produced and released by organisms such as bifidobacilli and lactobacilli, also known as postbiotics, can contribute to the anti-inflammatory effect of these organisms. These molecules, which are mainly short-chain fatty acids (SCFA), in particular propionate, acetate and butyrate, apparently exert their action by binding to specific receptors on intestinal epithelial cells (figure 10B.1). Association with these receptors induces the inhibition of the NF- $\kappa$ B signaling pathway and the production of pro-inflammatory cytokines by macrophages<sup>128,129</sup>. Similarly, these fatty acids can promote the induction of differentiation and expansion of regulatory T cells<sup>130</sup>. The encapsulation of some postbiotics with chitosan would be an alternative for the therapy of inflammatory diseases in immune-deficient patients, which could be affected by the administration of bacteria. This could become an interesting topic of study in the very near future.

In the treatment of uremia, a disorder associated with chronic kidney diseases, a genetically manipulated strain of a *Escherichia coli* DH5 harboring the gene encoding urease was used as a model for *in vitro* and *in vivo* evaluation of the ACA microcapsules in oral therapy of this disease; these studies revealed that encapsulation not only had a protective effect on the survival of cells in the gastric environment but also that encapsulated cells could remove urea from the medium<sup>63</sup> (figure 10B.2), suggesting that micro-encapsulation could allow safe and effective oral administration of live bacterial cells for various clinical applications (figure 10B.2).

### Concluding Remarks

Cell encapsulation has become a remarkably successful tool whose utilization seems to extend into different biotechnological fields given its potential to improve key aspects of *in vitro* and *in vivo* cell cultures, including proliferation and differentiation processes, especially in terms of providing greater protection to cells and avoid its recognition by the defense mechanism of the hosts. After 70 years of its initial implementation, it can be said that cell encapsulation is here to stay. Moreover, the development of new and exciting biomaterials over time, which has accelerated dramatically in recent years, seems to guarantee new successes in the years to come.

The valuable biological properties of chitosan, derived from its natural origin, have allowed its approval as an

excipient by the European and American pharmacopoeia (chitosan hydrochloride<sup>131</sup> and chitosan<sup>132</sup>, respectively). Thus, being chitosan a biomaterial so widely studied for promising applications in areas related to biotechnology such as biomedicine, food, agriculture, etc., it is believed that there will be a significant growth in research on new processes for obtaining it with higher purity indices and from new sources, as well as also in the preparation of derivatives specially designed to achieve specific objectives in cell encapsulation. In this context, click reactions can be seen as one the most logical routes to obtain new encapsulation methods using chitosan derivatives, although this field remains practically virgin due to the existence of a wide variety of others chemical reactions that could theoretically be incorporated into this scheme but they are still awaiting their experimental trial.

### References

1. TM Chang. Semipermeable microcapsules. *Science*, **146**, 524–525 (1964)
2. T Wang, J Adcock, W Kühtreiber, D Qiang, KJ Salleng, I Trenary, P Williams. Successful allotransplantation of encapsulated islets in pancreatectomized canines for diabetic management without the use of immunosuppression. *Transplantation*, **85**, 331–337 (2008).
3. Espona-Noguera, J Ciriza, A Cañibano-Hernández, G Orive, RM Hernández, L Saenz del Burgo *et al.* Review of Advanced Hydrogel-Based Cell Encapsulation Systems for Insulin Delivery in Type 1 Diabetes Mellitus. *Pharmaceutics*, **11(11)**, article number 597, 28 pages (2019).
4. M Hashemi, F Kalalinia. Application of encapsulation technology in stem cell therapy. *Life Sciences*, **143**, 139–146 (2015).
5. M Farina, JF Alexander, U Thekkedath, M Ferrari, A Gratttoni. Cell encapsulation: Overcoming barriers in cell transplantation in diabetes and beyond. *Advanced drug delivery reviews*, **139**, 92-115 (2019).
6. P De Vos, HA Lazarjani, D Poncelet, MM Faas. Polymers in cell encapsulation from an enveloped cell perspective. *Advanced Drug Delivery Reviews*, **67(68)**, 15–34 (2014).
7. JE Park, J Lee, ST Lee, E Lee E. *In vitro* maturation on ovarian granulosa cells encapsulated in agarose matrix improves developmental competence of porcine oocytes. *The riogenology*, **1(164)**, 42–50 (2021).
8. G Fundueanu, M Constantin, S Bucatariu, A Nicolescu, P Ascenzi, LG Moise *et al.* Simple and dual cross-linked chitosan millicapsules as a particulate support for cell culture. *International Journal of Biological Macromolecules*, **143**, 200-212 (2020).
9. A Blocki, F Löper, N Chirico, AT Neffe, F Jung, C Stamm *et al.* Engineering of cell-laden gelatin-based microgels for cell delivery and immobilization in regenerative therapies. *Clinical Hemorheology and Microcirculation*, **67(3-4)**, 251–259 (2017).

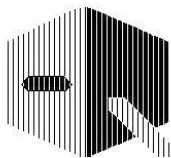
10. S Riedel, P Hietschold, C Krömmelbein, T Kunschmann, R Konieczny, W Knolle *et al.* Design of biomimetic collagen matrices by reagent-free electron beam induced crosslinking: Structure-property relationships and cellular response. **Materials & Design**, **168**, 107606 (2019).
11. J Cheng, D Park, Y Jun, J Lee, J Hyun, S Lee. Biomimetic spinning of silk fibers and *in situ* cell encapsulation. **Lab. Chip**, **16**(14), 2654-2661 (2016).
12. T Gao, T Chen, C Feng, X He, C Mu, J Anzai *et al.* Design and fabrication of flexible DNA polymer cocoons to encapsulate live cells. **Nat. Commun.**, **10**, 2946 (2019).
13. MS Mohammadi, MN Bureau, SN Nazhat. Polylactic acid (PLA) biomedical foams for tissue engineering. In: *Biomedical Foams for Tissue Engineering Applications*. Woodhead Publishing Limited, Chapter 11, pages 313–334 (2014).
14. E González, C Herencias, MA Prieto. A polyhydroxyalkanoate-based encapsulating strategy for “bioplasticizing” microorganisms. **Microbial Biotechnology**, **13**(1), 185–198 (2020).
15. J Sebastian, T Rouissi, SK Brar. Fungal chitosan: prospects and challenges. In: *Handbook of Chitin and Chitosan*. Volume 1: Preparation and Properties. Elsevier. Chapter 14, pages 419-452 (2020).
16. H Abdelkader, SA Hussain, N Abdullah, S Kmaruddin. Review on micro-encapsulation with Chitosan for pharmaceuticals applications. **MOJ Curr. Res. Rev.**, **1**(2), 77–84 (2018).
17. J Lizardi-Mendoza, W Argüelles-Monal, F Goycoolea-Valencia. Chemical characteristics and functional properties of chitosan. In: *Chitosan in the preservation of agricultural commodities*. Eds.: S Bautista-Baños, G Romanazzi, A Jiménez-Aparicio. Academic Press. Chapter 1 (2016).
18. C Lárez-Velásquez Chitosan-based nanomaterials on controlled bioactive agents delivery: a review. **J. Anal. Pharm. Res.**, **7**(4), 484-489 (2018).
19. N Boucard, C Viton, A Domard. New Aspects of the Formation of Physical Hydrogels of Chitosan in a Hydroalcoholic Medium. **Biomacromolecules**, **6**, 3227-3237 (2005).
20. J Berger, M Reist, JM Mayer, O Felt, R Gurny. Structure and interactions in chitosan hydrogels formed by complexation or aggregation for biomedical applications. **Eur. J. Pharm. Biopharm.**, **57**, 35–52 (2004).
21. J Berger, M Reist, JM Mayer, O Felt, NA Peppas, R Gurny. Structure and interactions in covalently and ionically cross-linked chitosan hydrogels for biomedical applications. **Eur. J. Pharm. Biopharm.**, **57**, 19–34 (2004).
22. KV HarishK,RN Tharanathan. Crosslinked chitosan — preparation and characterization. **Carbohydrate Research**, **341**(1), 169-173 (2006).
23. Y Hong, H Song, Y Gong, Z Mao, C Gao, J Shen. Covalently crosslinked chitosan hydrogel: Properties of *in vitro* degradation and chondrocyte encapsulation. **Acta Biomaterialia**, **3**(1), 23–31 (2007).
24. VX Truong, MP Ablett, HT Gilbert, J Bowen, SM Richardson, JA Hoyland, AP Dove. *In situ*-forming robust chitosan-poly(ethylene glycol) hydrogels prepared by copper-free azide–alkyne click reaction for tissue engineering. **Biomater. Sci.**, **2**, 167-175 (2014).
25. Crescenzi, D Imbriaco, C Lárez-Velásquez, M Dentini, A Ciferri. Novel types of polysaccharidic assemblies. **Macromolecular Chemistry and Physics**, **196**(9), 2873-2880 (1995).
26. Yu, DJ O'Sullivan. Immobilization of whole cells of *Lactococcus lactis* containing high levels of a hyperthermostable β-galactosidase enzyme in chitosan beads for efficient galactooligosaccharide production. **J. Dairy Sci.**, **101**(4), 2974-2983 (2018).
27. YF Poon, Y Cao, Y Liu, V Chan, M Chan-Park. Hydrogels Based on Dual Curable Chitosan-graft-Polyethylene Glycol-graft-Methacrylate: Application to Layer-by-Layer Cell Encapsulation. **ACS Applied Materials & Interfaces**, **2**(7), 2012–2025 (2010).
28. SA Young, SE Sherman, T Cooper, C Brown, F Anjum, DA Hess *et al.* Mechanically resilient injectable scaffolds for intramuscular stem cell delivery and cytokine release. **Biomaterials**, **159**, 146-160 (2018).
29. MA Azagarsamy, KS Anseth. Bioorthogonal Click Chemistry: An Indispensable Tool to Create Multifaceted Cell Culture Scaffolds. **ACS Macro Letters**, **2**, 5-9 (2013).
30. JP Chen, TH Cheng. Thermo-Responsive Chitosan-graft-poly(N-isopropylacrylamide) Injectable Hydrogel for Cultivation of Chondrocytes and Meniscus Cells. **Macromol. Biosci.**, **6**, 1026–1039 (2006).
31. C Lárez-Velásquez. Quitosano y nanopartículas. En: *Nanopartículas: fundamentos y aplicaciones*, Capítulo 8. Editores: C Lárez-Velásquez, S Koteich, F López. Comisión de Publicaciones del Departamento de Química, Universidad de Los Andes, Venezuela. Pags. 203–222 (2015).
32. Y Luo, Q Wang. Recent development of chitosan-based polyelectrolyte complexes with natural polysaccharides for drug delivery. **Int. J. Biol. Macromol.**, **64**, 353–367 (2014).
33. SR Bhatia, SF Khattak, SC Roberts. Polyelectrolytes for cell encapsulation. **Current Opinion in Colloid & Interface Science**, **10**, 45–51 (2005).
34. M Thanou, BI Florea, M Geldof, HE Junginger, G Borchard. Quaternized chitosan oligomers as novel gene delivery vectors in epithelial cell lines. **Biomaterials**, **23**(1), 153–159 (2002).
35. K Romøren, S Pedersen, G Smistad, Ø Evensen, BJ Thu. The influence of formulation variables on *in vitro* transfection efficiency and physicochemical properties of chitosan-based polyplexes. **International Journal of Pharmaceutics**, **261**(1-2), 115–127 (2003).
36. M Sahin, N Kocak, G Arslan, HI Ucan. Synthesis of cross-linked chitosan with epichlorohydrin possessing two novel polymeric ligands and its use in metal removal. **J. Inorganic & Organometallic Polymers and Materials**, **21**(1), 69-80 (2011).

37. WM Argüelles-Monal, J Lizardi-Mendoza, D Fernández-Quiroz, MT Recillas-Mota, M Montiel-Herrera. Chitosan derivatives: Introducing new functionalities with a controlled molecular architecture for innovative materials. **Polymers**, **10**(3), article number 342, 23 pages (2018).
38. Y Chen, Y Ye, R Li, Y Guo, H Tan. Synthesis of chitosan 6-OH immobilized cyclodextrin derivates via click chemistry. **Fibers & Polymers**, **14**, 1058–1065 (2013).
39. N Nishi, Y Maekita, SI Nishimura, O Hasegawa, S Tokura. Highly phosphorylated derivatives of chitin, partially deacetylated chitin and chitosan as new functional polymers: metal binding property of the insolubilized materials. **Int. J. Biol. Macromol.**, **9**(2), 109-114 (1987).
40. N R Kil'deeva, PA Perminov, LV Vladimirov, VV Novikov, SN Mikhailov. About Mechanism of Chitosan Cross-Linking with Glutaraldehyde. **Russian J. Bioorganic Chemistry**, **35**(3), 360–369 (2009).
41. L Wang, JP Stegemann. Glyoxal crosslinking of cell-seeded chitosan/collagen hydrogels for bone regeneration. **Acta Biomaterialia**, **7**(6), 2410-2417 (2011).
42. RAA Muzzarelli. Genipin-crosslinked chitosan hydrogels as biomedical and pharmaceutical aids. **Carbohydrate Polymers**, **77**, 1–9 (2009).
43. Q Zou, J Li, Y Li. Preparation and characterization of vanillin-crosslinked chitosan therapeutic bioactive microcarriers. **Int. J. Biol. Macromol.**, **79**, 736-747 (2015).
44. K Wegrzynowska-Drzymalska, P Grebicka, DT Mlynarczyk, D Chelminiak-Dudkiewicz, H Kaczmarek, T Goslinski, M Ziegler-Borowska. Crosslinking of Chitosan with Dialdehyde Chitosan as a New Approach for Biomedical Applications. **Materials**, **13**, 3413, 27 pages (2020).
45. LCR Carvalho, F Queda, C Almeida-Santos, MB Marques. Selective modification of chitin and chitosan: on the route to tailored oligosaccharides. **Chemistry—An Asian Journal**, **11**(24), 3468-3481 (2016).
46. AS Kritchenkova, YA Skorika. Click reaction in chitosan chemistry. **Russian Chemical Bulletin, International Edition**, **66**(5), 769—781 (2017).
47. BA Zielinski, P Aebischer. Chitosan as a matrix for mammalian cell encapsulation. **Biomaterials**, **15**, 1049–1056 (1994).
48. M Boido, M Ghiaudi, P Gentile, E Favaro, R Fusaro, C Tonda-Turo. Chitosan-based hydrogel to support the paracrine activity of mesenchymal stem cells in spinal cord injury treatment. **Sci. Rep.**, **9**, 6402 (2019).
49. K Roshanbinfar, S Salahshour Kordestani. Encapsulating Beta Islet Cells in Alginate, Alginate-Chitosan and Alginate-Chitosan-PEG Microcapsules and Investigation of Insulin Secretion. **J. Biomat. & Tissue Eng.**, **3**, 185–189 (2013).
50. V Chander, AK Singh, G Gangenahalli. Cell encapsulation potential of chitosan-alginate electrostatic complex in preventing natural killer and CD8+ cell-mediated cytotoxicity: an in vitro experimental study. **J. Microencapsul.**, **35**, 522–532 (2018).
51. A Vossoughi, HWT Matthew. Encapsulation of mesenchymal stem cells in glycosaminoglycans-chitosan polyelectrolyte microcapsules using electrospraying technique: Investigating capsule morphology and cell viability. **Bioeng. Transl. Med.**, **3**, 265–274 (2018).
52. S Itai, K Suzuki, Y Kurashina, H Kimura, T Amemiya, K Sato, M Nakamura, H Onoe. Cell-encapsulated chitosan-collagen hydrogel hybrid nerve guidance conduit for peripheral nerve regeneration. **Biomed. Microdevices**, **22**, 81 (2020).
53. S Ramesh, K Rajagopal, D Vaikkath, PD Nair, V Madhuri. Enhanced encapsulation of chondrocytes within a chitosan/hyaluronic acid hydrogel: a new technique. **Biotechnol. Lett.**, **36**, 1107–1111 (2014).
54. SM Oliveira, G Turner, PS Rodrigues, MA Barbosa, M Ali-khani, C Teixeira. Spontaneous chondrocyte maturation on 3D-chitosan scaffolds. **J. Tissue Science & Engineering**, **4**, (2012).
55. JS Choi, HS Yoo. Chitosan/Pluronic Hydrogel Containing bFGF/Heparin for Encapsulation of Human Dermal Fibroblasts. **J. Biomaterials Science, Polymer Edition**, **24**, 210–223 (2013).
56. RW Nurhayati, RD Cahyo, K Alawiyah, G Pratama, G Agustina, RD Antarianto, AR Prijanti, W Mubarok, AJ Rahyussalim. Development of double-layered alginate-chitosan hydrogels for human stem cell microencapsulation. **AIP Conference Proceedings**, **2193**, 020004 (2019).
57. A Mora-Boza, LM Mancipe Castro, RS Schneider, WM Han, AJ García, B Vázquez-Lasa, J San Román. Microfluidics generation of chitosan microgels containing glycerylphosphate crosslinker for *in situ* human mesenchymal stem cells encapsulation. **Materials Science and Engineering, C** **120**, 111716 (2021).
58. S Durkut, AE Elçin, YM Elçin. *In vitro* evaluation of encapsulated primary rat hepatocytes pre- and post-cryopreservation at -80°C and in liquid nitrogen. **Artif. Cells Nanomed. Biotechnol.**, **43**, 50–61 (2015).
59. S Mansouri, Y Merhi, FM Winnik, M Tabrizian. Investigation of Layer-by-Layer Assembly of Polyelectrolytes on Fully Functional Human Red Blood Cells in Suspension for Attenuated Immune Response. **Biomacromolecules**, **12**, 585–592 (2011).
60. M Sobol, A Bartkowiak, B de Haan, P de Vos. Cytotoxicity study of novel water-soluble chitosan derivatives applied as membrane material of alginate microcapsules. **J. Biomed. Materer. Res., A** **101**, 1907–1914 (2013).
61. Y Yeo, W Geng, T Ito, DS Kohane, JA Burdick, M Radisic. Photocrosslinkable hydrogel for myocyte cell culture and injection. **J. Biomed. Materer. Res. B Appl. Biomater.**, **81**, 312–322 (2007).
62. M Yang, S He, Z Su, Z Yang, X Liang, Y Wu. Thermosensitive Injectable Chitosan/Collagen/β-Glycerophosphate Composite Hydrogels for Enhancing Wound Healing by Encapsulating Mesenchymal Stem Cell Spheroids. **ACS Omega**, **5**, 21015–21023 (2020).

63. J Lin, W Yu, X Liu, H Xie, W Wang, X Ma. *In vitro* and *in vivo* characterization of alginate-chitosan-alginate artificial microcapsules for therapeutic oral delivery of live bacterial cells. **J. Biosci. Bioeng.**, **105**, 660–665 (2008).
64. X Luo, H Song, J Yang, B Han, Y Feng, Y Leng, Z Chen. Encapsulation of *Escherichia coli* strain Nissle 1917 in a chitosan—alginate matrix by combining layer-by-layer assembly with CaCl<sub>2</sub> cross-linking for an effective treatment of inflammatory bowel diseases. **Colloids and Surfaces B: Biointerfaces**, **189**, 110818 (2020).
65. M Kurakula, S Gorityala, DB Patel, P Basim, B Patel, S Kumar Jha. Trends of Chitosan Based Delivery Systems in Neuroregeneration and Functional Recovery in Spinal Cord Injuries. **Polysaccharides**, **2**, 519–537 (2021).
66. W Zhang, S Zhao, W Rao, J Snyder, JK Choi, L Wang *et al.* A novel core–shell microcapsule for encapsulation and 3D culture of embryonic stem cells. **J. Materials Chemistry B**, **1**(7), 1002–1009 (2013).
67. KC Yang, CC Wu, YH Cheng, TF Kuo, FH Lin. Chitosan/Gelatin Hydrogel Prolonged the Function of Insulinoma/Agarose Microspheres *In Vivo* During Xenogenic Transplantation. **Transplantation Proceedings**, **40**, 3623–3626 (2008).
68. YM Elçin, AE Elçin, RG Bretzel, T Linn. Pancreatic Islet Culture and Transplantation Using Chitosan and PLGA Scaffolds. In: *Tissue Engineering, Stem Cells, and Gene Therapies*. Ed YM Elçin, Springer USA. pp. 255–264 (2003).
69. S Graff, S Hussain, JC Chaumeil, C Charrueau. Increased intestinal delivery of viable *Saccharomyces boulardii* by encapsulation in microspheres. **Pharm. Res.**, **25**, 1290–1296 (2008).
70. MT Cook, G Tzortzis, VV Khutoryanskiy, D Charalampopoulos. Layer-by-layer coating of alginate matrices with chitosan-alginate for the improved survival and targeted delivery of probiotic bacteria after oral administration. **J. Mater. Chem., B** **1**, 52–60 (2013).
71. W Krasaecko, B Bhandari, H Deeth. The influence of coating materials on some properties of alginate beads and survivability of microencapsulated probiotic bacteria. **Int. Dairy Journal**, **14**, 737–743 (2004).
72. DC Vodnar, C Socaciu. Green tea increases the survival yield of Bifidobacteria in simulated gastrointestinal environment and during refrigerated conditions. **Chem. Cent. J.**, **6**, 61 (2012).
73. M Chávarri, I Marañón, R Ares, FC Ibáñez, F Marzo, M Villarán. Microencapsulation of a probiotic and prebiotic in alginate-chitosan capsules improves survival in simulated gastrointestinal conditions. **Int. J. Food Microbiology**, **142**, 185–189. (2010).
74. SM Koo, YH Cho, CS Huh, YJ Baek, J Park. Improvement of the stability of *Lactobacillus casei* YIT 9018 by microencapsulation using alginate and chitosan. **J. Microbiology and Biotechnology**, **11**, 376–383 (2001).
75. A Bepeyeva, JMS de Barros, H Albadran, AK Kakimov, ZK Kakimova, D Charalampopoulos, VV Khutoryanskiy. Encapsulation of *Lactobacillus casei* into Calcium Pectinate-Chitosan Beads for Enteric Delivery. **J. Food Sci.**, **82**, 2954–2959 (2017).
76. M Boido, D Garbossa, M Fontanella, A Ducati, A Vercelli. Mesenchymal Stem Cell Transplantation Reduces Glial Cyst and Improves Functional Outcome After Spinal Cord Compression. **World Neurosurgery**, **81**, 183–190. (2014).
77. FE Ezquer, MEEzquer, JM Vicencio, SD Calligaris. Two complementary strategies to improve cell engraftment in mesenchymal stem cell-based therapy: Increasing transplanted cell resistance and increasing tissue receptivity. **Cell Adh. Migr.**, **11**, 110–119 (2017).
78. Ai Arno, S Amini-Nik, PH Blit, M Al-Shehab, C Belo, E Herer, CH Tien, MG Jeschke. Human Wharton's jelly mesenchymal stem cells promote skin wound healing through paracrine signaling. **Stem Cell Res. Ther.**, **5**, 28 (2014).
79. DF Emerich, BR Frydel, TR Flanagan, M Palmatier, SR Winn, L Christenson. Transplantation of Polymer Encapsulated PC12 Cells: Use of Chitosan as an Immobilization Matrix. **Cell Transplant.**, **2**, 241–249 (1993).
80. CM Grau, LA Greene. Use of PC12 Cells and Rat Superior Cervical Ganglion Sympathetic Neurons as Models for Neuroprotective Assays Relevant to Parkinson's Disease. **Methods Mol. Biol.**, **846**, 201–211 (2012).
81. D Offen, I Ziv, A Barzilai, S Gorodin, E Glater, A Hochman, E Melamed. Dopamine-melanin induces apoptosis in PC12 cells; possible implications for the etiology of Parkinson's disease. **Neurochem. Int.**, **31**, 207–216 (1997).
82. P Belujon, AA Grace. Dopamine System Dysregulation in Major Depressive Disorders. **Int. J. Neuropsychopharmacol.**, **20**, 1036–1046 (2017).
83. E Dobryakova, HM Genova, J DeLuca, GR Wylie. The Dopamine Imbalance Hypothesis of Fatigue in Multiple Sclerosis and Other Neurological Disorders. **Frontiers in Neurology**, **6**, 52 (2015).
84. W Zhang. Encapsulation of Transgenic Cells for Gene Therapy. In: *Gene Therapy-Principles and Challenges*. In-techOpen (2015).
85. J Goldstein, G Siviglia, R Hurst, L Lenny, L Reich. Group B erythrocytes enzymatically converted to group O survive normally in A, B, and O individuals. **Science**, **215**, 168–170 (1982).
86. P Rahfeld, SG Withers. Toward universal donor blood: Enzymatic conversion of A and B to O type. **J. Biol. Chem.**, **295**, 325–334 (2020).
87. R Mitra, N Mishra, GP Rath. Blood groups systems. **Indian J. Anaesth.**, **58**, 524–528 (2014).
88. O Jahanpour, JJ Pyuza, EO Ntiyakunze, A Mremi, ER Shao. ABO and Rhesus blood group distribution and frequency among blood donors at Kilimanjaro Christian Medical Center, Moshi, Tanzania. **BMC Research Notes**, **10**(1), 1–5 (2017).
89. J Rosenberg, J Huang. CD8<sup>+</sup> T Cells and NK Cells: Parallel and Complementary Soldiers of Immunotherapy. **Curr. Opin. Chem. Eng.**, **19**, 9–20 (2018).

90. P Pontrelli, F Rascio, G Castellano, G Grandaliano, L Gessaldo, G Stallone. The Role of Natural Killer Cells in the Immune Response in Kidney Transplantation. **Front Immunol.**, **11**, 1454 (2020).
91. V Bueno, JOM Pestana. The role of CD8<sup>+</sup> T cells during allograft rejection. **Braz. J. Med. Biol. Res.**, **35**, 1247–1258 (2002).
92. M Rodríguez-Vázquez, B Vega-Ruiz, R Ramos-Zúñiga, DA Saldaña-Koppel, LF Quiñones-Olvera. Chitosan and Its Potential Use as a Scaffold for Tissue Engineering in Regenerative Medicine. **BioMed Research Int.**, **2015**, e821279 (2015).
93. Y Hong, H Song, Y Gong, Z Mao, C Gao, J Shen. Covalently crosslinked chitosan hydrogel: properties of in vitro degradation and chondrocyte encapsulation. **Acta Biomater.**, **3**, 23–31 (2007).
94. H Park, B Choi, J Hu, M Lee. Injectable chitosan hyaluronic acid hydrogels for cartilage tissue engineering. **Acta Biomater.**, **9**, 4779–4786 (2013).
95. H Tan, CR Chu, KA Payne, KG Marra. Injectable in situ forming biodegradable chitosan–hyaluronic acid based hydrogels for cartilage tissue engineering. **Biomaterials**, **30**, 2499–2506 (2009).
96. H Sá-Lima, SG Caridade, JF Mano, RL Reis. Stimuli-responsive chitosan-starch injectable hydrogels combined with encapsulated adipose-derived stromal cells for articular cartilage regeneration. **Soft Matter**, **6**, 5184–5195 (2010).
97. TC Tseng, L Tao, FY Hsieh, Y Wei, IM Chiu, S Hsu. An Injectable, Self-Healing Hydrogel to Repair the Central Nervous System. **Adv. Mater.**, **27**, 3518–3524 (2015).
98. FY Hsieh, TC Tseng, SH Hsu. Self-healing hydrogel for tissue repair in the central nervous system. **Neural Regeneration Research**, **10**(12), 1922 (2015).
99. HK Jahromi, A Farzin, E Hasanzadeh, SE Barough, N Mahmoodi, MRH Najafabadi, J Ai. Enhanced sciatic nerve regeneration by poly-L-lactic acid/multi-wall carbon nanotube neural guidance conduit containing Schwann cells and curcumin encapsulated chitosan nanoparticles in rat. **Mat. Sci. Eng.: C**, **109**, 110564 (2020).
100. K Bhatheja, J Field. Schwann cells: Origins and role in axonal maintenance and regeneration. **Int. J. Biochem. Cell Biology**, **38**, 1995–1999 (2006).
101. Sp Frostick, Q Yin, GJ Kemp. Schwann cells, neurotrophic factors, and peripheral nerve regeneration. **Microsurgery**, **18**, 397–405 (1998).
102. R Li, D Li, C Wu, L Ye, Y Wu, Y Yuan, J Xiao. Nerve growth factor activates autophagy in Schwann cells to enhance myelin debris clearance and to expedite nerve regeneration. **Theranostics**, **10**(4), 1649 (2020).
103. J Tello Velasquez, L Nazareth, RJ Quinn, J Ekberg, JA St John. Stimulating the proliferation, migration and lamellipodia of Schwann cells using low-dose curcumin. **Neuroscience**, **324**, 140–150 (2016).
104. IH Liu, SH Chang, HY Lin. Chitosan-based hydrogel tissue scaffolds made by 3D plotting promotes osteoblast proliferation and mineralization. **Biomed. Mater.**, **10**, 035004 (2015).
105. VJ Nelson, MFK Dinnunhan, PR Turner, JM Faed, JD Cabral. A chitosan/dextran-based hydrogel as a delivery vehicle of human bone-marrow derived mesenchymal stem cells. **Biomed. Mater.**, **12**, 035012 (2017).
106. L Dong, SJ Wang, XR ZhaoR, YF Zhu, JK Yu. 3D-Printed Poly( $\epsilon$ -caprolactone) Scaffold Integrated with Cell-laden Chitosan Hydrogels for Bone Tissue Engineering. **Sci. Rep.**, **7**, 13412 (2017).
107. H Naderi-Meshkin, H Naderi-Meshkin, MM Matin, A Heiranian-Tabasi, M Mirahmadi, M Irfan-Maqsood, MA Edalatmanesh *et al.* Injectable hydrogel delivery plus preconditioning of mesenchymal stem cells: exploitation of SDF-1/CXCR4 axis toward enhancing the efficacy of stem cells' homing. **Cell Biol. Int.**, **40**, 730–741 (2016).
108. W Jin, X Liang, A Brooks, K Futrega, X LiuX, MR Doran *et al.* Modelling of the SDF-1/CXCR4 regulated in vivo homing of therapeutic mesenchymal stem/stromal cells in mice. **PeerJ**, **6**, e6072 (2018).
109. B Cui, Y Zheng, L Sun, T Shi, Z Shi, L Wang *et al.* Heart regeneration in adult mammals after myocardial damage. **Acta Cardiológica Sinica**, **34**(2), 115 (2018).
110. L Xi. The use of chitosan to increase the stability of calcium alginate beads with entrapped yeast cells. **Biotechnology and Applied Biochemistry**, **23**(3), 269–272 (1996).
111. S Namthabad, R Chinta. Robust Encapsulation of Yeast for Bioethanol Production. Master Thesis, Engineering School, Industrial Biotechnology University of Boras, Sweden (2012).
112. M Guslandi, G Mezzi, M Sorghi, PA Testoni. *Saccharomyces boulardii* in maintenance treatment of Crohn's disease. **Dig. Dis. Sci.**, **45**, 1462–1464 (2000).
113. LV McFarland, CM Surawicz, RN Greenberg, GW Elmer, KA Moyer KA, SA Melcher *et al.* Prevention of beta-lactam-associated diarrhea by *Saccharomyces boulardii* compared with placebo. **Am. J. Gastroenterol.**, **90**, 439–445 (1995).
114. JP Buts, G Corthier, M Delmee. *Saccharomyces boulardii* for *Clostridium difficile*-associated enteropathies in infants. **J. Pediatr. Gastroenterol. Nutr.**, **16**, 419–425 (1993).
115. LF Călinoiu, BE Ștefănescu, ID Pop, L Muntean, DC Vodnar. Chitosan Coating Applications in Probiotic Microencapsulation. **Coatings**, **9**, 194 (2019).
116. A De Prisco, G Mauriello. Probiotication of foods: A focus on microencapsulation tool. **Trends in Food Science & Technology**, **48**, 27–39 (2016).
117. MT Cook, G Tzortzis, D Charalampopoulos, VV Khutoryanskiy. Microencapsulation of probiotics for gastrointestinal delivery. **J. Controlled Release**, **162**, 56–67 (2012).

118. R Gheorghita, L Anchidin-Norocel, R Filip, M Dimian, M Covasa. Applications of Biopolymers for Drugs and Probiotics Delivery. **Polymers**, **13**, 2729 (2021).
119. J Mirtić, T Rijavec, S Zupančič, A Zvonar Pobirk, A Lanjanje, J Kristl. Development of probiotic-loaded microcapsules for local delivery: Physical properties, cell release and growth. **Eur. J. Pharm. Sci.**, **121**, 178–187 (2018).
120. A Mortazavian, SH Razavi, MR Ehsani, S Sohrabvandi. Principles and Methods of Microencapsulation of Probiotic Microorganisms. **Iranian J. Biotechnology**, **5**, 1–18 (2007).
121. MT Cook, G Tzortzis, DCharalampopoulos, VV Khutoryanskiy. Microencapsulation of a symbiotic into PLGA/alginate multiparticulate gels. **Int. J. Pharm.**, **466**, 400–408 (2014).
122. IM Enache, AM Vasile, E Enachi, V Barbu, N Stănciu, C Vizireanu. Co-Microencapsulation of Anthocyanins from Black Currant Extract and Lactic Acid Bacteria in Biopolymeric Matrices. **Molecules**, **25**, 1700 (2020).
123. S Jantarathin, C Borompichaichartkul, R Sanguandeekul. Microencapsulation of probiotic and prebiotic in alginate-chitosan capsules and its effect on viability under heat process in shrimp feeding. **Materials Today: Proceedings**, **4**, 6166–6172 (2017).
124. M de Araújo-Etchepare, GC Raddatz, EM de Moraes-Flores, LQ Zepka, E Jacob-Lopes *et al.* Effect of resistant starch and chitosan on survival of *Lactobacillus acidophilus* microencapsulated with sodium alginate. **LWT - Food Science and Technology**, **65**, 511–517 (2016).
125. YA Ghouri, DM Richards, EF Rahimi, JT Krill, A Jelinek, AW DuPont. Systematic review of randomized controlled trials of probiotics, prebiotics, and symbiotics in inflammatory bowel disease. **Clin. Exp. Gastroenterol.**, **7**, 473–487 (2014).
126. F Cristofori, VN Dargenio, C Dargenio, VL Miniello, M Barone, R Francavilla. Anti-Inflammatory and Immuno-modulatory Effects of Probiotics in Gut Inflammation: A Door to the Body. **Frontiers in Immunology**, **12**, 178 (2021).
127. MAK Azad, M Sarker, D Wan. Immunomodulatory Effects of Probiotics on Cytokine Profiles. **BioMed Research Int.**, **2018**, e8063647 (2018).
128. SC Li, WF Hsu, JS Chang, CK Shih. Combination of *Lactobacillus acidophilus* and *Bifidobacterium animalis* subsp. *lactis* Shows a Stronger Anti-Inflammatory Effect than Individual Strains in HT-29 Cells. **Nutrients**, **11**, E969 (2019).
129. MAR Vinolo, HG Rodrigues, E Hatanaka, FT Sato, SC Sampaio, R Curi. Suppressive effect of short-chain fatty acids on production of proinflammatory mediators by neutrophils. **J. Nutr. Biochem.**, **22**, 849–855 (2011).
130. JS Park, EJ Lee, JC Lee, WK Kim, HS Kim. Anti-inflammatory effects of short chain fatty acids in IFN-gamma-stimulated RAW 264.7 murine macrophage cells: involvement of NF-kappa B and ERK signaling pathways. **Int. Immunopharmacol.**, **7**, 70–77 (2007).
131. Council of Europe. European Pharmacopoeia 6.0 1774. Chitosan Hydrochloride; Council of Europe: Strasbourg, Germany (2008).
132. United States Pharmacopeial Convection. United States Pharmacopeia 34/National Formulary. Chitosan; The United States Pharmacopeial Convection: Rockville, MD, USA (2011).



# Residuos lignocelulósicos como materia prima de segunda generación en procesos de biorrefinación

Andrea Briones Muñoz<sup>1\*</sup>, María Antonieta Riera<sup>2</sup>

<sup>1)</sup> Maestría Profesional en Química, Mención Química Ambiental. Instituto de Posgrado.  
Universidad Técnica de Manabí. Ecuador

<sup>2)</sup> Departamento de Procesos Químicos, Alimentos y Biotecnología.  
Facultad de Ciencias Matemáticas, Físicas y Químicas. Universidad Técnica de Manabí. Ecuador

(\*) [gbriones2108@utm.edu.ec](mailto:gbriones2108@utm.edu.ec)

Recibido: 17/10/2021

Revisado: 26/11/2021

Aceptado: 15/12/2021

## Resumen

Existe interés mundial en reemplazar los combustibles fósiles por fuentes renovables. La primera generación de biorrefinerías se basó en la utilización de cultivos alimentarios, lo que generó un debate sobre alimentos contra combustible y una sostenibilidad cuestionable. Para superar esto, se propuso el uso de materias primas lignocelulósicas incluyendo desde cultivos no alimentarios hasta residuos y desechos agro-forestales. Atendiendo a esta premisa, se realizó una revisión bibliográfica sobre el uso de residuos lignocelulósicos de segunda generación para la producción de bioproductos. Se investigó acerca de los procesos de transformación empleados, los bioproductos obtenidos y la cantidad de residuos de este tipo que están disponibles en Latinoamérica para su uso. El aprovechamiento de este tipo de residuos brinda una oportunidad para el desarrollo de la región al utilizar materia prima de bajo costo para la obtención de productos con valor agregado.

**Palabras claves:** Biomasa; Bioproducto; Biorrefinerías; Residuos agrícolas.

## Abstract

**Lignocellulosic waste as a second generation raw material in biorefining processes.** There is global interest in replacing fossil fuels with renewable sources. The first generation of biorefineries relied on the utilization of food crops, sparking a debate on food versus fuel and questionable sustainability. To overcome this, the use of lignocellulosic raw materials was proposed, ranging from non-food crops to agro-forestry residues and waste. Based on this premise, a bibliographic review was carried out on the use of second-generation lignocellulosic waste for the production of bioproducts. It was investigated about the transformation processes used, the bioproducts obtained and the amount of waste of this type that are available in Latin America for use. The exploitation of this type of waste provides an opportunity for the development of the region by using low-cost raw materials to obtain products with added value.

**Keywords:** Biomass; Bioproduct; Biorefinery; Agricultural waste.

## Introducción

El petróleo es un recurso fósil que existe desde la antigüedad, con el cual se han obtenido combustibles, fertilizantes, telas, detergentes, pinturas, plásticos, entre otros, demandados por la sociedad. El proceso de extracción, refinación y procesamiento del petróleo, requerido para la producción de diversos productos, ha generado consecuencias desfavorables a lo largo de los años en la calidad del aire, agua y suelo, visible además en los efectos del cambio climático.

De acuerdo a Sarmiento<sup>1</sup>, los compromisos ambientales como el convenio de Viena para la protección de la capa de ozono, el protocolo de Montreal, el protocolo de Kioto y el convenio marco de cambio climático, han impulsado en la actualidad medidas para sustituir las fuentes convencionales de producción de energía por otras de origen renovable, de modo que sean sustentables.

Una de ellas es la biomasa, presente en fuentes animales, vegetales, silvicultura e industrias conexas, así como en la fracción biodegradable de los residuos industriales y municipales<sup>2</sup>. Es un recurso constituido por carbono e hidrógeno, a partir de los cuales se puede obtener energía, combustibles y productos químicos<sup>3</sup>.

La biomasa lignocelulósica está conformada principalmente por celulosa (38-50%), hemicelulosa (23-32 %) y lignina (15-25 %)<sup>4</sup>. Dentro de esta clasificación están los residuos agrícolas e industriales, entre los cuales están la cáscara de arroz<sup>5</sup>, bagazo de caña de azúcar<sup>6</sup>, rastrojo de maíz<sup>7</sup>, pseudotallo del plátano<sup>8</sup>, residuos de palma africana<sup>9</sup>, cáscara y semillas de naranja<sup>4</sup>. Otra parte de la biomasa lignocelulósica está presente en los residuos forestales, de la silvicultura, cultivos energéticos y algunos residuos sólidos. Estos tienden a ser una opción viable para la producción de energía, debido a que las materias primas lignocelulósicas no compiten con los cultivos

alimentarios y además tienen un precio más competitivo que las materias primas agrícolas convencionales<sup>10</sup>.

La biorrefinación de biomasa residual también permite obtener diferentes subproductos de calidad que se procesan en la actualidad en la industria química<sup>11</sup>. Para ello, se han desarrollado nuevos procedimientos de síntesis orientados a una producción eficiente de bioproductos de segunda generación con un alto valor añadido.

Dentro de este contexto se desarrolló la presente revisión bibliográfica, con el propósito de conocer los residuos lignocelulósicos utilizados en la actualidad, los productos generados a partir de ella, las rutas de procesamiento existentes, además del potencial que tiene Latinoamérica (LA) como generadora de residuos de este tipo. Para tal fin se consultaron fuentes primarias y secundarias publicadas en los últimos años, seleccionando en primer lugar las de alto impacto. Se utilizó como motor de búsqueda Google Scholar, empleando como palabras clave: bioproductos, residuos lignocelulósicos y biorrefinería.

### Materia prima de segunda generación

Se define como materia prima de segunda generación a las fuentes agrícolas y forestales que no son parte de la alimentación y que además, son eficientes para la obtención de energía verde o renovable, lo que reduce la generación de gases de efecto invernadero (GEI) en el ambiente y contribuye a la disminución de contaminantes atmosféricos considerando todo su ciclo de vida<sup>12-16</sup>. Es un tipo de biomasa constituida en primer lugar por celulosa, que se define como un polisacárido compuesto por un solo tipo de monosacárido<sup>17</sup>. La celulosa es un producto biosintético de plantas, algunos animales y bacterias. Es el polímero más abundante de la naturaleza y tiene una estructura similar a una larga cadena lineal compuesta de unidades de glucopiranósilo con enlaces  $\beta$ -D (1,4)<sup>18</sup>.

La hemicelulosa es otro de los componentes que forman una estructura polimérica compleja, ramificada y consiste en la unión de diferentes unidades de azúcares: pentosas, hexosas y ácidos de estos azúcares<sup>19</sup>. Además, la hemicelulosa es un heteropolisacárido ramificado que interactúa con cadenas de celulosa y a veces se puede encontrar como un material de reticulación entre celulosa y lignina, principalmente impariendo estabilidad estructural mejorada a la pared celular<sup>20</sup>. Finalmente está la lignina, que se encuentra unida a la celulosa y hemicelulosa. Su diversidad estructural, compuesta principalmente por tres tipos de fenilpropano (p-hidroxifenil, guaiacil y siringil), unidos entre ellos por enlaces éter y carbono-carbono, además de su heterogenicidad química, dificultan su biodigestibilidad<sup>21</sup>. La composición de algunos residuos lignocelulósicos se presentan en la tabla 1.

Estos residuos no sólo son abundantes y económicos, sino que además son fuente de diversos azúcares poliméricos: glucosa (celulosa) y xilosa (hemicelulosa), que se pueden convertir por vía química o biotecnológica en productos de gran valor como azúcares, etanol, distintos productos químicos y enzimas<sup>31</sup>.

**Tabla 1.** Composición de residuos lignocelulósicos

Residuo	Celulosa (%)	Hemicelulosa (%)	Lignina (%)
Cáscara de plátano <sup>22</sup>	29,00 ± 3,61	26,67 ± 1,53	19,17 ± 0,68
Cáscara de yuca <sup>22</sup>	28,67 ± 1,53	6,67 ± 2,08	19,75 ± 0,64
Cáscara de limón <sup>23</sup>	21,60	6,00	8,90
Cáscara de mandarina <sup>23</sup>	20,20	7,80	9,10
Cáscara de naranja <sup>23</sup>	23,50	10,40	7,60
Paja de trigo <sup>24</sup>	38,70	30,00	12,40
Vaina de arveja <sup>24</sup>	44,90	28,40	15,10
Bagazo de maíz <sup>24</sup>	28,30	25,00	10,10
Raquis de palma africana <sup>25,26</sup>	46,14 ± 1,05	2,28 ± 0,22	26,31 ± 2,81
Hojas de yuca <sup>27</sup>	40,90	15,63	ND
Tallo de yuca <sup>27,28</sup>	39,83	13,00	11,80
Bagazo de caña <sup>29</sup>	32,7 ± 0,7	21,3 ± 1,3	15,3 ± 0,5
Cascarrilla de arroz <sup>29</sup>	34,4 ± 0,1	9,5 ± 0,2	22,1 ± 0,4
Asperín <sup>29</sup>	36,6 ± 0,9	7,0 ± 0,7	38,8 ± 0,5
Residuos de poda <sup>30</sup>	35,52	ND	45,45

ND: No determinado

### Productos biobasados y procesos de transformación

El desarrollo de productos biobasados se lleva a cabo bajo un modelo bioeconómico de producción piramidal o circuito de cascada, que busca el crecimiento económico a la vez que minimiza los impactos negativos en el ambiente y la sociedad. Este concepto se enfoca en la reducción de la cantidad de residuos para dar un valor más prolongado, mediante la creación de plantas de producción integradas que utilizan biomasa o materias primas derivadas de la biomasa y con ello producir una gama de productos de valor agregado y energía<sup>32</sup>.

Los productos de base biológica son diversos y entre ellos se encuentran: bioetanol, biobutanol, biohidrógeno, biodiesel, bioenergía, bioplástico, biometanol, bioaceite, biofertilizante, biogás y otros bioproductos, a partir de diferentes residuos lignocelulósicos (tabla 2).

**Tabla 2.** Productos obtenidos a partir de residuos lignocelulósicos

Productos	Residuos agrícolas
Bioetanol	Corteza del cacao <sup>32</sup> Pasto mombaza <sup>34</sup> Cáscara de piña <sup>35</sup> Paja de arroz <sup>36</sup> Mazorcas de maíz <sup>37</sup> Tallo de yuca <sup>38</sup>
Biobutanol	Rastrojo de maíz <sup>39</sup> Bagazo de la caña de azúcar <sup>40</sup>
Biohidrógeno	Cáscara de naranja y plátano <sup>41</sup> Rastrojo de maíz <sup>42</sup> Residuos de frutas <sup>43</sup>
Biometanol	Residuos de la palma de aceite <sup>44</sup>
Bionergía	Residuos agroindustriales <sup>45</sup> Madera de eucalipto y residuos de cultivo de café <sup>46</sup> Residuo de arroz <sup>47</sup>
Bioplástico	Cascarilla de cacao y bagazo de caña de azúcar <sup>48</sup> Residuo de la caña de azúcar <sup>49</sup> Pectina de fruta de pitahaya <sup>50</sup> Semilla de aguacate <sup>51</sup> Cáscara de yuca <sup>52</sup> Cáscaras del plátano <sup>53</sup>
Bioaceite	Residuo del plátano <sup>54</sup> Residuos de semillas <sup>55</sup> Residuos de la piel de naranja <sup>56</sup>
Biofertilizante y Biogás	Residuos de alimentos <sup>57</sup> Residuos hortofrutícolas <sup>58</sup> Residuos agrícolas <sup>59</sup>

Representa una opción futurista para hacer frente a los desafíos globales, asociados con el desarrollo de una economía baja en carbono, para reducir el agotamiento de los recursos no renovables y el cambio climático<sup>33</sup>.

Los biocombustibles de segunda generación se producen a partir de biomasa lignocelulósica, que es la única fuente renovable que contiene carbono e hidrógeno y está disponible en grandes cantidades a un coste relativamente bajo<sup>60</sup>. Su uso reduce los impactos ambientales y representa una fuente alternativa al uso de hidrocarburos, para cumplir la demanda energética actual a nivel nacional y mundial<sup>61,62</sup>.

El bioetanol se puede producir a partir de fermentación, por la acción de microorganismos como *Saccharomyces cerevisiae*<sup>63</sup>. El biobutanol se produce a través de la fermentación anaeróbica con acetona-butanol-etanol (ABE)<sup>64,65</sup>. En la actualidad, el biohidrógeno se obtiene por medio de procesos fotosintéticos y fermentativos, haciendo uso de biomasa y bacterias anaeróbicas. Es un proceso que se puede llevar a cabo a temperatura y presión ambiente, lo que lo hace idóneo para la producción a largo plazo<sup>64,66</sup>. Estos biocombustibles, dada su biodegradabilidad, no toxicidad y estar libres de azufre y aromáticos, presentan ventajas frente al combustible convencional. Emiten menos contaminantes atmosféricos y gases de efecto invernadero distintos de los óxidos de nitrógeno<sup>67,68</sup>.

Los plásticos de base biológica (bioplásticos) son una alternativa a los plásticos derivados de la industria petroquímica debido a su potencial biodegradabilidad y su origen a partir de fuentes renovables<sup>69</sup>. En la actualidad se producen mayoritariamente a partir de residuos industriales y urbanos con alta carga de materia orgánica, aunque también pueden producirse a partir de gases como el CO o el CO<sub>2</sub><sup>70</sup>.

Los biofertilizantes son sustancias que contienen microorganismos vivos que, al ser aplicados a semillas, superficies de plantas o suelo, colonizan la rizósfera o el interior de la planta y promueve su crecimiento aumentando el suministro o la disponibilidad de nutrientes primarios<sup>71</sup>.

La producción de biogás es una tecnología bien establecida principalmente para la generación de energía renovable y también para la valorización de residuos orgánicos. El biogás es el producto final de un proceso biológico, la llamada digestión anaeróbica, en el que diferentes microorganismos siguen diversas vías metabólicas para descomponer la materia orgánica<sup>72</sup>.

En general la biomasa lignocelulosa presente en algunos residuos, puede transformarse usando diversas técnicas físicas, térmicas, fisicoquímicas, químicas y biológicas o sus combinaciones<sup>73</sup> (figura 1). Se incluyen en este caso procesos como la combustión, pirólisis, gasificación y licuefacción<sup>74</sup>.

### Biorrefinerías de segunda generación

Las biorrefinerías son complejos industriales que usan la biomasa como insumo principal y tienen un concepto de fun-

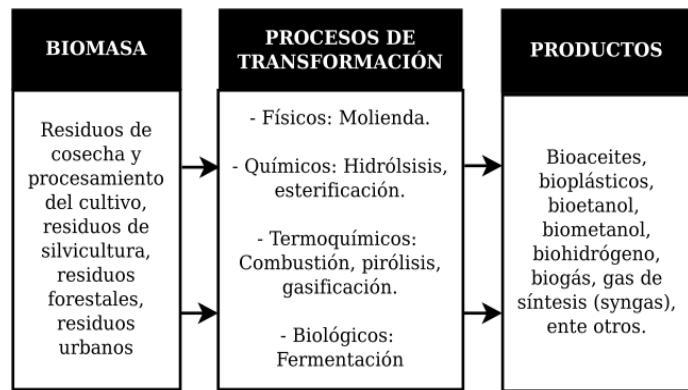


Fig. 1: Procesos de transformación de biomasa.

cionamiento similar a las refinerías de petróleo, donde se producen múltiples productos. Según los procesos separativos las biorrefinerías pueden ser de cuatro tipos: cultivo entero, insumos lignocelulosicos, verdes y plataforma syngas. Otra distinción señala la existencia de biorrefinerías de primera generación, segunda generación e integradas<sup>75,76</sup>.

Una biorrefinería lignocelulósica es aquella instalación de ingeniería de procesos y biotecnología que se encarga del procesamiento de biomasa lignocelulósica, para la obtención de productos de base biológica<sup>77</sup>. Los procesos de transformación incluyen la recolección y almacenamiento de la biomasa recolectada, pretratamiento y transporte de la biomasa procesada<sup>78</sup>. La conversión bioquímica de biomasas lignocelulósicas implica la hidrólisis de carbohidratos en azúcares solubles, seguida de fermentación microbiana o digestión anaeróbica directa con o sin fermentación, mientras que la ruta termoquímica implica combustión directa, pirólisis, gasificación o torrefacción<sup>79</sup>.

Las biorrefinerías de segunda generación (2G) han mostrado gran potencial para convertir desechos lignocelulosicos en combustibles, energía y otros productos de valor agregado. Un ejemplo de ello es la brasileña GranBio, donde se emplean un conjunto de tecnologías (pre-tratamiento, hidrólisis enzimática y fermentación), para la transformación de residuos de la caña de azúcar en etanol 2G<sup>80</sup>. Por su parte la canadiense Iogen Corporation, utiliza residuos agrícolas para producir biogás como combustible del sector transporte<sup>81</sup>. Enerkem, en Canadá, transforma los residuos sólidos urbanos no reciclables y no compostables, a través de un proceso de preparación, gasificación, limpieza de gas de síntesis y conversión catalítica, en etanol para el sector transporte y metanol para aplicaciones químicas<sup>82,83</sup>. Otro caso es el de Bioliq®, quien emplea biomasa residual (residuos de la agricultura, la silvicultura o el paisajismo), para obtener gas de síntesis y productos químicos, mediante pirólisis rápida y refinación a escala industrial<sup>82,84</sup>.

Se necesitan procesos avanzados para la transformación de biomasa lignocelulósica en bioproductos, donde el material se fraccione mediante tecnologías respetuosas con el ambiente<sup>85</sup>. Sin embargo, existen diversas barreras por superar y lograr una exitosa operación y rentabilidad<sup>86</sup>.

## Latinoamérica como generadora de residuos lignocelulósicos

Latinoamérica es una de las regiones con mayor diversidad biológica y disponibilidad de biomasa en el mundo. Debido a su privilegiada ubicación geográfica cuenta con buen suelo, clima adecuado, tierras disponibles y bajos costos laborales; siendo la combinación perfecta para la producción de bioproductos<sup>87</sup>.

Cada año se generan en LA gran cantidad de productos agrícolas, residuos sólidos forestales y urbanos, con gran potencial de ser convertidos en productos con valor agregado<sup>88</sup>. El proyecto S2Biom estimó que para el año 2030, se necesitará un total de 476 millones de toneladas de biomasa lignocelulósica, para cubrir la demanda de bioproductos requeridos por la sociedad<sup>79</sup>. Aunque se desconoce de la existencia de un registro oficial de las cantidades de residuos disponibles por tipo y por nación, se pueden usar las estimaciones de la FAO para Centroamérica y Suramérica, concernientes a las cantidades de CH<sub>4</sub> que se generan por quema de residuos agrícolas (figura 2).

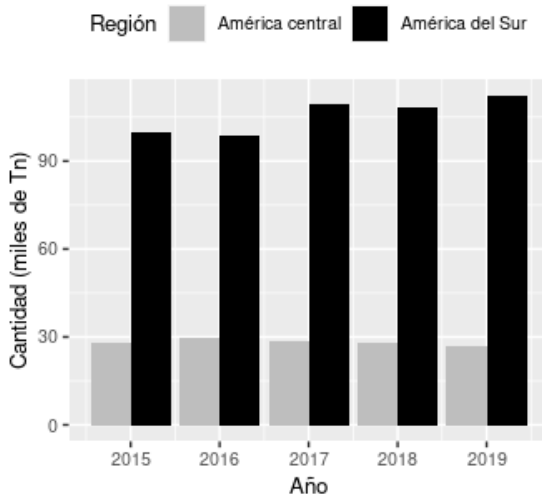


**Fig. 2:** Emisiones de CH<sub>4</sub> por quema de residuos. Elaborado con información reportada por la FAO<sup>89</sup>

Toda esta biomasa que es quemada, podría ser útil en procesos de biorrefinería. Especialmente en la labor agrícola se generan residuos de diferentes partes del cultivo, que contienen propiedades aprovechables debidas a la presencia de nutrientes y materiales orgánicos en su composición<sup>17</sup>.

En los últimos años LA ha registrado un notable crecimiento en la labor agropecuaria, enfocada hacia la sostenibilidad en el ámbito ambiental y las desigualdades socioeconómicas<sup>85</sup>. Así mismo la región registra un aumento en la superficie de tierra cultivable, pasando de 7,21% en el año 2014 a 7,72% en el 2018<sup>86</sup>. Específicamente sudamericana se caracteriza por ser productor de caña de azúcar, arroz, maíz, papa, plátano, banano, naranja y yuca. Otros productos como el aceite de palma y la soya se obtienen solamente en 5 países del área. En el caso de la soya, Brasil y Argentina, son líderes mundiales en este rubro<sup>90</sup>.

El potencial que contienen estos residuos, representa una alternativa prometedora para la producción de nuevos productos de manera sustentable. Sin embargo, un alto rendimiento de transformación de la materia prima y un mínimo costo del residuo, son requisitos básicos para el éxito de la utilización de la biomasa en las biorrefinerías<sup>91</sup>.

Pese a que los residuos lignocelulosos han jugado un papel importante en la implementación de una biorrefinería, en el contexto de la bioeconomía circular<sup>92</sup>, es necesaria una cantidad significativa de residuos para alcanzar altos volúmenes de productos en los procesos de producción<sup>29</sup>. Aunque en LA se han desarrollado e implementado tecnologías de conversión de residuos lignocelulosicos, se necesitan más esfuerzos, tanto en la investigación como a nivel de política de Estado, para lograr tratar los grandes volúmenes de desechos generados en la región y con ello abastecer la demanda regional de bioproductos<sup>93</sup>.

## Conclusiones

Los residuos lignocelulosicos son biomasas constituidas principalmente por celulosa y hemicelulosa, las cuales son fuentes de azúcares capaces de ser transformadas a través de procesos químicos, biotecnológicos o una combinación de ellos, en una variedad de productos que comúnmente se obtienen a partir de recursos fósiles. En los últimos años se han desarrollado biorrefinerías lignocelulósicas y de segunda generación, como industria emergente para el procesamiento de este tipo de recursos. Existen algunos casos de éxito en el mundo, donde se emplean residuos de este tipo para la obtención de productos de 2G. Aunque Latinoamérica es una región privilegiada para la actividad agrícola y, por ende, hay una abundante generación de residuos lignocelulosicos, aún se requieren esfuerzos de investigación, inversión y políticos para su aprovechamiento. El uso adecuado de estos recursos representa una oportunidad para la región, no sólo desde el punto de vista ambiental sino también comercial y de generación de nuevos empleos, si se logra la implementación de biorrefinerías para la producción de productos a gran escala.

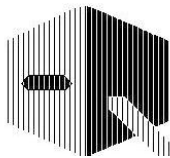
## Referencias

1. J Sarmiento. Migration for climate change in Colombia: Between environmental refugees and economic migrants. *Rev. Derecho*, **15**(2), 53–69 (2019).
2. SCot. Influencia de las condiciones de pretratamiento en la gasificación eficiente de biomasa vegetal producción de energía sostenible. Trabajo final de grado de Máster en Química Sostenible. Universidad Politécnica de Valencia, Valencia, España (2017).
3. M Chávez, S Salvador, E Salvador. La biomasa: fuente alternativa de combustibles y compuestos químicos. *An. Quím.*, **115**(5), 399–407 (2019).
4. A Otto, N Mira, E Prem, N Markt, P Illmer. Biological pretreatment strategies for second-generation lignocellulosic resources to enhance biogas production. *Energies*, **11**(7), 1–14 (2018).
5. BA Goodman. Utilization of waste straw and husks from rice production: A review. *Journal of Bioresources and Biopro-*

- ducts, 5(3)**, 143-162 (2020). DOI: 10.1016/j.jobab.2020.07.001.
6. J Fernández-Rodríguez, JA Pérez-Hernández, F González-Águila. Obtención de biocombustible piroleñoso a partir del bagazo de caña de azúcar en una planta experimental cubana. **Rev. Inst. Cubano Deriv. Caña Azucar (ICIDCA)**, **46(2)**, 42-48 (2012).
  7. L Orlandi. Análisis de factibilidad económica de la producción de bioetanol ligno-celulósico a partir de una fuente como el rastrojo de maíz y, eventualmente, de sorgo. Trabajo final de grado de Máster en Producción e Industrialización de Cereales y Oleaginosas. Universidad Nacional de Lomas de Zamora, Lomas de Zamora, Argentina (2017).
  8. A Guarnizo-Franco, PN Martínez-Yepes, ML Pinzón-Bedoya. Azúcares del pseudotallo de plátano: una opción para la obtención de alcohol de segunda generación. **Bistua: Revista de la Facultad de Ciencias Básicas**, **10(1)**, 39-51 (2012).
  9. A González, I Jiménez, M Rodríguez, S Restrepo, J Gómez. Biocombustibles de segunda generación y Biodiesel: Una mirada a la contribución de la Universidad de los Andes. **Rev. Ing., 1(28)**, 70 (2008).
  10. M Pineda. Dynamics of land use and land cover in a Mexican national park. **Madera y Bosques**, **23(3)**, 87-99 (2017).
  11. Y Vargas, L Peréz. Aprovechamiento de residuos agroindustriales en el mejoramiento de la calidad del ambiente. **Rev. Fac. Ciencias Básicas**, **14(1)**, 59-72 (2018).
  12. J Vilaboa-Arroniz, J Lopez-Collado, D Platas-Rosado, I Vilaboa-Arroniz. El mito de los biocombustible en México. **Trop. Subtrop. Agroecosystems**, **22**, 431-441 (2019).
  13. C Andrade, A Corredor, L Buitrago, A Lache. Procesos bioquímicos utilizados para la producción de bioetanol, biodiésel y biogás y su estado en Colombia. **Semilleros Formación Investigativa**, **3(1)**, 101-117 (2017).
  14. S Subía, R Rubio. Evaluación de biomasa de microalgas de la laguna Limoncocha como materia prima para la obtención de biocombustibles. **Enfoque UTE**, **9(2)**, 106-116 (2018).
  15. RM Balán-Chan, I. Elizalde-Martínez. Algunos aspectos de producción de diésel verde a partir de materias primas de segunda generación y la tecnología del hidrotratamiento. **Rev. Int. Investig. Innov. Tecnol.**, **6 (31)**, 1-15 (2017).
  16. D Krasznai, R Champagne, H Roy, P Champagne, M Cunningham. Compositional analysis of lignocellulosic biomass: conventional methodologies and future outlook. **Crit. Rev. Biotechnol.**, **38(2)**, 199-217 (2018).
  17. J Galaz. Efecto de la Temperatura de Operación en Biorreactores de Biogás con Lactosa y Celulosa. Trabajo de grado de Maestría en Ciencias de la Ingeniería. Pontificia Universidad Católica de Chile, Santiago de Chile, Chile (2020).
  18. A Sharma, M Thakur, M Bhattacharya, T Mandal, S Goswami. Commercial application of cellulose nano-composites – A review. **Biotechnology Reports**, **21**, e00316 (2019). DOI: 10.1016/j.btre.2019.e00316.
  19. J Cai, Y He, X Yu, SW Banks, Y Yang, X Zhang, et al. Review of physicochemical properties and analytical characterization of lignocellulosic biomass. **Renewable and Sustainable Energy Reviews**, **76(1)**, 309-322 (2017).
  20. R Naveda, P Montalvo, L Pinto L, V Figueroa .Remoción de lignina en el pretratamiento de cascarilla de arroz por explosión con vapor. **Rev. Soc. Quim. Perú**, **85 (3)**, 352-361 (2019).
  21. SS Hassan, GA Williams, AKJaiswal. Emerging technologies for the pretreatment of lignocellulosic biomass. **Bioresource Technology**, **262**, 310-318 (2018). DOI: 10.1016/j.biortech.2018.04.099.
  22. J Vera, R Zambrano. Evaluación físico-química de los residuos del procesamiento de yuca (*Manihotesculenta*) y plátano (*Musa paradisiaca*) para la obtención de bioplástico. Trabajo de grado. Universidad Técnica de Manabí, Portoviejo, Ecuador (2021).
  23. L Tejeda, W Marimón, M Medina. Evaluación del potencial de las cáscaras de frutas en la obtención de bioetanol. **Hechos Microbiol.**, **5(1)**, 4-9 (2014).
  24. I Ramos. Caracterización química de tres residuos lignocelulosicos generados en la región del Cantón Alausí. **Rev. Inst. Investig. Fac. Minas, Metalurgia y Ciencias Geográficas**, **20(40)**, 80-85 (2017).
  25. LV Valle Alvarez, J Kreiker, B Raggiotti, F Cadena. Aprovechamiento de desechos lignocelulosicos derivados de la producción industrial de aceite de palma en el desarrollo de materiales compuestos. En: AJEA – Actas de Jornadas y Eventos Académicos de UTN V Jornada de Intercambio y Difusión de los Resultados de Investigaciones de los Doctorados en Ingeniería. 2019. DOI: 10.33414/ajea.4.393.2019 Consultado: 10/12/2021
  26. I Chico. Caracterización del material compuesto Raquis-Cemento. Trabajo de grado. Universidad de los Andes, Bogotá, Colombia (2015).
  27. L Niño López, A Acosta Cardenas, R Gelvez Zambrano. Evaluación de pre-tratamientos químicos para la hidrólisis enzimática de residuos lignocelulosicos de yuca (*Manihote sculentaCrantz*). **Rev. Fac. Ing. Univ. Antioquia**, **69**, 317-326 (2013).
  28. JG Reales, HI Castaño, JE Zapata. Evaluación de Tres Métodos de Pretratamiento Químico sobre la Deslignificación de Tallos de Yuca. **Información tecnológica**, **27(3)**, 11-22 (2016).
  29. D Torres Jaramillo, SP Morales Vélez, JC Quintero Díaz. Evaluación de pretratamientos químicos sobre materiales lignocelulosicos. **Ingeniare. Revista Chilena de Ingeniería**, **25(4)**, 733-743 (2017).
  30. C Natagaima. Obtención de celulosa a partir de residuos de la poda de pasto común por medio de líquido iónico (cloruro de 1-butil-3-metilimidazolio). Trabajo de grado. Universidad Nacional Abierta y a Distancia, Bogotá, Colombia (2018).
  31. R Potumarthi, RR Baadhe, S Bhattacharya S. Fermentable Sugars from Lignocellulosic Biomass: Technical Challenges. En: *Biofuel Technologies*. Eds. V Gupta y M Tuohy. Springer, Berlin. (2013). DOI: 10.1007/978-3-642-34519-7\_1
  32. J Sigüencia, J Delgado, F Posso, J Sánchez. Estimación del potencial de producción de bioetanol para los residuos de la corteza del cacao en Ecuador. **Rev. Cienc. Tecnol. Agropec.**, **21(3)**, 1-20 (2020).
  33. S Dahiya, R Katakojwala, S Ramakrishna, S Venkata. Bio-based products and life cycle assessment in the context of circular economy and sustainability. **Mater. Circ. Econ.**, **2**, 7 (2020). DOI: 10.1007/s42824-020-00007-x

34. J Ventura, MA Santiago, IC Barrera, P Álvarez, P Carrillo, JA Honorato. Caracterización del pasto mombaza como materia prima para producir bioetanol. **Rev. Mex. Ciencias Agric.**, **12(2)**, 235-246 (2021).
35. A Segura, A Manriquez, D Santos, E Ambriz, P Casas, A Serafín. Obtención de bioetanol a partir de residuos de cáscara de piña (*Ananas comosus*). **Jóvenes en la Ciencia**, **8**, 1–8 (2020).
36. S Prasad, S Kumar, K Kumar, J Choudhry, H Kamyab, QV Bach, *et al.* Screening and evaluation of cellulolytic fungal strains for saccharification and bioethanol production from rice residue. **Energy**, **190**, 116422 (2020).
37. A Arumugam, V Malolan, V Ponnusami . Contemporary Pretreatment Strategies for Bioethanol Production from Corn-cobs: A Comprehensive Review. **Waste and Biomass Valor**, **12**, 577–612 (2021).
38. S Sivamani, R Baskar, APChandrasekaran. Response surface optimization of acid pretreatment of cassava stem for bioethanol production. **Environ. Prog. Sustain. Energy**, **39**, e13335 (2020).
39. X Lin, Y Liu, X Zheng, N Qureshi. High-efficient cellulosic butanol production from deep eutectic solvent pretreated corn stover without detoxification. **Ind. Crops Prod.**, **162**, 113258 (2021).
40. P Narueworanon, L Laopaiboon, P Laopaiboon. Capability of immobilized *Clostridium beijerinckii* TISTR 1461 on lotus stalk pieces to produce butanol from sugarcane molasses. **Processes**, **9(4)**, 573 (2021). DOI: [10.3390/pr9040573](https://doi.org/10.3390/pr9040573)
41. PM Melero-Carrizosa, RB García-Reyes, MM Atilano-Camino, A García-González. Obtención de biohidrógeno a partir de cáscaras de naranja y plátano mediante fermentación obscura con *Clostridium beijerinckii*. En: *VII Simposio Nacional de Ciencias Farmacéuticas y Biomedicina y el V Simposio Nacional de Microbiología Aplicada*. 2020. Disponible en: <https://rcfb.uanl.mx/index.php/rcfb/article/view/350> Consultado: 10/12/2021
42. F Nadeem, D Jiang, N Tahir, M Alam, Z Zhang, W Yi, *et al.* Defect engineering in SnO<sub>2</sub> nanomaterials: Pathway to enhance the biohydrogen production from agricultural residue of corn stover. **Appl. Mater. Today**, **21**, 100850 (2020).
43. R Mahato, D Kumar, G Rajagopalan. Biohydrogen production from fruit waste by *Clostridium* strain BOH3. **Renew. Energy**, **153**, 1368–1377 (2020).
44. K Im-Orb, ANPhan, AArpornwichanop. Bio-methanol production from oil palm residues: A thermodynamic analysis. **Energy Conversion Management**, **226**, 113493 (2020).
45. SR Naqvi, I Ali, S Nasir, SA Ammar, AE Atabani, WH Chen. Assessment of agro-industrial residues for bioenergy potential by investigating thermo-kinetic behavior in a slow pyrolysis process. **Fuel**, **278**, 118259 (2020).
46. HJPL de Souza, MD Chaves, G Baptista, CR Andrade, AC Oliveira, DPL de Souza, *et al.* Pelletization of eucalyptus wood and coffee growing wastes: Strategies for biomass valorization and sustainable bioenergy production. **Renew. Energy**, **149**, 128–140 (2020).
47. KH Chang, KR Lou, CH Ko. Potential of bioenergy produc-
- tion from biomass wastes of rice paddies and forest sectors in Taiwan. **Journal of Cleaner Production**, **206**, 460-476 (2019).
48. SNHM Azmin, NABM Hayat, MS Mat. Development and characterization of food packaging bioplastic film from cocoa pod husk cellulose incorporated with sugarcane bagasse fibre. **Journal of Bioresources and Bioproducts**, **5(4)**, 248–255 (2020). DOI: [10.1016/j.jobab.2020.10.003](https://doi.org/10.1016/j.jobab.2020.10.003)
49. LC de Azevedo, R Suzimara, S Jonnatan, D Djalma, N Sandi, O Fábio, *et al.* Biodegradable Films Derived from Corn and Potato Starch and Study of the Effect of Silicate Extracted from Sugarcane Waste Ash. **ACS Appl. Polym. Mater.**, **2(6)**, 2160–2169 (2020). DOI: [10.1021/acsapm.0c00124.s001](https://doi.org/10.1021/acsapm.0c00124.s001)
50. R Listyarini, P Susilawati, E Nukung, M Yua. Bioplastic from Pectin of Dragon Fruit (*Hylocereus polyrhizus*) Peel. **J. Kim. Sains dan Apl.**, **23(6)**, 203–208 (2020).
51. H Sánchez, W Ponce, B Brito, W Viera, R Baquerizo, M Riera. Biofilms Production from Avocado Waste. **Ingeniería y Universidad**, **25**, 1-16 (2021).
52. Maulida, M Siagian, P Tarigan. Production of Starch Based Bioplastic from Cassava Peel Reinforced with Microcrystalline CelluloseAvicel PH101 Using Sorbitol as Plasticizer. **J. Phys. Conf. Ser.**, **710**, 012012 (2016). DOI: [10.1088/1742-6596/710/1/012012](https://doi.org/10.1088/1742-6596/710/1/012012)
53. N Azieyanti, AAmirul, S Othman, H Misran. Mechanical and Morphology Studies of Bioplastic-Based Banana Peels. **J. Phys. Conf. Ser.**, **1529(3)**, 32–50 (2020).
54. AGAdeniyi, JOIghalo, MKAmosa. Modelling and simulation of banana (*Musa spp.*) waste pyrolysis for bio-oil production. **Biofuels**, **12(7)**, 879-883 (2019).
55. M Oladipupo, A Achazhiyath, K Rambabu, G Bharath, F Banat, GS Nirmala, *et al.* Extraction, characterization and optimization of high quality bio-oil derived from waste date seeds. **Chemical Engineering Communications**, **208(6)**, 801–811 (2021).
56. D Aboagye, N Banadda, N Kiggundu, I Kabenge. Assessment of orange peel waste availability in ghana and potential bio-oil yield using fast pyrolysis. **Renewable and Sustainable Energy Reviews**, **70(C)**, 814–821 (2017).
57. Y Ma, Y Yin, Y Liu. New insights into co-digestion of activated sludge and food waste: Biogas versus biofertilizer. **Bioresour. Technol.**, **241**, 448–453 (2017).
58. I Chakravarty, SAMandavgane. Valorization of fruit and vegetable waste for biofertilizer and biogas. **J. Food Process Eng.**, **44**, e13512 (2021).
59. S Achinas, GJWEuverink. Elevated biogas production from the anaerobic co-digestion of farmhouse waste: Insight into the process performance and kinetics. **Waste Manag. Res.**, **37(12)**, 1240–1249 (2019).
60. JM Campos-Martín, A Chica, ME Domíne, T García, B Pawelec, JL Pinilla, *et al.* Biocombustibles. **Boletín del Grupo Español del Carbón**, **58**, 38–44 (2020).
61. L Santos, F Ramos. Analytical strategies for the detection and quantification of antibiotic residues in aquaculture fishes: A review. **Trends in Food Science and Technology**, **52**, 16–30

- (2016).
62. M Garrido. Biocombustibles y producción de biohidrógeno. **MoleQla: Rev. de Ciencias de la Universidad Pablo de Olavide**, **38**, 26-30 (2020).
63. M Balat, H Balat, C Öz. Progress in bioethanol processing. **Prog. Energy Combust. Sci.**, **34**(5), 551–573 (2008).
64. M Ibrahim, N Ramli, E Kamal, S Abd-Aziz. Cellulosic biobutanol by Clostridia: Challenges and improvements. **Renew. Sustainable Energy Rev.**, **79**, 1241–1254 (2017).
65. TY Tsai, YC Loa, CD Dong, D Nagarajan, JS Chang, DJ Lee. Biobutanol production from lignocellulosic biomass using immobilized Clostridium acetobutylicum. **Appl. Energy**, **277**(1), 1115531 (2020).
66. Preethi, TM Mohamed, J Rajesh, M Gunasekaran, G Kumar. Biohydrogen production from industrial wastewater: An overview. **Bioresour. Technol. Reports**, **7**, 100287 (2019).
67. SN Gebremariam, JM Marchetti. Economics of biodiesel production: Review. **Energy Convers. Manag.**, **168**, 74–84 (2018).
68. ST Keera, SM El Sabagh, AR Taman. Castor oil biodiesel production and optimization. **Egypt. J. Pet.**, **27**(4), 979–984 (2018).
69. A Prieto. Los bioplásticos, ¿qué son? ¿cuántos hay? ¿cómo se producen? **Centro de Investigaciones Biológicas Margarita Salas (CIB)** (2020). DOI: 10.18567/sebbmdv\_ANC.2020.08.1
70. M Alcaide, C Collado, J Sancho. Bioplástico degradable. **Ingeniería Materiales**, **2**, 9–13 (2020). Disponible en: [http://polired.upm.es/index.php/ingenieria\\_materiales/article/view/4424/4599](http://polired.upm.es/index.php/ingenieria_materiales/article/view/4424/4599)
71. M Quiroga, D Agüero, R Zapata, H Busilacchi, M Bueno. Activadores de crecimiento y biofertilizante como alternativa al uso de fertilizantes químicos en cultivo de chía (*Salvia hispanica* L.). **Energías Renovables y Medio Ambiente**, **35**(1), 31–40 (2020).
72. N Scarlat, JFDallemand, F Fahl. Biogas: developments and perspectives in Europe. **Renew. Energy**, **129**(A), 457–472 (2018).
73. L Mezule, B Dalecka, T Juhna. Fermentable Sugar Production from Lignocellulosic Waste. **Chemical Engineering Transactions**, **43**, 619–624 (2015).
74. A Parra, ES Cajiao, AR Cerón, HS Villada. Efecto del método de pre-gelatinización de harina de yuca sobre propiedades mecánicas de matrices moldeadas. **Agronomía Colombiana**, **34**(1), S89–S91 (2020).
75. E Trigo, M Regúnaga, M Aquaroni, F Giménez, J Peña. Biorrefinerías en la República Argentina: análisis del mercado potencial para las principales cadenas de valor. MINCyT, Ciudad Autónoma de Buenos Aires, Argentina (2012).
76. R Salazar, G Cárdenas. La bioeconomía y las biorrefinerías. **Avance Agroindustrial**, **34**(3), 3134 (2013).
77. MS Romano, V Corne, R Azario, MC García. Aprovechamiento de residuos lignoceluloso para la remoción de cadmio. **Avances en Ciencias e Ingeniería**, **11**(3), 11-22 (2020).
78. SS Hassan, GA Williams, AKJaiswal. Lignocellulosic Biorefineries in Europe: Current State and Prospects. **Trends in Biotechnology**, **37**(3), 231–234 (2019).
79. SS Hassan, GA Williams, AKJaiswal. Moving towards the second generation of lignocellulosic biorefineries in the EU: Drivers, challenges, and opportunities. **Renewable and Sustainable Energy Reviews**, **101**, 590–599 (2019).
80. <http://www.granbio.com.br/en/conteudos/biofuels/> Consultado: 11/12/2021
81. <https://www.iogen.ca/iogen-technology>. Consultado: 11/12/2021
82. F Gírio, S Marques, F Pinto, AC Oliveira, P Costa, A Reis, et al. Biorefineries in the World. En: *Biorefineries*. Eds. M Rabaçal, A Ferreira, C Silva, M Costa. Lecture Notes in Energy, vol 57. Springer, Cham. (2017) DOI: 10.1007/978-3-319-48288-0\_9
83. <https://enerkem.com/company/facilities-projects/> Consultado: 11/12/2021
84. <https://www.bioliq.de/english/55.php> Consultado: 11/12/2021
85. M Rizo. Agricultura, desarrollo sostenible, medioambiente, saber campesino y universidad. **Ciencia en su PC**, **2**, 106–120 (2017).
86. Banco Mundial. Tierras cultivables (% del área de tierra) – Latin America & Caribbean (2021). Disponible en: <https://datos.bancomundial.org/indicator/AG.LND.ARBL.ZS?locations=ZJ> Consultado: 06/12/2021
87. RJanssen, DDRutz. Sustainability of biofuels in Latin America: Risks and opportunities. **Energy Policy**, **39**(10), 5717–5725 (2011). DOI: 10.1016/j.enpol.2011.01.047
88. RD Silva-Martínez, ASanches-Pereira. Organic waste to energy in Latin America and the Caribbean (Lac); state-of-the-art literature review. En: *26th European Biomass Conference and Exhibition*. 2018:14-17. Disponible en: <https://repositorio.unesp.br/handle/11449/171299> Consultado: 11/12/2021
89. <https://www.fao.org/faostat/es/#data/GT> Consultado: 11/12/2021
90. M Stojanovic. Biomimicry in Agriculture: Is the Ecological System-Design Model the Future Agricultural Paradigm? **J. Agric. Environ. Ethics**, **32**, 789–804 (2019).
91. AK Chandel, VK Garlapati, AK Singh, FAF Antunes, SS da Silva. The path forward for lignocellulose biorefineries: Bottlenecks, solutions, and perspective on commercialization. **Bioresource Technology**, **264**, 370–381 (2018).
92. MA Osejos-Merino, JJ Jaramillo-Véliz, MV Merino-Conforme, AJ Quimis-Gómez, JL Alcívar-Cobeña. Producción de biogás con estiércol de cerdo a partir de un biodigestor en la Granja EMAVIMA Jipijapa – Ecuador. **Dominio de Ciencia**, **4**(1), 709–733 (2018).
93. RD Silva-Martínez, A Sanches-Pereira, W Ortiz, MF Gómez, S Teixeira. The state-of-the-art of organic waste to energy in Latin America and the Caribbean: Challenges and opportunities. **Renewable Energy**, **156**, 509–525 (2020).



## Cell encapsulation using chitosan: chemical aspects and applications

Maura Rojas Pirela<sup>1,2</sup>, Verónica Rojas<sup>2</sup>, Elizabeth Pérez Pérez<sup>1</sup>, Cristóbal Lárez Velásquez<sup>3\*</sup>

<sup>1)</sup> Laboratorio de Análisis Biotecnológico y Molecular (ANBIOMOL) "Prof. Guillermo López Corcuera"  
Facultad de Farmacia y Bioanálisis, Universidad de Los Andes. Mérida 5101, Venezuela.

<sup>2)</sup> Instituto de Biología, Facultad de Ciencias, Pontificia Universidad Católica de Valparaíso,  
Valparaíso, Chile.

<sup>3)</sup> Laboratorio de Polímeros, Departamento de Química,  
Universidad de Los Andes, Mérida 5101, Venezuela

(\*) [clarez@ula.ve](mailto:clarez@ula.ve); [larezcristobal@gmail.com](mailto:larezcristobal@gmail.com)

Recibido: 07/10/2021

Revisado: 14/11/2021

Aceptado: 03/12/2021

### Abstract

In this work, the main approaches for the preparation of encapsulating matrices using chitosan-containing formulations have been reviewed. Various methodologies have been considered, such as physical intermolecular bonds and chemical cross-linking reactions, including the click reactions which have become novel in the cross-linking of systems containing this biopolymer. Likewise, the formation of different macroscopic assemblies such as spheroids, vesicles, layer by layer polycomplexes, etc., has been addressed. In the final part of the work, the main achievements reported with these matrices in the encapsulation of cells, both eukaryotic and prokaryotic, are discussed, emphasizing their potential applications and perspectives in different fields as medicine (treatment of traumatic diseases, diabetes, venous diseases, tissue regeneration, transplantation and tolerance); food (administration of probiotics); industrial applications (bioethanol production); etc.

**Keywords:** Cell encapsulating matrices; Click reaction; chemical crosslinking; ionotropic gelation

### Resumen

**Encapsulación de células usando quitosano: aspectos químicos y aplicaciones.** En este trabajo se han revisado los principales enfoques para la preparación de matrices encapsulantes utilizando formulaciones que contienen quitosano. Se han considerado diversas metodologías, como las uniones intermoleculares físicas y las reacciones químicas de entrecruzamiento, incluidas las reacciones *click*, las cuales se han vuelto una novedad en la reticulación de sistemas que contienen este biopolímero. Asimismo, se ha abordado la formación de diferentes ensamblajes macroscópicos como esferoides, vesículas, policomplejos capa a capa, etc. En la parte final del trabajo se discuten los principales logros reportados con estas matrices en el encapsulado de células, tanto eucariotas como procariotas, enfatizando sus potenciales aplicaciones y perspectivas en diferentes campos como la medicina (tratamiento de enfermedades traumáticas, diabetes, enfermedades venosas, regeneración de tejidos, trasplante y tolerancia); en la industria alimentaria (administración de probióticos); aplicaciones industriales (producción de bioetanol); etc.

**Palabras claves:** Matrices encapsulantes de células; reacción *click*; reacciones de entrecruzamiento; gelación ionotrópica

### Introduction

Cell encapsulation basically consists of confining living cells within non-living matrices in order to protect their physical integrity, preserving also their normal metabolic activities, for their subsequent transit or use in risky environments for them. The method was proposed for the first time by Chang in the 60s of the previous century, showing different experimental approaches that allow it to be achieved<sup>1</sup>.

One of the main reasons for the encapsulation of cells is the protection that the encapsulating coating gives them, which is usually formed by a partially permeable polymeric membrane artificially created. Thus, in the case of transplanted cells,

encapsulation could prevent their rejection if it manages to "hide" them from the host's immune system (a process known as immunoisolation), without the need to use immunosuppressants<sup>2</sup>.

Research on new systems for cell encapsulation, or the improvement of already known systems, will always be very topical because the results are potentially applicable in the treatment of disorders associated with various diseases such as diabetes, neurological degeneration, hemophilia, cancer, kidney failure, etc.<sup>3-5</sup>. In a broader sense, the search for new matrices for the encapsulation of proteins, peptides, DNA, cells, and even microorganisms, has been oriented towards

the use of biomaterials such as polysaccharides, i.e., alginates<sup>6</sup>, agarose<sup>7</sup>, chitosan<sup>8</sup> (see chemical structures in figure 1); proteins, i.e., gelatin<sup>9</sup>, collagen<sup>10</sup>, silk fiber<sup>11</sup>; polynucleotides (RNA and DNA<sup>12</sup>) and some biodegradable polymers such as polylactic and polyglycolic acids and their copolymers<sup>13</sup> and polyhydroxyalcanoates<sup>14</sup> (see chemical structures in figure 2). Among the current most important reasons for the preference of these materials is their biodegradability, since it is intended that they not only be able to transport cells but also allow the design of controlled release systems towards well pre-established therapeutic targets.

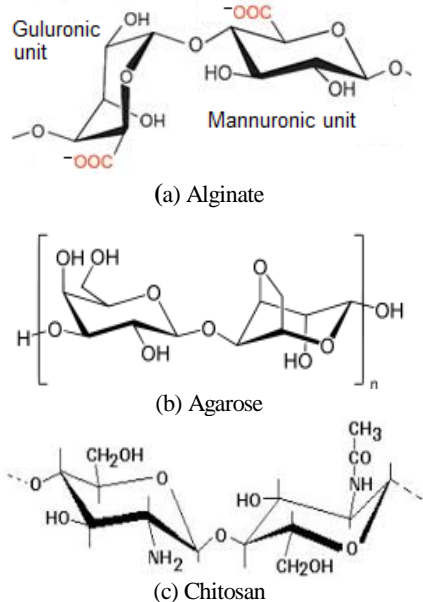


**Fig. 1:** Chemical structure of some polysaccharides employed in the cell encapsulation.

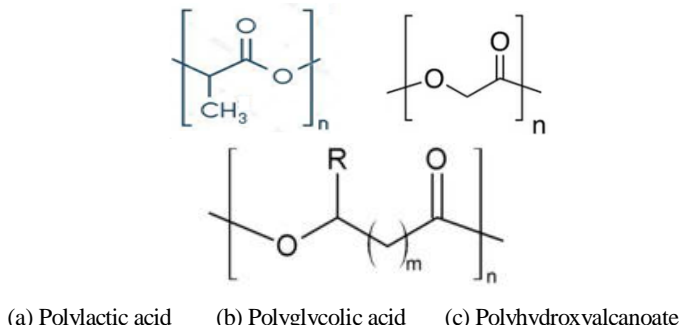


**Fig. 2:** Chemical structure of some biodegradable polymers employed in the cell encapsulation.

In this work, the main approaches using chitosan-containing formulations for the encapsulation of cells are reviewed. Different methodologies have been considered for the formation of the encapsulating matrix, such as physical and chemical cross-linking reactions, including click reactions. Likewise, the formation of different macroscopic structures such as spheroids, vesicles, layer-by-layer polycomplexes, etc., has been addressed. On the other hand, a brief discussion of the main achievements reported for the chitosan-containing matrices obtained during encapsulation of both, eukaryotic and

prokaryotic cells, is also presented, emphasizing their potential applications.

### Chemical aspects of the encapsulation of cells using chitosan

Chitosan is a highly versatile polysaccharide which is usually obtained by deacetylation of chitin, a relatively inexpensive material routinely extracted from industrial crustacean processing wastes. However, for applications in the health field, in recent years there has been a tendency to produce it from fungi to minimize the intoxication risks associated to marine product derivatives<sup>15</sup>. It is considered a prominent candidate for the encapsulation of a diversity of materials<sup>16</sup>, including cells, to be used in living systems because it has adequate properties for these purposes, such as its non-toxicity, biodegradability, and biocompatibility<sup>17,18</sup>. However, it is essential to consider that for such uses it is necessary to work with materials of high degrees of purity.

From a chemical point of view, some relevant chitosan-characteristic reactions can be established in this kind of applications. Thus, encapsulation of materials within envelopes or matrices containing chitosan in their composition can be achieved using various experimental approaches, such as:

- Formation of three-dimensional networks generated by intermolecular crosslinking due to physical interactions, which can be of various nature (hydrophobic<sup>19</sup>, hydrogen bonds<sup>19</sup>, molecular entanglement<sup>20</sup>, ionic interactions<sup>21</sup>, etc.).
- Three-dimensional networks formation caused by covalent bonds linking different polymer chains, which can be achieved through chemical reactions that do not include crosslinking agents<sup>22</sup> or that require their presence, whether they are low or high molecular weight<sup>23</sup>. Among these reactions have recently been included the so-called “click reactions”, also known as orthogonal reactions<sup>24</sup>, based on chitosan derivatives which are specially prepared for such purposes.

One of the most exploited characteristics of chitosan for this type of application is its cationic nature in aqueous acidic medium, which is enhanced in some derivatives such as quaternary ammonium salts in a wide pH range. This cationic character allows its electrostatic interaction with materials carrying anionic residues, as it has been shown in the preparation of microspheres encapsulating solutions of an anionic polyelectrolyte obtained by oxidation of the polysaccharide scleroglucan (generating pendant carboxylate residues along its chain) within a skin formed by the chitosan/scleroglucan polyelectrolyte complex<sup>25</sup>. Spheres are formed by simply dropping a polyanion solution into a chitosan solution in an acid medium. Similarly, the encapsulation of chitosan solutions within the skin formed by the polyelectrolyte complex of both biopolymers is also possible. An idealized picture of this type of sphere is shown in figure 3.

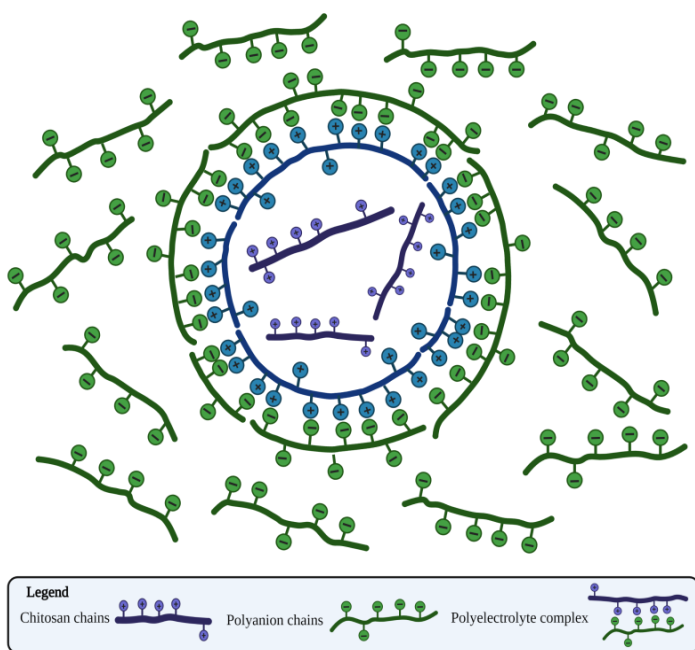


**Fig. 3:** Idealized structure of a sphere formed by interfacial polycomplexation of chitosan and a polyanion when a drop of chitosan solution is dropped into the polyanion solution.

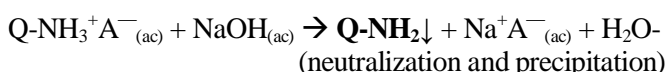
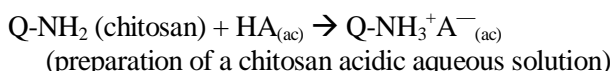
Some of the most common experimental methods of encapsulation that have been reported using containing-chitosan formulations are: spheres formation by ionotropic crosslinking, i.e., a suspension of cells in a aqueous chitosan solution is dropped over an aqueous solution of sodium tripolyphosphate (STPP) under agitation<sup>26</sup>; cell assemblies confined between layers of chitosan (built layer by layer)<sup>27</sup>; preparation of the gelling mixture containing the cells and its subsequent covalent crosslinking by various chemical routes, i.e., polymerization reactions with thermal initiation<sup>28</sup>; bioorthogonal reactions, in which the experimental conditions must be refined in order to achieve functional materials (considering the complex biological mixtures employed and the presence of living cells)<sup>29</sup>; etc.

#### *Chitosan cross-linking processes in the formation of encapsulating matrices*

A great variety of cross-linking processes using chitosan-containing formulations have been reported in the formation of encapsulating matrices. A summary of the most common ones is presented in the following sections.

#### Cross-linking by physical interactions:

- Precipitation due to pH change: neutralization of an acidic aqueous solution of chitosan ( $\text{Q}-\text{NH}_3^+ \text{A}^-_{(\text{ac})}$ ) with a base ( $\text{NaOH}$ ) leads to decreasing of chitosan cationic groups, favoring hydrogen bonding and/or hydrophobic interactions and causing its precipitation according to the following reactions:



- Aggregation by changing the solvent properties: addition of a miscible solvent (but less polar than water such as 1,2-propanediol) to an aqueous solution of chitosan, in acid medium, causes changes in the properties of the solvent, whose dielectric constant becomes lower<sup>19</sup>, unfailingly leading to gelation if right conditions are reached. As in the previous case, hydrogen bonding and hydrophobic interactions will be favored under the new conditions.

- Aggregation due to temperature changes: when the temperature of aqueous solutions of specific chitosan derivatives is increased, hydrophobic aggregates are formed due to the occurrence of a conformational transition which causes gelling of the system, i.e., aqueous solutions of poly(isopropyl-acrylamide)-grafted chitosan undergo gelling around 29.5 °C<sup>30</sup>.

- Ionotropic cross-linking: neutralization of the cationic charges of chitosan with low molecular weight polyanions, such as STPP, generates spherically assembled hydrogels with controllable size. The occurrence of this kind of process has also been reported with other similar polyanions, i.e., adenosine triphosphate (ATP), trisodium citrate, and sodium sulfate<sup>31</sup> (see structures in figure 4).

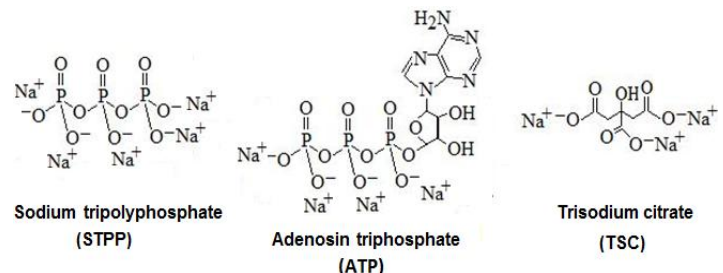


**Fig. 4:** Chemical structure of some low molecular weight polyanions used as crosslinking agents in ionotropic hydrogelation.

- Formation of polyelectrolyte complexes (PEC): neutralization of electrical charges of opposite sign (positive in chitosan and negative in polyanions) generates composite materials known as chitosan-based polyelectrolyte complexes<sup>32,33</sup>, which are also denominated as “chitoplexes”<sup>34</sup>. An important group of these materials, mainly due to their natural origin, are the so-called polyplexes, in which the polyanionic part would be made up of nucleic acids, i.e., plasmidic DNA<sup>35</sup>.

#### Chitosan chemical cross-linking:

- Through hydroxyl groups: a specific example of this type of reaction is its cross-linking with epichlorohydrin<sup>36</sup>; however, it is important to consider that to achieve the selective reaction of the -OH groups in chitosan, usually the primary hydroxyls of the C6 carbon, the amine groups must be previously protected by reactions such as phthaloylation<sup>37</sup> and formation of Schiff bases with aryl-aldehydes<sup>38</sup>, which allow their subsequent regeneration. The use of methanesulfonic acid as a solvent has also been reported as a method of protecting amine groups<sup>39</sup>. Other reactions that can lead to cross-linking through the -OH groups, after protection of the amine groups, are reactions with diacyl halides, i.e., adipoyl chloride<sup>39</sup>.

- Through amine groups: the most frequently reported covalent cross-linking reaction of chitosan, through the amine groups present on carbon C2, is the formation of Schiff bases with dialdehydes. In this regard, cross-linking using glutaraldehyde has been one of the most studied reactions (see simplified scheme in figure 5), although it has not yet been fully understood due to the complexity involved in this multifactorial process<sup>40</sup>. Although other dialdehydes have also been used for this purpose, such as glyoxal (figure 6a)<sup>41</sup>, the current emphasis has been moving to some related compounds, especially those of natural origin, such as genipin (figure 6b)<sup>42</sup> and vanillin (figure 6c)<sup>43</sup>, seeking to reduce toxic effects of aldehydes, among other things; nevertheless, it should be noted that cross-linking with this kind of compounds also proceeds through complex mechanisms. Macromolecular dialdehydes has also been assayed to chemical cross-linking of chitosan, i.e., scleroglucan-dialdehyde (figure 6d) obtained by the Malaprade reaction of scleroglucan (oxidation with potassium periodate of the polysaccharide produced by fungi of the genus Sclerotium)<sup>25</sup>. Similarly, a very interesting cross-linking reaction has been achieved using a chitosan-dialdehyde (figure 6e) generated by this same reaction to obtain a cross-linking material containing only chitosan and its dialdehyde derivative<sup>44</sup>.

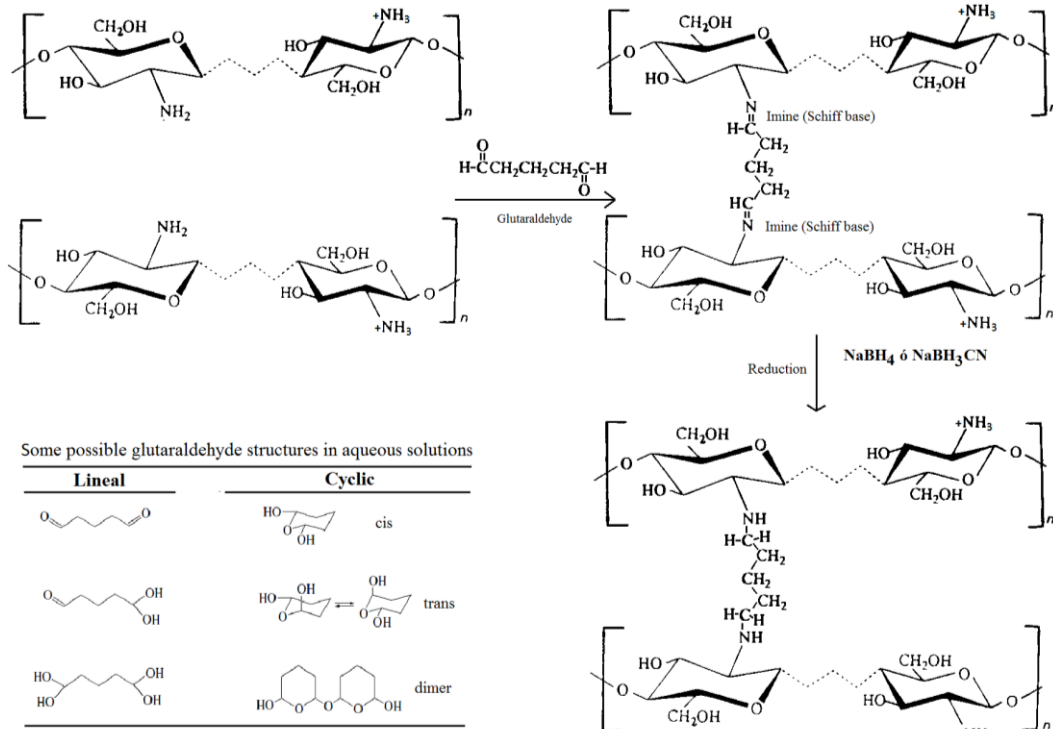


**Fig. 5:** Simplified scheme of the cross-linking reaction of chitosan with glutaraldehyde via Schiff base formation. The subsequent reduction of the imines and glutaraldehyde structures that can coexist in aqueous solutions are also shown.

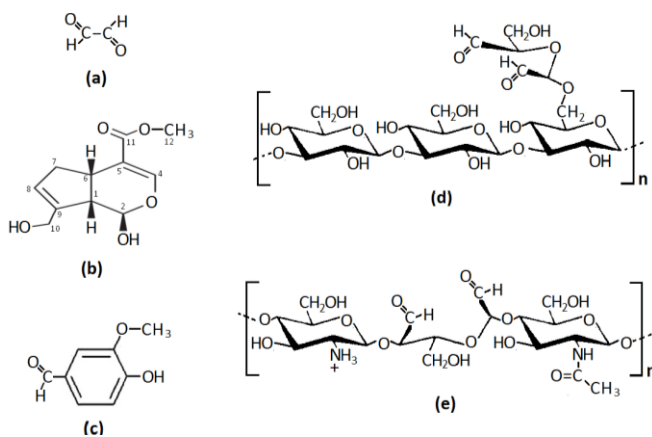


**Fig. 6:** Chemical structure of some compounds used in the chemical cross-linking of chitosan through the amine group at the C2 carbon: (a) glyoxal, (b) genipin and (c) vanillin, (d) scleroglucan-dialdehyde and (e) chitosan-dialdehyde.

- Through pendant groups added by derivatization: addition of

new pendant groups to the chitosan polymer chain can lead to new cross-linking reactions, which allow to obtain novel materials and open new horizons to the versatility of chitosan as a material for use in bioapplications. Generation of these pendant groups can be achieved through a wide variety of chitosan modification reactions, many of which can already be considered routine reactions, through both: amine group at the C2 carbon (acylation, alkylation, quaternization, phosphorylation, sulfation, etc.) as well as hydroxyl groups at C3 and C6 carbons (acylation, alkylation, silylation, halogenation, azidation, etc.)<sup>45</sup>. These derivatives can be subsequently manipulated to establish new processes for cell encapsulation, i.e., coupling of the derivative from 5-azido pentanoic acid and chitosan with ethoxylated glycerol tripropionate through a click reaction (figure 7), whose product has been assayed with good results in mesenchymal cell encapsulation<sup>24</sup>. Thus, click reactions have increased the prospects for chitosan as promising materials for such applications<sup>29,46</sup>.

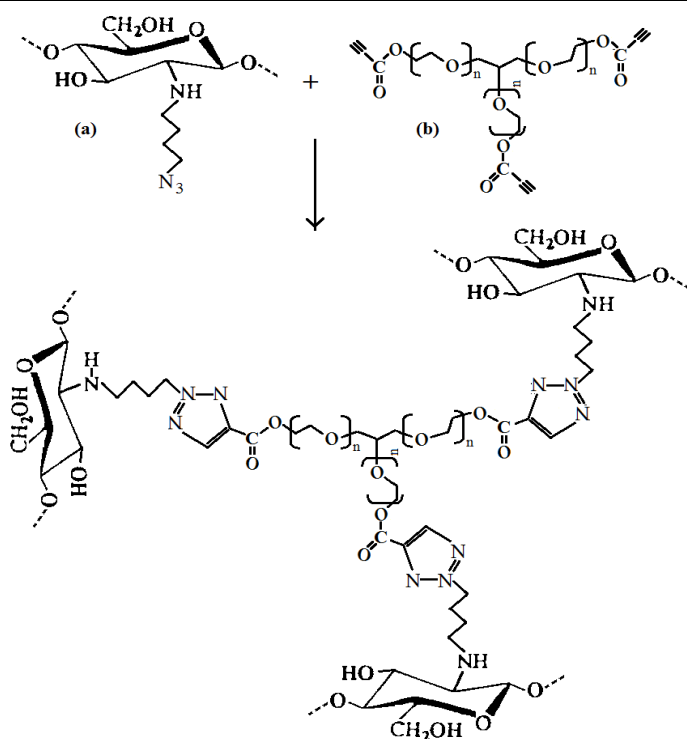


**Fig. 7:** Chemical cross-linking via click reaction between the derivative from 5-azido pentanoic acid/chitosan (a) and the ethoxylated glycerol tripropionate (b).

### Cell encapsulation using chitosan

Chitosan derivatives, and their combinations with other natu-

ral and synthetic polymers, are among the most studied polymeric materials for cell encapsulation<sup>47-52</sup>. Various types of eukaryotic and prokaryotic cells have been used in numerous studies of cell encapsulation with these biopolymers (figures 8-10). Encapsulation of some eukaryotic cells such as chondrocytes<sup>53,54</sup>, fibroblasts<sup>47,55</sup>, stem cells<sup>56</sup>, mesenchymal cells<sup>57</sup>, hepatocytes<sup>58</sup>, erythrocytes<sup>59</sup>, pancreatic  $\beta$ -cells<sup>60</sup>, cardiomyocytes<sup>61</sup>, etc., have served as the basis for studies focused on cell therapy for the treatment of certain pathologies<sup>48,49,62-65</sup>, transplantation and immune tolerance<sup>50,59,65-68</sup>, tissue regeneration<sup>47,68</sup> and industrial applications<sup>69</sup>. On the other hand, the encapsulation of bacteria<sup>70-76</sup> has been focused mainly on the oral administration of probiotics<sup>70</sup> and the treatment of some diseases<sup>53</sup>. Each of these topics will be briefly discussed in the following sections.

#### Eukaryote cells encapsulation

**Pathology treatments:** chitosan has been used as encapsulating material for mesenchymal stem cells (MSCs) in the treatment of traumatic diseases in which a traumatic injury has occurred, i.e., in the spinal cord (figure 8A); chitosan not only maintains the cellular viability of MSCs but also allows these cells to release vesicles and extracellular trophic factors (growth factors, chemokines, and cytokines), as well as maintain their antioxidant characteristics<sup>48</sup>. MSCs appear to exert a paracrine action that can therapeutically enhance spinal cord regeneration, limiting glial cicatrization<sup>76</sup>, reducing cell death at the injured site<sup>77</sup>, and acting as

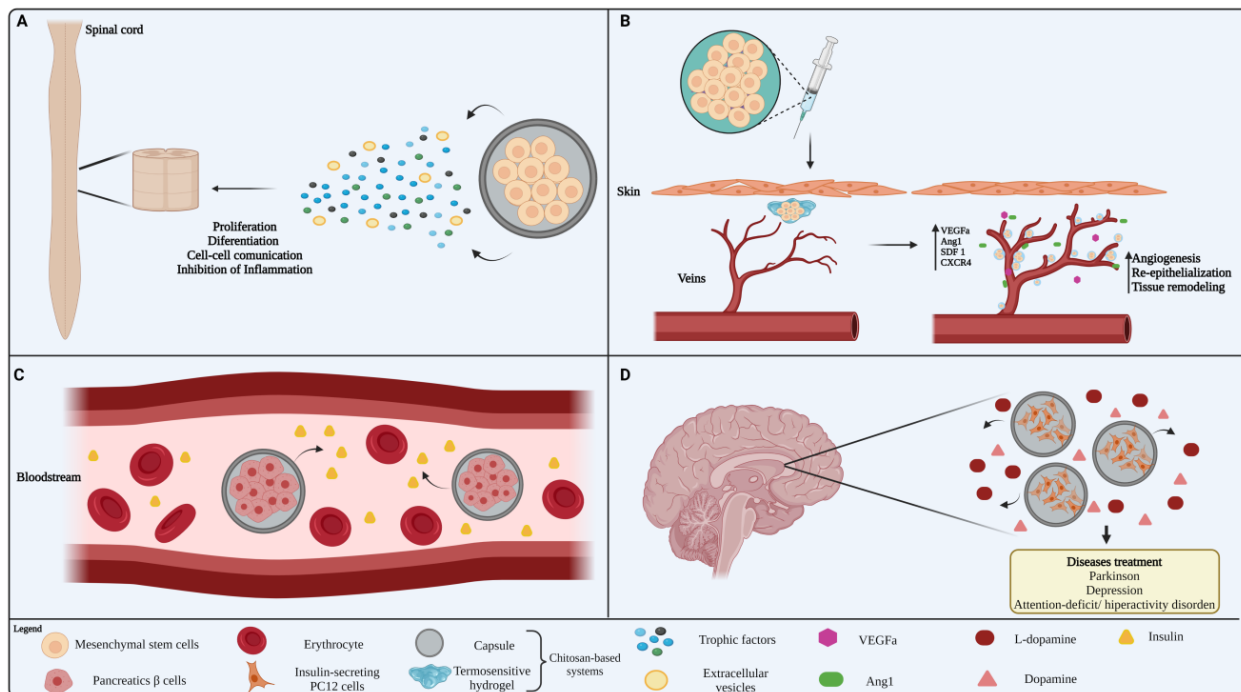


**Fig. 8:** Encapsulation of eukaryotic cells in chitosan-based systems for treatment of some pathologies. **A.** Traumatic diseases: the release of trophic factors and extracellular vesicles by MSCs promotes the regeneration of the nervous tissue; **B.** Venous diseases: encapsulated MSCs release paracrine factors that modulate inflammation, angiogenesis, and tissue remodeling; **C.** Metabolic diseases such as diabetes: encapsulated pancreatic  $\beta$ -cells could be used as a controlled insulin delivery system for the control of blood glucose; **D.** Neuropathies: encapsulation of some neurotransmitter-secreting cells, such as PC12 cells, would be used as a strategy for the treatment of diseases associated with neurotransmitter deficiency or secretory cell dysfunction.

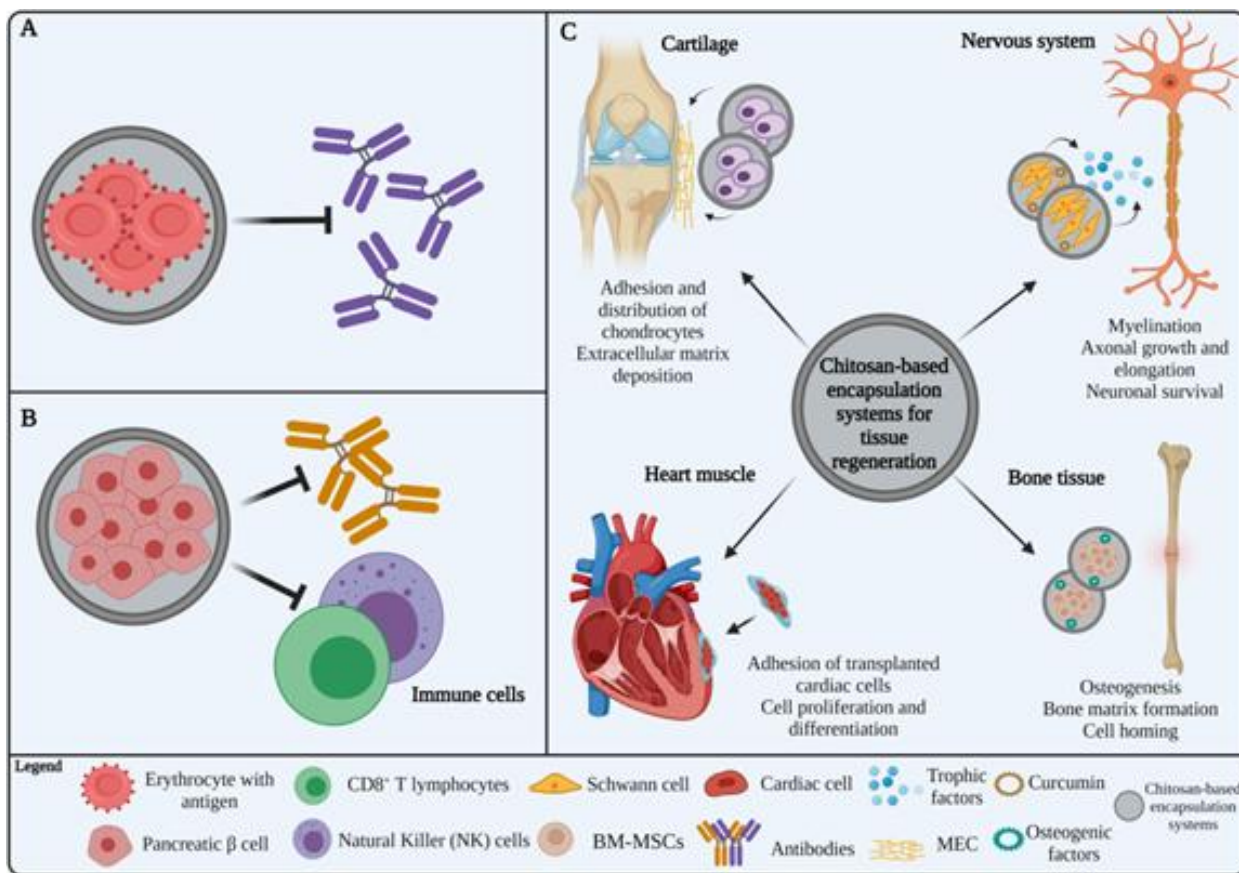


**Fig. 9:** Encapsulation of eukaryotic cells in chitosan-based systems for tissue transplantation and regeneration: **A.** Erythrocyte transfusion: encapsulation of erythrocytes expressing surface antigens could prevent the antibodies binding to them and, consequently, attenuate recognition of the system host immune; **B.** Pancreatic cell implantation: encapsulation of  $\beta$ -cells would inhibit the adhesion of antibodies to these cells, preventing cytotoxicity mediated by natural killer (NK) and CD8<sup>+</sup> T cells; **C.** Tissue regeneration: the encapsulation of different types of cells could be a strategy for the regeneration of various tissues (cartilage, nervous system, bone, heart muscle, etc.).

a carrier of signal molecules that regulate cell-to-cell and cell-extracellular matrix communications<sup>48</sup>. Together with MSCs, chitosan could orchestrate the modulation of inflammation, promoting the establishment of a less hostile environment after traumatic injury and, subsequently, the survival of transplanted cells<sup>48</sup>.

In other cases, such as diabetes and venous diseases, the injection of heat-sensitive hydrogels of chitosan/collagen/ $\beta$ -glycerophosphate ( $\beta$ -GP) containing three-dimensional spheroidal mesenchymal stem cells (3D MSC) has been studied to accelerate the healing of chronic wounds<sup>62</sup> (figure 8B). The combination of these polymers promotes a conducive environment for encapsulated MSCs, especially accelerating the adhesion, proliferation, secretion, and expression of paracrine factors, such as vascular endothelial growth factor A (VEGFA), angiopoietin 1 (Ang1), factor 1 derived from stromal cells (SDF1) and its chemokine receptor 4 with CXC motif (CXCR4) which, in addition, to reduce inflammation, also promote angiogenesis, re-epithelialization and tissue remodeling in the wound<sup>78</sup>.

Besides being proposed for the treatment of venous insufficiency linked to diabetes, encapsulation of pancreatic  $\beta$ -cells in microcapsules of alginate/chitosan (AC) and algi-

nate/chitosan/PEG (ACPEG) could be used as a delivery system for insulin-controlled release for blood glucose control (figure 8C)<sup>49</sup>. These materials could represent a suitable system for pancreatic cell support and insulin secretion. Its permeable-selective nature allows the diffusion of nutrients and the production and release of insulin<sup>49</sup>, offering a therapeutic alternative to traditional treatments of insulin injections and diet. Encapsulation of PC12 cells with chitosan has been evaluated (figure 8D) as a therapeutic strategy for neurodegenerative diseases associated with the loss of dopamine in the cerebral striatum, i.e., Parkinson's disease<sup>79</sup>. PC12 is a dopamine-secreting cell line of great interest in studies of neuroprotective models for Parkinson's disease<sup>80,81</sup>. Besides promoting the viability of PC12 cells, its encapsulation with chitosan stimulates them to produce and release catecholamines and their precursors, such as L-dopa and dopamine, even four weeks after encapsulation<sup>80</sup>. The difference in the secretory capacities of these encapsulated cells is attributed to a possible chitosan interaction with some adhesion molecules present on the cell surface<sup>80</sup>. Therefore, the use of dopamine-secreting cells can be considered as a strategy for treatments of Parkinson's and other diseases associated with dopamine deficiency or secretory cell dysfunction<sup>82,83</sup>. Transplantation and tolerance: microencapsulation is considered a very

promising tool for immuno-isolation in transplantation and immune tolerance studies<sup>84</sup>. In addition to re-presenting an alternative to the chronic suppression of the patient's immune system, which makes these patients vulnerable to other diseases, the encapsulation of living cells serves as an immuno-permeable barrier, increasing cell viability after transplantation. Additionally, these encapsulation systems act as selectively permeable barriers, allowing the free diffusion of nutrients and metabolic waste, and improving cell survival<sup>84</sup>.

Some studies have suggested that cell encapsulation with this polymer is a novel and effective strategy in tissue engineering<sup>50,59,65-68,79</sup> (figure 9). Cell transplantation has been proposed as a strategy for the immuno-camouflage of living and functional red blood cells<sup>69</sup>. Encapsulation of erythrocytes in ACPEG capsules could be used to prevent the binding of antibodies to red blood cells and, consequently, to attenuate the recognition of the host's immune system<sup>69</sup> (figure 9A) This strategy would be a great advance in transfusion therapies, since it would allow the production of universal red blood cells, without the use of specific enzymes for the elimination of surface antigens<sup>85,86</sup>. Furthermore, it would be a great advantage in transfusion therapies, especially for rare blood groups<sup>86</sup> or in regions where the frequency of certain blood groups is very low<sup>11</sup>. Transplantation of encapsulated pancreatic  $\beta$ -cells in chitosan-based systems in the treatment of diabetes, additionally to being an alternative for the production of insulin, would function as a barrier minimizing the damage induced by the inflammatory responses to the transplanted cells<sup>49</sup> (figure 9A), contributing to longer life and function during a xenogeneic transplantation<sup>53</sup>. A similar situation can occur for Parkinson's disease, where encapsulation of cells such as PC12 will not only allow the controlled release of dopamine but would also be a method to safely confine these tumor cells and isolate them from the immune system<sup>79</sup>.

It should be noted that the immuno-isolating capacity of chitosan microencapsulation is not only attributed to the ability to inhibit the adhesion of antibodies (including IgG) to the transplanted cells<sup>55</sup>, but also to the prevention of cytotoxicity mediated by natural T killer cells (NK) and CD8<sup>+50</sup> (figure 9B). These cells are crucial in the vertebrate immune system because they act as regulatory agents of the alloimmune response in transplanted patients<sup>89-91</sup>. Notably, CD8<sup>+</sup> cells can escape to the immunosuppressive effects of drugs such as cyclosporin and rapamycin<sup>91</sup>, whereby cell encapsulation with polymers such as chitosan could be an alternative for immune suppression therapy in transplanted patients because of an attenuating effect on immune cells escaping of immunosuppressive drugs effects could be additionally obtained.

**Tissue regeneration:** due to its biological properties, chitosan has been widely studied as a very promising material in regenerative medicine, being used as scaffolds or platforms

for the repair and/or regeneration of various tissues, including skin, bone, liver, cartilage, nerves, and muscle<sup>81</sup> (figure 8C).

**Cartilage regeneration:** encapsulation of chondrocytes with chitosan-containing systems is considered a great tool in tissue engineering and orthopedics<sup>53,92-95</sup>. The covering obtained with chitosan/hyaluronic acid (HA) fulfilling a temporary function of extracellular matrix (ECM) and creates a favorable chondrogenic microenvironment due to the promotion of deposition of cartilaginous extracellular matrix (CCEM) components by encapsulated chondrocytes<sup>93</sup>, facilitating adhesion and uniform distribution of chondrocytes at the implant site<sup>53,94</sup> (figure 9C.1). Furthermore, proliferative activity and differentiation of chondrocytes are stimulated by the presence of these polymers<sup>93</sup>. It should be noted that the encapsulation of adipose tissue-derived stromal cells (ADSC) with chitosan/ $\beta$ -glycerophosphate/starch has been considered as an alternative for the regeneration of cartilage tissue; encapsulation of these cells with these polymers promotes chondrocytic differentiation and CEM accumulation<sup>95</sup>.

**Nervous system regeneration:** several studies have evaluated the encapsulation of neuronal stem cells (NMCs) with chitosan derivatives as a strategy for the repair of nervous tissue<sup>96,97</sup> (figure 9C.1). In murine nerve cells encapsulation studies and injection of neural progenitors-spheroid-type aggregates with self-healing hydrogels (SH-H) of glycol-chitosan and benzaldehyde-difunctionalized PEG, at both ends (DF-PEG), induced proliferation and differentiation to neuron-like cells was observed. In addition, cells encapsulated with SH-Hs had the ability to regenerate and rescue neural function in the central nervous system (CNS) of a zebrafish embryo neural injury model (*Danio rerio*), caused by exposure to ethanol<sup>96</sup>. Similarly, the SH-Hs treatment loaded with spheroid neural stem cells (NSCs), additionally to restoring neuronal functions, had a positive influence on the development and hatching rate of treated embryos. The advantage of these neural progenitors encapsulated with SH-Hs could be attributed to their ability to fill physical spaces associated with injuries<sup>97</sup> and facilitate metabolism, oxygen availability, migration and cell-cell communication, creating an adequate microenvironment for the proliferation of encapsulated NSCs<sup>96,97</sup>. On the other hand, the encapsulation of Schwann cells (SCs) with chitosan has also been studied<sup>98</sup> (figure 9C.1). SCs are glial cells that play an important role in the regeneration of the injured peripheral nervous system (PNS)<sup>99</sup>. In this study, the sciatic nerve regeneration was evaluated *in vivo* using artificial neural guide channels of poly-L-lactic acid contained with SCs and curcumin encapsulated in chitosan nanoparticles<sup>98</sup>. Treatment with these nanoparticles induced a significant increase in the number of axons in the injured sciatic nerve, as well as a restoration of motor and sensory function<sup>99</sup>.

In these systems, SCs would play an important role in nerve regeneration through the release of neurotrophic factors, i.e., neurotrophic factor derived from the glial cell line (GDNF)<sup>100</sup> and growth factors such as nerve growth factor (NGF)<sup>101</sup>, which contribute to the myelination process, promotion of growth and axonal elongation, as well as survival of neurons<sup>100,101</sup> (figure 9C.1). On the other hand, curcumin would act as a factor to decrease apoptosis<sup>98</sup> and stimulate the proliferation of SCs<sup>102</sup> and, consequently, improve the regeneration and functional recovery of injured nerve. Encapsulation and transplantation of SCs together with compounds that facilitate their activity could have a great influence on the therapeutic activity of these cells, notably improving neuronal regeneration therapy.

**Bone regeneration:** the encapsulation of osteoblasts with chitosan hydrogels has been proposed as a method to transport osteoblast cells in bone disorders treatments<sup>103</sup> (figure C.3). A greater adhesion, proliferation, and expression of type 1 collagen (collagen more abundant in the vertebrate ECM) was achieved through the manufacture of a 3D tracing system to make tissue scaffolds based on pure chitosan and chitosan cross-linked with pectin and genipin, as well as a higher mineralization activity in osteoblast cells *in vitro*<sup>103</sup>. Likewise, some reports based on the encapsulation of stromal MSCs derived from human bone marrow (BM-MSCs), which can self-renew and differentiate into multiple cell lines, demonstrated that its encapsulation in chitosan/dextran hydrogels not only maintained their viability but could also differentiate into adipocytes and osteocytes<sup>104</sup>. Similarly, encapsulation of BM-MSCs together with osteogenic factors, such as bone morphogenic protein-2 (BMP2), in chitosan/poly ( $\epsilon$ -caprolactone) heat-sensitive gels have a positive effect on osteogenesis and bone matrix formation<sup>105</sup> (figure 9C.3). More importantly, the encapsulation of these MSCs not only influences their proliferation and differentiation, but they could also serve as an alternative to take advantage of some signaling pathway, such as the stromal cell-derived factor-1 (SDF-1)/CXC receptor 4 (CXCR4) route, very important in the process of mobilization and relocation or "homing" of MSCs<sup>106,107</sup>. Studies focused on MSCs derived from human adipose tissue (hASCs) revealed that after being injected and promoted the over-expression of their chemokine receptor CXC type 4 (CXCR4) these cells had the ability to respond and migrate towards the derived stromal cell factor (SDF-1a), which was released from a injectable thermosensitive hydrogels of chitosan/ glycerolphosphate/ hydroxylethylcellulose (CH/GP/ HEC)<sup>107</sup>. The expression of CXCR4 in cells and the concomitant release of its ligand SDF-1a from CH/GP/HEC hydrogels led to increased localization/retention of hASCs<sup>107</sup>. In addition to the massive infiltration of hASCs, in response to SDF-1a, a process of close vascularization was observed, which could indicate that these hydrogels would act as optimal supports for the migration of endogenous cells, which could facilitate repair and regeneration of tissues.

**Regeneration of cardiac muscle tissue:** options for the treatment of myocardial infarction are very limited<sup>62</sup> due to the inability of the mature myocardium to regenerate<sup>109</sup>. However, encapsulation of cardiac cells (cardiomyocytes and myoblasts) in photo-crosslinkable hydrogels, obtained from azidobenzoic acid-chitosan- and acryloyl-poly(ethylene glycol)-RGDS (Az-chitosan/Acr-PEG-RGDS), was evaluated as an alternative for regeneration of cardiac tissue (figure 9C.4), obtaining evidence of adhesion, proliferation and differentiation of encapsulated C2C12 myoblasts<sup>62</sup>. Likewise, a high viability of neonatal rat cardiomyocytes encapsulated in these photo-crosslinkable hydrogels was observed. Importantly, when adhesion of these hydrogels in the cardiac tissue was evaluated, it was evident that they remained adhered in the different parts of the heart where were applied, both on the surface (epicardium) and within the ventricle, a relevant fact for the treatment of myocardial infarction<sup>62</sup>.

**Other applications:** chitosan microencapsulation of some yeasts has also been studied for therapeutic and industrial purposes<sup>76,110,111</sup>. Encapsulation of the probiotic *Saccharomyces boulardii* in alginate/chitosan (AC) microspheres showed to have positive effects on its survival, protecting it from acid degradation and accelerating its transit through the gastrointestinal tract<sup>76</sup>; the use of this yeast with similar microencapsulation systems could be of great application not only for the therapies of inflammatory bowel diseases<sup>112</sup> but also for infectious enteritis<sup>113</sup> and enterocolopathies associated with *Clostridium difficile*<sup>114</sup>. On the other hand, the use of alginate/chitosan/alginate (ACA) and genipin/alginate/chitosan (GAC) has been proposed for industrial applications as an attractive method for the encapsulation of yeasts in the production of bioethanol<sup>111</sup>; these systems would improve the stability of the cells and the tolerance to the inhibitors, increasing the amount of biomass inside the reactor and decreasing the cost of recovery, as well as recycling and subsequent processing of the cells. Apparently, encapsulation with systems such as ACA and GAC attenuates the effect of ethanol concentration on yeast growth, which would imply a protective action related to tolerance to stress conditions in the culture.

#### *Encapsulation of bacteria*

**Administration of probiotics:** one of the main challenges in supplementing food with probiotics is that these can remain active in different environmental conditions. In addition to resisting oxygen exposure while functional food products are in storage, probiotics must face up to the host's harsh gastrointestinal conditions (such as gastric pH, bile salts, and enzymes) once ingested<sup>115,116</sup>. Thus, microencapsulation is classified as one of the main solutions for the preservation of probiotics, especially that based on some polymers such as chitosan<sup>71,116-119</sup>. Chitosan has been used in the protection of probiotic cells mainly as a coating/covering, and not as the capsule itself<sup>72,73,120</sup>. Some studies carried out with different bacterial strains have shown that the use of alginate microcapsules

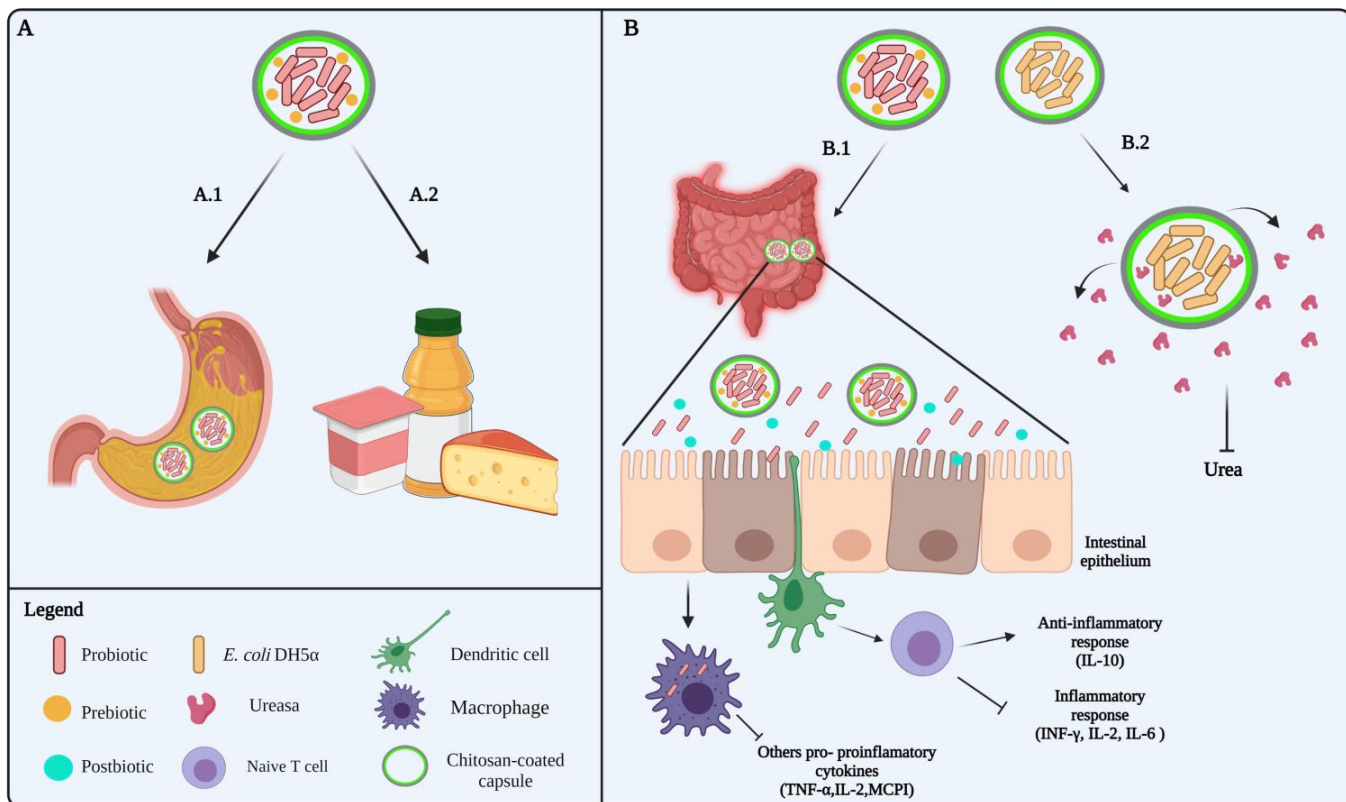


**Fig. 10:** Encapsulation of prokaryotic cells in systems containing chitosan. **A.** Probiotic protection would allow the storage and protection of the organism in different environmental conditions: **A.1** Efficient protection of probiotics in extreme conditions of stomach pH, bile and digestive enzymes, resulting in a greater number of viable cells in the intestine, **A.2** Confinement of probiotics could contribute to the stability of the microorganism in food matrices; **B.** Encapsulation of probiotics could be used in the treatment of some pathologies such as: **B.1** Bowel inflammatory diseases taking advantage of its anti-inflammatory effect, **B.2** Disorders associated with chronic kidney diseases, i.e., uremia, through overexpression and release of recombinant urease in genetically modified bacteria.

coated with chitosan is the best option for the storage and protection of probiotic bacteria, such as *Lactobacillus* and *Bifidobacterium* spp., under different experimental conditions<sup>64,65,67</sup>. Furthermore, chitosan-coated pectin capsules have been reported to efficiently protect *Lactobacillus casei* CIMB 30185 from extreme stomach pH conditions, resulting in increased numbers of viable cells in the intestine<sup>68</sup>.

In addition to protecting or improving the efficiency of the probiotic, some symbiotic encapsulation systems based on chitosan have been developed<sup>71</sup>. In these systems, contrary to others, a prebiotic or a specific carbon source of this is added<sup>120</sup> (figures 10A and 10B) which, in addition to serving as a substrate, can contribute to the stability and survival of the probiotic. A study using symbiotic systems based on AC/*L. casei*/selenium-enriched green tea (TVS) showed that the presence of TVS increases the probiotic survival at a storage temperature of 4 °C, under experimentally simulated gastric and bile solution conditions<sup>71</sup>. Similarly, the co-encapsulation of anthocyanins with *L. casei*, in addition to having a positive effect on the survival of the probiotic in simulated gastric conditions, improves the stability of the microorganism in food matrices such as yogurt<sup>121</sup>. Fur-

thermore, the use of other prebiotics such as inulin and starch has been reported in the co-encapsulation of lactic bacteria such as *Lactobacillus acidophilus*<sup>122,123</sup>. Comprehensively considered, these studies prompt that chitosan encapsulation and/or coating systems can lead to remarkable advances in the development of food and nutraceutical ingredients with markedly improved functionalities.

**Treatment of diseases:** the encapsulation of bacterial cells in AC gels has been proposed as an oral therapy strategy for some disorders such as inflammatory bowel diseases (Crohn's disease and ulcerative colitis) and uremia<sup>63,64</sup> (figures 10B.1 and 10B.2, respectively). Encapsulation of bacteria such as *Escherichia coli* strain Nissle 1917 (EcN), an organism with probiotic properties, was shown to have an anti-inflammatory and immunomodulatory effect in a colitis rat model<sup>64</sup>. The anti-inflammatory effect of probiotics is attributed to the modulation of the immune system in the intestinal micro-environment<sup>124</sup>, specifically through the modulation of the function of some immune cells, such as dendritic cells (DCs) and macrophages, and intestinal epithelial cells, mediating the activation of pattern recognition receptors (PRR) such as Toll-like receptors (TLR) expressed on cell surfaces<sup>125</sup>. Probiotic binding to some of the

TLRs, i.e., TLR2, can inhibit the secretion of cytokines and pro-inflammatory mediators, such as monocyte chemoattractant protein 1 (MCP1), tumor necrosis factor-alpha (TNF- $\alpha$ ), interleukins (IL-6, IL-2), but in turn promotes an increased expression of anti-inflammatory cytokines (IL-10)<sup>64,125,126</sup> (figure 10B.1) through the regulation of some signaling pathways, such as the NF- $\kappa$ B pathway and others such as that one triggered by mitogen-activated protein kinases (MAP kinases)<sup>127</sup>. Furthermore, some molecules produced and released by organisms such as bifidobacilli and lactobacilli, also known as postbiotics, can contribute to the anti-inflammatory effect of these organisms. These molecules, which are mainly short-chain fatty acids (SCFA), in particular propionate, acetate and butyrate, apparently exert their action by binding to specific receptors on intestinal epithelial cells (figure 10B.1). Association with these receptors induces the inhibition of the NF- $\kappa$ B signaling pathway and the production of pro-inflammatory cytokines by macrophages<sup>128,129</sup>. Similarly, these fatty acids can promote the induction of differentiation and expansion of regulatory T cells<sup>130</sup>. The encapsulation of some postbiotics with chitosan would be an alternative for the therapy of inflammatory diseases in immune-deficient patients, which could be affected by the administration of bacteria. This could become an interesting topic of study in the very near future.

In the treatment of uremia, a disorder associated with chronic kidney diseases, a genetically manipulated strain of a *Escherichia coli* DH5 harboring the gene encoding urease was used as a model for *in vitro* and *in vivo* evaluation of the ACA microcapsules in oral therapy of this disease; these studies revealed that encapsulation not only had a protective effect on the survival of cells in the gastric environment but also that encapsulated cells could remove urea from the medium<sup>63</sup> (figure 10B.2), suggesting that micro-encapsulation could allow safe and effective oral administration of live bacterial cells for various clinical applications (figure 10B.2).

### Concluding Remarks

Cell encapsulation has become a remarkably successful tool whose utilization seems to extend into different biotechnological fields given its potential to improve key aspects of *in vitro* and *in vivo* cell cultures, including proliferation and differentiation processes, especially in terms of providing greater protection to cells and avoid its recognition by the defense mechanism of the hosts. After 70 years of its initial implementation, it can be said that cell encapsulation is here to stay. Moreover, the development of new and exciting biomaterials over time, which has accelerated dramatically in recent years, seems to guarantee new successes in the years to come.

The valuable biological properties of chitosan, derived from its natural origin, have allowed its approval as an

excipient by the European and American pharmacopoeia (chitosan hydrochloride<sup>131</sup> and chitosan<sup>132</sup>, respectively). Thus, being chitosan a biomaterial so widely studied for promising applications in areas related to biotechnology such as biomedicine, food, agriculture, etc., it is believed that there will be a significant growth in research on new processes for obtaining it with higher purity indices and from new sources, as well as also in the preparation of derivatives specially designed to achieve specific objectives in cell encapsulation. In this context, click reactions can be seen as one the most logical routes to obtain new encapsulation methods using chitosan derivatives, although this field remains practically virgin due to the existence of a wide variety of others chemical reactions that could theoretically be incorporated into this scheme but they are still awaiting their experimental trial.

### References

1. TM Chang. Semipermeable microcapsules. *Science*, **146**, 524–525 (1964)
2. T Wang, J Adcock, W Kühtreiber, D Qiang, KJ Salleng, I Trenary, P Williams. Successful allotransplantation of encapsulated islets in pancreatectomized canines for diabetic management without the use of immunosuppression. *Transplantation*, **85**, 331–337 (2008).
3. Espona-Noguera, J Ciriza, A Cañibano-Hernández, G Orive, RM Hernández, L Saenz del Burgo *et al.* Review of Advanced Hydrogel-Based Cell Encapsulation Systems for Insulin Delivery in Type 1 Diabetes Mellitus. *Pharmaceutics*, **11(11)**, article number 597, 28 pages (2019).
4. M Hashemi, F Kalalinia. Application of encapsulation technology in stem cell therapy. *Life Sciences*, **143**, 139–146 (2015).
5. M Farina, JF Alexander, U Thekkedath, M Ferrari, A Gratttoni. Cell encapsulation: Overcoming barriers in cell transplantation in diabetes and beyond. *Advanced drug delivery reviews*, **139**, 92-115 (2019).
6. P De Vos, HA Lazarjani, D Poncelet, MM Faas. Polymers in cell encapsulation from an enveloped cell perspective. *Advanced Drug Delivery Reviews*, **67(68)**, 15–34 (2014).
7. JE Park, J Lee, ST Lee, E Lee E. *In vitro* maturation on ovarian granulosa cells encapsulated in agarose matrix improves developmental competence of porcine oocytes. *The riogenology*, **1(164)**, 42–50 (2021).
8. G Fundueanu, M Constantin, S Bucatariu, A Nicolescu, P Ascenzi, LG Moise *et al.* Simple and dual cross-linked chitosan millicapsules as a particulate support for cell culture. *International Journal of Biological Macromolecules*, **143**, 200-212 (2020).
9. A Blocki, F Löper, N Chirico, AT Neffe, F Jung, C Stamm *et al.* Engineering of cell-laden gelatin-based microgels for cell delivery and immobilization in regenerative therapies. *Clinical Hemorheology and Microcirculation*, **67(3-4)**, 251–259 (2017).

10. S Riedel, P Hietschold, C Krömmelbein, T Kunschmann, R Konieczny, W Knolle *et al.* Design of biomimetic collagen matrices by reagent-free electron beam induced crosslinking: Structure-property relationships and cellular response. **Materials & Design**, **168**, 107606 (2019).
11. J Cheng, D Park, Y Jun, J Lee, J Hyun, S Lee. Biomimetic spinning of silk fibers and *in situ* cell encapsulation. **Lab. Chip**, **16(14)**, 2654-2661 (2016).
12. T Gao, T Chen, C Feng, X He, C Mu, J Anzai *et al.* Design and fabrication of flexible DNA polymer cocoons to encapsulate live cells. **Nat. Commun.**, **10**, 2946 (2019).
13. MS Mohammadi, MN Bureau, SN Nazhat. Polylactic acid (PLA) biomedical foams for tissue engineering. In: *Biomedical Foams for Tissue Engineering Applications*. Woodhead Publishing Limited, Chapter 11, pages 313–334 (2014).
14. E González, C Herencias, MA Prieto. A polyhydroxyalkanoate-based encapsulating strategy for “bioplasticizing” microorganisms. **Microbial Biotechnology**, **13(1)**, 185–198 (2020).
15. J Sebastian, T Rouissi, SK Brar. Fungal chitosan: prospects and challenges. In: *Handbook of Chitin and Chitosan*. Volume 1: Preparation and Properties. Elsevier. Chapter 14, pages 419-452 (2020).
16. H Abdelkader, SA Hussain, N Abdullah, S Kmaruddin. Review on micro-encapsulation with Chitosan for pharmaceuticals applications. **MOJ Curr. Res. Rev.**, **1(2)**, 77–84 (2018).
17. J Lizardi-Mendoza, W Argüelles-Monal, F Goycoolea-Valencia. Chemical characteristics and functional properties of chitosan. In: *Chitosan in the preservation of agricultural commodities*. Eds.: S Bautista-Baños, G Romanazzi, A Jiménez-Aparicio. Academic Press. Chapter 1 (2016).
18. C Lárez-Velásquez Chitosan-based nanomaterials on controlled bioactive agents delivery: a review. **J. Anal. Pharm. Res.**, **7(4)**, 484-489 (2018).
19. N Boucard, C Viton, A Domard. New Aspects of the Formation of Physical Hydrogels of Chitosan in a Hydroalcoholic Medium. **Biomacromolecules**, **6**, 3227-3237 (2005).
20. J Berger, M Reist, JM Mayer, O Felt, R Gurny. Structure and interactions in chitosan hydrogels formed by complexation or aggregation for biomedical applications. **Eur. J. Pharm. Biopharm.**, **57**, 35–52 (2004).
21. J Berger, M Reist, JM Mayer, O Felt, NA Peppas, R Gurny. Structure and interactions in covalently and ionically cross-linked chitosan hydrogels for biomedical applications. **Eur. J. Pharm. Biopharm.**, **57**, 19–34 (2004).
22. KV HarishK,RN Tharanathan. Crosslinked chitosan — preparation and characterization. **Carbohydrate Research**, **341(1)**, 169-173 (2006).
23. Y Hong, H Song, Y Gong, Z Mao, C Gao, J Shen. Covalently crosslinked chitosan hydrogel: Properties of *in vitro* degradation and chondrocyte encapsulation. **Acta Biomaterialia**, **3(1)**, 23–31 (2007).
24. VX Truong, MP Ablett, HT Gilbert, J Bowen, SM Richardson, JA Hoyland, AP Dove. *In situ*-forming robust chitosan-poly(ethylene glycol) hydrogels prepared by copper-free azide–alkyne click reaction for tissue engineering. **Biomater. Sci.**, **2**, 167-175 (2014).
25. Crescenzi, D Imbriaco, C Lárez-Velásquez, M Dentini, A Ciferri. Novel types of polysaccharidic assemblies. **Macromolecular Chemistry and Physics**, **196(9)**, 2873-2880 (1995).
26. Yu, DJ O'Sullivan. Immobilization of whole cells of *Lactococcus lactis* containing high levels of a hyperthermostable β-galactosidase enzyme in chitosan beads for efficient galactooligosaccharide production. **J. Dairy Sci.**, **101(4)**, 2974-2983 (2018).
27. YF Poon, Y Cao, Y Liu, V Chan, M Chan-Park. Hydrogels Based on Dual Curable Chitosan-graft-Polyethylene Glycol-graft-Methacrylate: Application to Layer-by-Layer Cell Encapsulation. **ACS Applied Materials & Interfaces**, **2(7)**, 2012–2025 (2010).
28. SA Young, SE Sherman, T Cooper, C Brown, F Anjum, DA Hess *et al.* Mechanically resilient injectable scaffolds for intramuscular stem cell delivery and cytokine release. **Biomaterials**, **159**, 146-160 (2018).
29. MA Azagarsamy, KS Anseth. Bioorthogonal Click Chemistry: An Indispensable Tool to Create Multifaceted Cell Culture Scaffolds. **ACS Macro Letters**, **2**, 5-9 (2013).
30. JP Chen, TH Cheng. Thermo-Responsive Chitosan-graft-poly(N-isopropylacrylamide) Injectable Hydrogel for Cultivation of Chondrocytes and Meniscus Cells. **Macromol. Biosci.**, **6**, 1026–1039 (2006).
31. C Lárez-Velásquez. Quitosano y nanopartículas. En: *Nanopartículas: fundamentos y aplicaciones*, Capítulo 8. Editores: C Lárez-Velásquez, S Koteich, F López. Comisión de Publicaciones del Departamento de Química, Universidad de Los Andes, Venezuela. Pags. 203–222 (2015).
32. Y Luo, Q Wang. Recent development of chitosan-based polyelectrolyte complexes with natural polysaccharides for drug delivery. **Int. J. Biol. Macromol.**, **64**, 353–367 (2014).
33. SR Bhatia, SF Khattak, SC Roberts. Polyelectrolytes for cell encapsulation. **Current Opinion in Colloid & Interface Science**, **10**, 45–51 (2005).
34. M Thanou, BI Florea, M Geldof, HE Junginger, G Borchard. Quaternized chitosan oligomers as novel gene delivery vectors in epithelial cell lines. **Biomaterials**, **23(1)**, 153–159 (2002).
35. K Romøren, S Pedersen, G Smistad, Ø Evensen, BJ Thu. The influence of formulation variables on *in vitro* transfection efficiency and physicochemical properties of chitosan-based polyplexes. **International Journal of Pharmaceutics**, **261(1-2)**, 115–127 (2003).
36. M Sahin, N Kocak, G Arslan, HI Ucan. Synthesis of cross-linked chitosan with epichlorohydrin possessing two novel polymeric ligands and its use in metal removal. **J. Inorganic & Organometallic Polymers and Materials**, **21(1)**, 69-80 (2011).

37. WM Argüelles-Monal, J Lizardi-Mendoza, D Fernández-Quiroz, MT Recillas-Mota, M Montiel-Herrera. Chitosan derivatives: Introducing new functionalities with a controlled molecular architecture for innovative materials. **Polymers**, **10**(3), article number 342, 23 pages (2018).
38. Y Chen, Y Ye, R Li, Y Guo, H Tan. Synthesis of chitosan 6-OH immobilized cyclodextrin derivates via click chemistry. **Fibers & Polymers**, **14**, 1058–1065 (2013).
39. N Nishi, Y Maekita, SI Nishimura, O Hasegawa, S Tokura. Highly phosphorylated derivatives of chitin, partially deacetylated chitin and chitosan as new functional polymers: metal binding property of the insolubilized materials. **Int. J. Biol. Macromol.**, **9**(2), 109-114 (1987).
40. N R Kil'deeva, PA Perminov, LV Vladimirov, VV Novikov, SN Mikhailov. About Mechanism of Chitosan Cross-Linking with Glutaraldehyde. **Russian J. Bioorganic Chemistry**, **35**(3), 360–369 (2009).
41. L Wang, JP Stegemann. Glyoxal crosslinking of cell-seeded chitosan/collagen hydrogels for bone regeneration. **Acta Biomaterialia**, **7**(6), 2410-2417 (2011).
42. RAA Muzzarelli. Genipin-crosslinked chitosan hydrogels as biomedical and pharmaceutical aids. **Carbohydrate Polymers**, **77**, 1–9 (2009).
43. Q Zou, J Li, Y Li. Preparation and characterization of vanillin-crosslinked chitosan therapeutic bioactive microcarriers. **Int. J. Biol. Macromol.**, **79**, 736-747 (2015).
44. K Wegrzynowska-Drzymalska, P Grebicka, DT Mlynarczyk, D Chelminiak-Dudkiewicz, H Kaczmarek, T Goslinski, M Ziegler-Borowska. Crosslinking of Chitosan with Dialdehyde Chitosan as a New Approach for Biomedical Applications. **Materials**, **13**, 3413, 27 pages (2020).
45. LCR Carvalho, F Queda, C Almeida-Santos, MB Marques. Selective modification of chitin and chitosan: on the route to tailored oligosaccharides. **Chemistry—An Asian Journal**, **11**(24), 3468-3481 (2016).
46. AS Kritchenkova, YA Skorika. Click reaction in chitosan chemistry. **Russian Chemical Bulletin, International Edition**, **66**(5), 769—781 (2017).
47. BA Zielinski, P Aebischer. Chitosan as a matrix for mammalian cell encapsulation. **Biomaterials**, **15**, 1049–1056 (1994).
48. M Boido, M Ghibaudi, P Gentile, E Favaro, R Fusaro, C Tonda-Turo. Chitosan-based hydrogel to support the paracrine activity of mesenchymal stem cells in spinal cord injury treatment. **Sci. Rep.**, **9**, 6402 (2019).
49. K Roshanbinfar, S Salahshour Kordestani. Encapsulating Beta Islet Cells in Alginate, Alginate-Chitosan and Alginate-Chitosan-PEG Microcapsules and Investigation of Insulin Secretion. **J. Biomat. & Tissue Eng.**, **3**, 185–189 (2013).
50. V Chander, AK Singh, G Gangenahalli. Cell encapsulation potential of chitosan-alginate electrostatic complex in preventing natural killer and CD8+ cell-mediated cytotoxicity: an in vitro experimental study. **J. Microencapsul.**, **35**, 522–532 (2018).
51. A Vossoughi, HWT Matthew. Encapsulation of mesenchymal stem cells in glycosaminoglycans-chitosan polyelectrolyte microcapsules using electrospraying technique: Investigating capsule morphology and cell viability. **Bioeng. Transl. Med.**, **3**, 265–274 (2018).
52. S Itai, K Suzuki, Y Kurashina, H Kimura, T Amemiya, K Sato, M Nakamura, H Onoe. Cell-encapsulated chitosan-collagen hydrogel hybrid nerve guidance conduit for peripheral nerve regeneration. **Biomed. Microdevices**, **22**, 81 (2020).
53. S Ramesh, K Rajagopal, D Vaikkath, PD Nair, V Madhuri. Enhanced encapsulation of chondrocytes within a chitosan/hyaluronic acid hydrogel: a new technique. **Biotechnol. Lett.**, **36**, 1107–1111 (2014).
54. SM Oliveira, G Turner, PS Rodrigues, MA Barbosa, M Ali-khani, C Teixeira. Spontaneous chondrocyte maturation on 3D-chitosan scaffolds. **J. Tissue Science & Engineering**, **4**, (2012).
55. JS Choi, HS Yoo. Chitosan/Pluronic Hydrogel Containing bFGF/Heparin for Encapsulation of Human Dermal Fibroblasts. **J. Biomaterials Science, Polymer Edition**, **24**, 210–223 (2013).
56. RW Nurhayati, RD Cahyo, K Alawiyah, G Pratama, G Agustina, RD Antarianto, AR Prijanti, W Mubarok, AJ Rahyussalim. Development of double-layered alginate-chitosan hydrogels for human stem cell microencapsulation. **AIP Conference Proceedings**, **2193**, 020004 (2019).
57. A Mora-Boza, LM Mancipe Castro, RS Schneider, WM Han, AJ García, B Vázquez-Lasa, J San Román. Microfluidics generation of chitosan microgels containing glycerylphosphate crosslinker for *in situ* human mesenchymal stem cells encapsulation. **Materials Science and Engineering, C** **120**, 111716 (2021).
58. S Durkut, AE Elçin, YM Elçin. *In vitro* evaluation of encapsulated primary rat hepatocytes pre- and post-cryopreservation at -80°C and in liquid nitrogen. **Artif. Cells Nanomed. Biotechnol.**, **43**, 50–61 (2015).
59. S Mansouri, Y Merhi, FM Winnik, M Tabrizian. Investigation of Layer-by-Layer Assembly of Polyelectrolytes on Fully Functional Human Red Blood Cells in Suspension for Attenuated Immune Response. **Biomacromolecules**, **12**, 585–592 (2011).
60. M Sobol, A Bartkowiak, B de Haan, P de Vos. Cytotoxicity study of novel water-soluble chitosan derivatives applied as membrane material of alginate microcapsules. **J. Biomed. Materer. Res., A** **101**, 1907–1914 (2013).
61. Y Yeo, W Geng, T Ito, DS Kohane, JA Burdick, M Radisic. Photocrosslinkable hydrogel for myocyte cell culture and injection. **J. Biomed. Materer. Res. B Appl. Biomater.**, **81**, 312–322 (2007).
62. M Yang, S He, Z Su, Z Yang, X Liang, Y Wu. Thermosensitive Injectable Chitosan/Collagen/β-Glycerophosphate Composite Hydrogels for Enhancing Wound Healing by Encapsulating Mesenchymal Stem Cell Spheroids. **ACS Omega**, **5**, 21015–21023 (2020).

63. J Lin, W Yu, X Liu, H Xie, W Wang, X Ma. *In vitro* and *in vivo* characterization of alginate-chitosan-alginate artificial microcapsules for therapeutic oral delivery of live bacterial cells. **J. Biosci. Bioeng.**, **105**, 660–665 (2008).
64. X Luo, H Song, J Yang, B Han, Y Feng, Y Leng, Z Chen. Encapsulation of *Escherichia coli* strain Nissle 1917 in a chitosan—alginate matrix by combining layer-by-layer assembly with CaCl<sub>2</sub> cross-linking for an effective treatment of inflammatory bowel diseases. **Colloids and Surfaces B: Biointerfaces**, **189**, 110818 (2020).
65. M Kurakula, S Gorityala, DB Patel, P Basim, B Patel, S Kumar Jha. Trends of Chitosan Based Delivery Systems in Neuroregeneration and Functional Recovery in Spinal Cord Injuries. **Polysaccharides**, **2**, 519–537 (2021).
66. W Zhang, S Zhao, W Rao, J Snyder, JK Choi, L Wang *et al.* A novel core–shell microcapsule for encapsulation and 3D culture of embryonic stem cells. **J. Materials Chemistry B**, **1**(7), 1002–1009 (2013).
67. KC Yang, CC Wu, YH Cheng, TF Kuo, FH Lin. Chitosan/Gelatin Hydrogel Prolonged the Function of Insulinoma/Agarose Microspheres *In Vivo* During Xenogenic Transplantation. **Transplantation Proceedings**, **40**, 3623–3626 (2008).
68. YM Elçin, AE Elçin, RG Bretzel, T Linn. Pancreatic Islet Culture and Transplantation Using Chitosan and PLGA Scaffolds. In: *Tissue Engineering, Stem Cells, and Gene Therapies*. Ed YM Elçin, Springer USA. pp. 255–264 (2003).
69. S Graff, S Hussain, JC Chaumeil, C Charrueau. Increased intestinal delivery of viable *Saccharomyces boulardii* by encapsulation in microspheres. **Pharm. Res.**, **25**, 1290–1296 (2008).
70. MT Cook, G Tzortzis, VV Khutoryanskiy, D Charalampopoulos. Layer-by-layer coating of alginate matrices with chitosan-alginate for the improved survival and targeted delivery of probiotic bacteria after oral administration. **J. Mater. Chem., B** **1**, 52–60 (2013).
71. W Krasaecko, B Bhandari, H Deeth. The influence of coating materials on some properties of alginate beads and survivability of microencapsulated probiotic bacteria. **Int. Dairy Journal**, **14**, 737–743 (2004).
72. DC Vodnar, C Socaciu. Green tea increases the survival yield of Bifidobacteria in simulated gastrointestinal environment and during refrigerated conditions. **Chem. Cent. J.**, **6**, 61 (2012).
73. M Chávarri, I Marañón, R Ares, FC Ibáñez, F Marzo, M Villarán. Microencapsulation of a probiotic and prebiotic in alginate-chitosan capsules improves survival in simulated gastrointestinal conditions. **Int. J. Food Microbiology**, **142**, 185–189. (2010).
74. SM Koo, YH Cho, CS Huh, YJ Baek, J Park. Improvement of the stability of *Lactobacillus casei* YIT 9018 by microencapsulation using alginate and chitosan. **J. Microbiology and Biotechnology**, **11**, 376–383 (2001).
75. A Bepeyeva, JMS de Barros, H Albadran, AK Kakimov, ZK Kakimova, D Charalampopoulos, VV Khutoryanskiy. Encapsulation of *Lactobacillus casei* into Calcium Pectinate-Chitosan Beads for Enteric Delivery. **J. Food Sci.**, **82**, 2954–2959 (2017).
76. M Boido, D Garbossa, M Fontanella, A Ducati, A Vercelli. Mesenchymal Stem Cell Transplantation Reduces Glial Cyst and Improves Functional Outcome After Spinal Cord Compression. **World Neurosurgery**, **81**, 183–190. (2014).
77. FE Ezquer, MEEzquer, JM Vicencio, SD Calligaris. Two complementary strategies to improve cell engraftment in mesenchymal stem cell-based therapy: Increasing transplanted cell resistance and increasing tissue receptivity. **Cell Adh. Migr.**, **11**, 110–119 (2017).
78. Ai Arno, S Amini-Nik, PH Blit, M Al-Shehab, C Belo, E Herer, CH Tien, MG Jeschke. Human Wharton's jelly mesenchymal stem cells promote skin wound healing through paracrine signaling. **Stem Cell Res. Ther.**, **5**, 28 (2014).
79. DF Emerich, BR Frydel, TR Flanagan, M Palmatier, SR Winn, L Christenson. Transplantation of Polymer Encapsulated PC12 Cells: Use of Chitosan as an Immobilization Matrix. **Cell Transplant.**, **2**, 241–249 (1993).
80. CM Grau, LA Greene. Use of PC12 Cells and Rat Superior Cervical Ganglion Sympathetic Neurons as Models for Neuroprotective Assays Relevant to Parkinson's Disease. **Methods Mol. Biol.**, **846**, 201–211 (2012).
81. D Offen, I Ziv, A Barzilai, S Gorodin, E Glater, A Hochman, E Melamed. Dopamine-melanin induces apoptosis in PC12 cells; possible implications for the etiology of Parkinson's disease. **Neurochem. Int.**, **31**, 207–216 (1997).
82. P Belujon, AA Grace. Dopamine System Dysregulation in Major Depressive Disorders. **Int. J. Neuropsychopharmacol.**, **20**, 1036–1046 (2017).
83. E Dobryakova, HM Genova, J DeLuca, GR Wylie. The Dopamine Imbalance Hypothesis of Fatigue in Multiple Sclerosis and Other Neurological Disorders. **Frontiers in Neurology**, **6**, 52 (2015).
84. W Zhang. Encapsulation of Transgenic Cells for Gene Therapy. In: *Gene Therapy-Principles and Challenges*. In-techOpen (2015).
85. J Goldstein, G Siviglia, R Hurst, L Lenny, L Reich. Group B erythrocytes enzymatically converted to group O survive normally in A, B, and O individuals. **Science**, **215**, 168–170 (1982).
86. P Rahfeld, SG Withers. Toward universal donor blood: Enzymatic conversion of A and B to O type. **J. Biol. Chem.**, **295**, 325–334 (2020).
87. R Mitra, N Mishra, GP Rath. Blood groups systems. **Indian J. Anaesth.**, **58**, 524–528 (2014).
88. O Jahanpour, JJ Pyuza, EO Ntiyakunze, A Mremi, ER Shao. ABO and Rhesus blood group distribution and frequency among blood donors at Kilimanjaro Christian Medical Center, Moshi, Tanzania. **BMC Research Notes**, **10**(1), 1–5 (2017).
89. J Rosenberg, J Huang. CD8<sup>+</sup> T Cells and NK Cells: Parallel and Complementary Soldiers of Immunotherapy. **Curr. Opin. Chem. Eng.**, **19**, 9–20 (2018).

90. P Pontrelli, F Rascio, G Castellano, G Grandaliano, L Gessaldo, G Stallone. The Role of Natural Killer Cells in the Immune Response in Kidney Transplantation. **Front Immunol.**, **11**, 1454 (2020).
91. V Bueno, JOM Pestana. The role of CD8<sup>+</sup> T cells during allograft rejection. **Braz. J. Med. Biol. Res.**, **35**, 1247–1258 (2002).
92. M Rodríguez-Vázquez, B Vega-Ruiz, R Ramos-Zúñiga, DA Saldaña-Koppel, LF Quiñones-Olvera. Chitosan and Its Potential Use as a Scaffold for Tissue Engineering in Regenerative Medicine. **BioMed Research Int.**, **2015**, e821279 (2015).
93. Y Hong, H Song, Y Gong, Z Mao, C Gao, J Shen. Covalently crosslinked chitosan hydrogel: properties of in vitro degradation and chondrocyte encapsulation. **Acta Biomater.**, **3**, 23–31 (2007).
94. H Park, B Choi, J Hu, M Lee. Injectable chitosan hyaluronic acid hydrogels for cartilage tissue engineering. **Acta Biomater.**, **9**, 4779–4786 (2013).
95. H Tan, CR Chu, KA Payne, KG Marra. Injectable in situ forming biodegradable chitosan–hyaluronic acid based hydrogels for cartilage tissue engineering. **Biomaterials**, **30**, 2499–2506 (2009).
96. H Sá-Lima, SG Caridade, JF Mano, RL Reis. Stimuli-responsive chitosan-starch injectable hydrogels combined with encapsulated adipose-derived stromal cells for articular cartilage regeneration. **Soft Matter**, **6**, 5184–5195 (2010).
97. TC Tseng, L Tao, FY Hsieh, Y Wei, IM Chiu, S Hsu. An Injectable, Self-Healing Hydrogel to Repair the Central Nervous System. **Adv. Mater.**, **27**, 3518–3524 (2015).
98. FY Hsieh, TC Tseng, SH Hsu. Self-healing hydrogel for tissue repair in the central nervous system. **Neural Regeneration Research**, **10**(12), 1922 (2015).
99. HK Jahromi, A Farzin, E Hasanzadeh, SE Barough, N Mahmoodi, MRH Najafabadi, J Ai. Enhanced sciatic nerve regeneration by poly-L-lactic acid/multi-wall carbon nanotube neural guidance conduit containing Schwann cells and curcumin encapsulated chitosan nanoparticles in rat. **Mat. Sci. Eng.: C**, **109**, 110564 (2020).
100. K Bhatheja, J Field. Schwann cells: Origins and role in axonal maintenance and regeneration. **Int. J. Biochem. Cell Biology**, **38**, 1995–1999 (2006).
101. Sp Frostick, Q Yin, GJ Kemp. Schwann cells, neurotrophic factors, and peripheral nerve regeneration. **Microsurgery**, **18**, 397–405 (1998).
102. R Li, D Li, C Wu, L Ye, Y Wu, Y Yuan, J Xiao. Nerve growth factor activates autophagy in Schwann cells to enhance myelin debris clearance and to expedite nerve regeneration. **Theranostics**, **10**(4), 1649 (2020).
103. J Tello Velasquez, L Nazareth, RJ Quinn, J Ekberg, JA St John. Stimulating the proliferation, migration and lamellipodia of Schwann cells using low-dose curcumin. **Neuroscience**, **324**, 140–150 (2016).
104. IH Liu, SH Chang, HY Lin. Chitosan-based hydrogel tissue scaffolds made by 3D plotting promotes osteoblast proliferation and mineralization. **Biomed. Mater.**, **10**, 035004 (2015).
105. VJ Nelson, MFK Dinnunhan, PR Turner, JM Faed, JD Cabral. A chitosan/dextran-based hydrogel as a delivery vehicle of human bone-marrow derived mesenchymal stem cells. **Biomed. Mater.**, **12**, 035012 (2017).
106. L Dong, SJ Wang, XR ZhaoR, YF Zhu, JK Yu. 3D- Printed Poly( $\epsilon$ -caprolactone) Scaffold Integrated with Cell-laden Chitosan Hydrogels for Bone Tissue Engineering. **Sci. Rep.**, **7**, 13412 (2017).
107. H Naderi-Meshkin, H Naderi-Meshkin, MM Matin, A Heiranian-Tabasi, M Mirahmadi, M Irfan-Maqsood, MA Edalatmanesh *et al.* Injectable hydrogel delivery plus preconditioning of mesenchymal stem cells: exploitation of SDF-1/CXCR4 axis toward enhancing the efficacy of stem cells' homing. **Cell Biol. Int.**, **40**, 730–741 (2016).
108. W Jin, X Liang, A Brooks, K Futrega, X LiuX, MR Doran *et al.* Modelling of the SDF-1/CXCR4 regulated in vivo homing of therapeutic mesenchymal stem/stromal cells in mice. **PeerJ**, **6**, e6072 (2018).
109. B Cui, Y Zheng, L Sun, T Shi, Z Shi, L Wang *et al.* Heart regeneration in adult mammals after myocardial damage. **Acta Cardiológica Sinica**, **34**(2), 115 (2018).
110. L Xi. The use of chitosan to increase the stability of calcium alginate beads with entrapped yeast cells. **Biotechnology and Applied Biochemistry**, **23**(3), 269–272 (1996).
111. S Namthabad, R Chinta. Robust Encapsulation of Yeast for Bioethanol Production. Master Thesis, Engineering School, Industrial Biotechnology University of Boras, Sweden (2012).
112. M Guslandi, G Mezzi, M Sorghi, PA Testoni. *Saccharomyces boulardii* in maintenance treatment of Crohn's disease. **Dig. Dis. Sci.**, **45**, 1462–1464 (2000).
113. LV McFarland, CM Surawicz, RN Greenberg, GW Elmer, KA Moyer KA, SA Melcher *et al.* Prevention of beta-lactam-associated diarrhea by *Saccharomyces boulardii* compared with placebo. **Am. J. Gastroenterol.**, **90**, 439–445 (1995).
114. JP Buts, G Corthier, M Delmee. *Saccharomyces boulardii* for *Clostridium difficile*-associated enteropathies in infants. **J. Pediatr. Gastroenterol. Nutr.**, **16**, 419–425 (1993).
115. LF Călinoiu, BE Ștefănescu, ID Pop, L Muntean, DC Vodnar. Chitosan Coating Applications in Probiotic Microencapsulation. **Coatings**, **9**, 194 (2019).
116. A De Prisco, G Mauriello. Probiotication of foods: A focus on microencapsulation tool. **Trends in Food Science & Technology**, **48**, 27–39 (2016).
117. MT Cook, G Tzortzis, D Charalampopoulos, VV Khutoryanskiy. Microencapsulation of probiotics for gastrointestinal delivery. **J. Controlled Release**, **162**, 56–67 (2012).

118. R Gheorghita, L Anchidin-Norocel, R Filip, M Dimian, M Covasa. Applications of Biopolymers for Drugs and Probiotics Delivery. **Polymers**, **13**, 2729 (2021).
119. J Mirtić, T Rijavec, S Zupančič, A Zvonar Pobirk, A Lanjanje, J Kristl. Development of probiotic-loaded microcapsules for local delivery: Physical properties, cell release and growth. **Eur. J. Pharm. Sci.**, **121**, 178–187 (2018).
120. A Mortazavian, SH Razavi, MR Ehsani, S Sohrabvandi. Principles and Methods of Microencapsulation of Probiotic Microorganisms. **Iranian J. Biotechnology**, **5**, 1–18 (2007).
121. MT Cook, G Tzortzis, DCharalampopoulos, VV Khutoryanskiy. Microencapsulation of a symbiotic into PLGA/alginate multiparticulate gels. **Int. J. Pharm.**, **466**, 400–408 (2014).
122. IM Enache, AM Vasile, E Enachi, V Barbu, N Stănciu, C Vizireanu. Co-Microencapsulation of Anthocyanins from Black Currant Extract and Lactic Acid Bacteria in Biopolymeric Matrices. **Molecules**, **25**, 1700 (2020).
123. S Jantarathin, C Borompichaichartkul, R Sanguandeekul. Microencapsulation of probiotic and prebiotic in alginate-chitosan capsules and its effect on viability under heat process in shrimp feeding. **Materials Today: Proceedings**, **4**, 6166–6172 (2017).
124. M de Araújo-Etchepare, GC Raddatz, EM de Moraes-Flores, LQ Zepka, E Jacob-Lopes *et al.* Effect of resistant starch and chitosan on survival of *Lactobacillus acidophilus* microencapsulated with sodium alginate. **LWT - Food Science and Technology**, **65**, 511–517 (2016).
125. YA Ghouri, DM Richards, EF Rahimi, JT Krill, A Jelinek, AW DuPont. Systematic review of randomized controlled trials of probiotics, prebiotics, and symbiotics in inflammatory bowel disease. **Clin. Exp. Gastroenterol.**, **7**, 473–487 (2014).
126. F Cristofori, VN Dargenio, C Dargenio, VL Miniello, M Barone, R Francavilla. Anti-Inflammatory and Immuno-modulatory Effects of Probiotics in Gut Inflammation: A Door to the Body. **Frontiers in Immunology**, **12**, 178 (2021).
127. MAK Azad, M Sarker, D Wan. Immunomodulatory Effects of Probiotics on Cytokine Profiles. **BioMed Research Int.**, **2018**, e8063647 (2018).
128. SC Li, WF Hsu, JS Chang, CK Shih. Combination of *Lactobacillus acidophilus* and *Bifidobacterium animalis* subsp. *lactis* Shows a Stronger Anti-Inflammatory Effect than Individual Strains in HT-29 Cells. **Nutrients**, **11**, E969 (2019).
129. MAR Vinolo, HG Rodrigues, E Hatanaka, FT Sato, SC Sampaio, R Curi. Suppressive effect of short-chain fatty acids on production of proinflammatory mediators by neutrophils. **J. Nutr. Biochem.**, **22**, 849–855 (2011).
130. JS Park, EJ Lee, JC Lee, WK Kim, HS Kim. Anti-inflammatory effects of short chain fatty acids in IFN-gamma-stimulated RAW 264.7 murine macrophage cells: involvement of NF-kappa B and ERK signaling pathways. **Int. Immunopharmacol.**, **7**, 70–77 (2007).
131. Council of Europe. European Pharmacopoeia 6.0 1774. Chitosan Hydrochloride; Council of Europe: Strasbourg, Germany (2008).
132. United States Pharmacopeial Convection. United States Pharmacopeia 34/National Formulary. Chitosan; The United States Pharmacopeial Convection: Rockville, MD, USA (2011).